Luz Catarina Neves Fernandes

MSc. in Technology and Food Quality

Development of new analytical methods for Matrix Assisted Laser Desorption Ionization Mass Spectrometry-based applications. Focus on proteins, polymers and small molecules

Dissertação para obtenção do Grau de Doutor em
Química Sustentável

Orientador: Prof. Doutor José Luis Capelo Martinez, Professor Auxiliar
Faculdade de Ciências e Tecnologia
Universidade Nova de Lisboa, Portugal

Co-orientadores: Prof. Doutor Carlos Lodeiro Espiño, Professor Auxiliar
Faculdade de Ciências e Tecnologia
Universidade Nova de Lisboa, Portugal

Prof. Doutora Isabel Maria Andrade Martins Galhardas de Moura,
Professora Catedrática Aposentada
Faculdade de Ciências e Tecnologia
Universidade Nova de Lisboa, Portugal

Júri:

Presidente: Prof. Doutor José Júlio Alves Alferes

Arguentes: Prof. Doutor Francisco Manuel Lemos Amado
Doutora Deborah Penque

Vogais: Doutor Hugo Miguel Baptista Carreira dos Santos
Doutora Elisabete de Jesus Oliveira Marques

FACULDADE DE CIÊNCIAS E TECNOLOGIA
UNIVERSIDADE NOVA DE LISBOA

Setembro 2016

Development of new analytical methods for Matrix Assisted Laser Desorption Ionization Mass Spectrometry-based applications, focus on proteins, polymers and small molecules.

To my lovely children...

"Sometimes we feel that what we do is nothing but a drop in the sea. But the ocean would be less if it lacked a drop."

Mother Teresa

"... podemos muito mais do que imaginamos."

José Saramago

Acknowledgements

In Portuguese

Quando dei o primeiro passo estava longe de pensar que me iria entregar a uma tarefa que iria demorar anos… Foram muitos os altos e baixos ao longo deste percurso, muitas vitórias, mas também algumas derrotas. Termino assim esta etapa, onde ultrapassei muitos desafios e dificuldades imensas, com o sentimento de dever cumprido.

Estou muito reconhecida por tudo quanto recebi e estarei eternamente grata a todos os que me ajudaram neste desafio. Ainda assim, gostaria de agradecer particularmente :

Ao Professor Doutor José Luis Capelo Martinez, orientador deste trabalho, expressando a minha profunda admiração e reconhecimento. Um simples agradecimento não será porventura suficiente para expressar a minha gratidão por tudo quanto me ensinou e proporcionou. Agradeço a excelente orientação científica, a ajuda, o apoio, a paciência, a compreensão manifestada, as suas críticas e reflexões únicas e sobretudo, a confiança que em mim depositou quando me iniciou no mundo da espectrometria de massa MALDI-TOF e da proteómica, confiando-me o serviço de análises em 2006, de onde, posteriormente nasceu o convite para realização deste projeto. Sempre me soube motivar com a sua forma única de ser. Com a sua enorme generosidade, sempre se recusou deixar-me desfalecer nos momentos mais difíceis, servindo inúmeras vezes de trampolim para alcançar objetivos. Reconheço-lhe sem dúvida notáveis capacidades de liderança sendo, para mim, um exemplo claro de dedicação genuína à Ciência. Para sempre, obrigada!

Ao Professor Doutor Carlos Lodeiro Espiño, co-orientador, agradeço o apoio incondicional, a disponibilidade e encorajamento que sempre demonstrou ao longo deste trabalho, assim como as barreiras que, ao longo deste percurso, me foi ajudando a erguer. Foi sem dúvida a pessoa que mais me incentivou e motivou desde o primeiro dia. A força e confiança que sempre me transmitiu transformou-se em energia positiva necessária para tudo conseguir. Agradeço ainda a sincera amizade que ao longo destes anos se foi criando e consolidando. Sinto-me imensamente privilegiada por isso. Muito muito obrigada!

Agradeço à Professora Doutora Isabel Moura, co-orientadora, pelo apoio, disponibilidade, simpatia, amizade e a ajuda proporcionada durante todos estes anos, quer no período em que presidia ao DQ, quer posteriormente.

À FCT/UNL, na pessoa do Senhor Diretor, Professor Doutor Fernando Santana, pela oportunidade facultada que permitiu levar a cabo este trabalho de Doutoramento nesta instituição, onde exerço funções de Técnica Superior no laboratório de análises da REQUI*M*TE desde 2003.

Ao Doutor Hugo Santos e à Doutora Elisabete Oliveira, colegas do grupo Bioscope, agradeço a amizade sincera, dedicação, disponibilidade e paciência sempre demonstrada ao longo destes anos. Um agradecimento muito especial ao Doutor Hugo Santos, pelos preciosos ensinamentos; amigo a quem recorrentemente bati à porta para resolver muitas questões de ordem técnica entre outras, auxiliando-me com preciosas indicações sempre com a paciência, disponibilidade e a calma que o caracteriza. Um imenso obrigado Hugo!

Aos restantes colegas do grupo Bioscope, que viram crescer este trabalho e que com paciência e amizade deram resposta à minhas questões intermináveis. Assim agradeço aos ex-membros (Doutora Raquel Rial, Doutor Ricardo Carreira, Doutor Gonçalo Vale, Doutor Marco Galésio, Doutor Bruno Pedras, Doutora Cristina Nuñes e Doutor Mário Diniz), e aos actuais membros (Javier, Eduardo, Adrián, Susana, Joana, Jessica, aos Gonçalos, Ana, Marta e Jamila). Muito obrigada por toda a ajuda ao longo destes anos!

Agradeço à Professora Doutora Ana Lourenço, coordenadora do laboratório de análises, pela oportunidade que me concedeu de poder conciliar, sempre que necessário, o meu trabalho diário do laboratório de análises com a finalização deste projeto.

Aos meus colegas do laboratório de análises, Carla Rodrigues e Nuno Costa, agradeço o companheirismo diário e o incentivo.

Um especial agradecimento à Ana Teresa Lopes pela amizade e pelas palavras de incentivo.

Agradeço às amigas de batalhas, Alaíde Agripino e Isabel Pinto, que como eu também tiveram que percorrer este caminho até ao fim. Muito obrigada pela amizade, carinho, paciência, disponibilidade, ajuda e pelas inúmeras palavras de incentivo.

Finalmente um agradecimento essencial à minha família que é o meu combustível e me ajudou na conquista de mais um sonho. Assim agradeço aos meus irmãos pelo amor que nos une e por serem quem são. Agradeço à minha mãe, sempre! Por tudo, pelo amor incondicional, pela ajuda, pelo incentivo, mesmo estando longe. Pelas inúmeras viagens feitas para Lisboa para acorrer ao meu auxílio sempre que era solicitada. Obrigada Mãe!

Um agradecimento muito muito especial à melhor pessoa do mundo, do meu mundo. Uma grande SENHORA, cuja pureza, humildade e bondade me conquistou desde o primeiro dia, a minha sogra, D. Felisbela. A quem agradeço do fundo do coração por ter

sido minha mãe na ausência da minha; mãe dos meus filhos na minha ausência e com quem sempre pudemos contar nos dias mais complicados. Ser-lhe-ei eternamente grata. O meu agradecimento é extensível ao meu sogro, Sr. Guido, que muito admiro. Muito obrigada.

Ao Nuno, o meu marido, pela paciência e por conseguir como ninguém suportar com grande sabedoria os meus desabafos, o meu mau humor e falta de paciência, que ao longo destes últimos tempos foram uma constante. Obrigada para sempre!

Às pessoas que não precisam de me dar motivos para sorrir, elas já são o motivo do meu sorriso, os meus filhos Tiago e André. Obrigada por serem o sol dos meus dias mesmo quando a vida está nublada. Mil e uma desculpas pelas longas horas de ausência, não tanto física mas sobretudo em espírito. Obrigada meus amores por existirem!

Por fim agradeço a todas as pessoas que direta ou indiretamente, embora não expressamente referidas, contribuíram para que este trabalho tivesse sido elaborado.

A todos, um sincero, muito obrigado!

Pelo suporte com o financiamento agradeço:

- À FCT-MCTES, projecto PTDC/QUI/6650/2006, pelo financiamento do trabalho desenvolvido nos capítulos IV e V.

- À InOu 2009-UVIGO and Canterbury Christ Church University Research Fund, pelo financiamento do trabalho desenvolvido no capítulo IV.

-À FCT, projectos POCI/QUI/55519/2004 FCT-FEDER e PTDC/QUI-QUI/099907/2008, pelo financiamento do trabalho desenvolvido no capítulo VI.

- À Associação Científica Proteomass pelo financiamento da investigação do trabalho laboratorial executado desde o ano de 2009.

Abstract

During the early life of Matrix-assisted laser desorption/ionization (MALDI), it took the (bio)scientific community a while to realize the great potential of the technique over a wide range of analytical problems, from the discovery or identification of (mostly) organic (macro)molecules through to structure analysis and function. Since then, the practical use of MALDI-MS has grown almost exponentially and it is today an indispensable laboratory tool, particularly in the life sciences.

Matrix-assisted laser desorption/ionization (MALDI) is a "soft" ionization technique, which allows for the sensitive detection of large, non-volatile and labile molecules by mass spectrometry. It is fast, allowing the analysis of hundreds of samples per day. It is expensive, as almost all mass spectrometry techniques, yet it is cost-effective. Currently the tandem MS and ion different fragmentation capabilities of most MALDI systems add an extra value to this technique as it allows for structural characterization of (bio)molecules. In addition to molecular identification and characterization, MALDI is an invaluable tool to profile and classify complex samples.

In spite of its many advantages, MALDI has one achilles tendon. If the sample is not conveniently prepared, the ionization is hampered and then the analysis is not possible. This is the reason why sample treatment for MALDI analysis is a never-ending hot topic in analytical chemistry. Thus, the methods used to identify proteins do not work with polymers and vice versa. In other words, for each new molecule a sample treatment optimization is needed so an adequate, well-defined, method of analysis is obtained. For this reason this thesis focused in the development of new sample treatments for MALDI-based applications. To this end and when possible, ultrasonic energy is used as a tool to simplify the sample handling by matching the analytical minimalism concept as defined by Halls[1]. The molecules for which the new sample treatments were developed were proteins, polymers and small inorganic molecules.

MALDI is the technique of preference for the analysis of polymers as with one single analysis the polymer´s typical values of number-average molecular weight, Mn,

[1] D. J. Halls, "Analytical minimalism applied to the determination of trace elements by atomic spectrometry. Invited lecture," *J. Anal. At. Spectrom*, vol. 10, pp. 169–175, 1995.

and weight-average molecular weight, Mw, can be obtained. A detailed characterization of these materials is important to relate their chemical structure and composition to their functions. In this work a rapid sample treatment based on ultrasonic energy for the characterization of polymers was developed. Thus, a number of variables affect the efficiency of the ultrasonic energy and thus they were investigated over different polymers to study their influence in the Mn and Mw values. Different ultrasonic devices including ultrasonic bath with dual frequency, sonoreactor and ultrasonic probe were used. The selected variables were (i) Utrasonic frequency (35 kHz, 40 kHz and 130 kHz), (ii) ultrasonic amplitude and (iii) time of ultrasonication. This study was done over three standard polymers: poly(styrene) 2000 Da and 10,000 Da and poly(ethylene glycol) 1000 Da. Furthermore, two common standard matrices, dithranol and 2,5-dihydroxybenzoic acid were used throughout the study. The results obtained show that the ultrasonic bath at 35 kHz is the best option for the purpose of fast sample treatment for polymer characterization. The Mn and Mw values obtained for this ultrasonic device and for the three polymers tested using dithranol as MALDI matrix, were not statistically different from the ones acquired with vortex mixing and also were in concordance with the values recommended by the polymer manufacturers.

MALDI as a tool for the study of small molecules and complexes has evolved slowly but constantly. During a time the main problem to deal with was the interfering peaks of the matrixes used. Their m/z signals used to interfere with the masses of the small molecules as they are of the same range. However, the discovering on new matrices, the development of MALDI-based MS/MS applications and specifically, the ability some molecules have to get ionized in the absence of matrix have pushed forward MALDI as a reference tool in research related to small molecules. In this thesis anionic and cationic interactions with a new emissive imine-based b-naphthol molecular probe is assessed using MALDI. In addition, the results from the MALDITOF-MS studies suggest that L can be used to sense Cu2+ in positive mode, and cyanide in negative mode. Density functional theory (DFT) studies showed that the copper(II) complex is formed by the unprotonated L2 species as it was predicted experimentally. However, the anionic complexes with fluoride and cyanide take place via supramolecular interactions with the diprotonated L form. This clearly demonstrated that L is not deprotonated upon anion interaction. Furthermore, MALDI was used in the study of the synthesis, characterization

and spectroscopic studies of two new schiff-base bithienyl pendant-armed 15-crown-5 molecular probes.

Complex proteomes are deciphered using gel- or off-gel based protocols. In this work an ultrasonic multiprobe was assayed as a tool to develop a fast method to identify proteins from complex proteomes. The optimization is done using a pool of standard proteins and complex proteome derived from *D. Desulfuricansa and Cyprinus carpio*. Proteins are first separated from complex proteomes using gel electrophoresis. The gel spots containing the protein(s) are then excised, washed and submitted to the action of the enzyme trypsin, that cleaves the protein in small peptides. The pool of peptides obtained is used to identify the protein using peptide mass fingerprint. When compared to the traditional method, the use of the ultrasonic multiprobe allows the following features: (i) the number of steps and the handling is greatly reduced; (ii) the total time since the spot is excised till the protein is ready to be identified is reduced from twelve hours to eight minutes and (iii) the risk of contamination is greatly reduced.

Keywords: MALDI-TOF MS, sample treatment, Ultrasound, Polymers, Protein identification, Chemosensor.

Resumo

A espectrometria de massa com ionização e dessorção a laser assistida por matriz (MALDI-TOF MS) é uma tecnologia extremamente poderosa e amplamente usada na análise de macromoléculas, embora não limitada a estas, por se tratar de uma técnica com inúmeras vantagens na obtenção de um espectro de massa: é rápida, de elevada sensibilidade e seletividade. Apesar destas vantagens, uma das principais limitações da técnica prende-se com a preparação da amostra que necessita de um tratamento especifico prévio à análise. Neste sentido, o trabalho desta tese pretende contribuir para o desenvolvimento de novos tratamentos de amostra, mais simples e eficientes. Foram escolhidos três tipos de analises, (i) identificação de proteínas por Peptide Mass Fingerprint (PMF), (ii) caracterização de polímeros e (iii) caracterização de moléculas pequenas.

No tratamento de amostras para a caracterização de polímeros foram testados diversos dispositivos ultrassónicos. Foram explorados os efeitos das seguintes variáveis sobre a distribuição dos pesos moleculares: (i) frequência de ultrassons, (ii) amplitude de ultrassons, e (iii) tempo de sonicação. Procedeu-se à avaliação do efeito destas variáveis em três polímeros padrão, recorrendo a duas matrizes MALDI. Os resultados obtidos demonstram que o banho de ultrassons a 35 kHz é a melhor opção para o tratamento célere das amostras. Os valores de Mn e Mw obtidos para este dispositivo de ultrassons e para os três polímeros testados usando ditranol como matriz, não foram estatisticamente diferentes dos adquiridos com a metodologia padrão de agitação com vortex.

No âmbito das moléculas pequenas, a tecnologia MALDI-TOF MS foi empregue no estudo de novas moléculas orgânicas com absorção no ultravioleta, verificando-se a sua capacidade de sensor, em fase gasosa, relativamente a catiões tais como Cu^{2+}, Zn^{2+} e Al^{3+}, e a aniões como F^- e CN^- , comportando-se de forma estável nas condições da análise MALDI-TOF MS.

Relativamente ao tratamento de amostras de proteínas, o trabalho refere-se à aplicação de uma multi-sonda de ultrassons de 4 pontas, para desenvolver procedimentos rápidos para digestão de proteínas em proteomas complexos. As proteínas são separadas com recurso à eletroforese em gel. A utilização de ultrassons com uma multi-sonda,

permite (i) diminuir o número de etapas do tratamento e a manipulação da amostra, (ii) diminuir os tempos necessários para completar o tratamento, (iii) diminuir o riscos de contaminação. O tratamento completo desde que a proteína é separada no gel até à sua identificação é realizado em poucos minutos comparado com o método clássico. Foi ainda usado o método de marcação isotópica com ^{18}O para estudar o tipo de péptidos extraídos dos géis, assim como a eficiência da extração. A otimização da metodologia foi feita com recurso a proteínas padrão, sendo que proteínas separadas por eletroforese em gel, a partir de extratos de *D. desulfuricans*, e de *Cyprinus carpio*, foram utilizadas como "proof of concept".

Palavras-chave: MALDI-TOF MS, tratamento de mostras, proteómica, ultrassons, identificação de proteínas, polímeros, quimiossensores

Index

List of Figures

List of Tables

Symbols and Abreviations

Symbols

A	Absorbance
λ_{em}	Emission wavelength
λ_{exc}	Excitation wavelength
λ_{max}	Wavelength of maximum emission or absorption
m/z	Mass-to-charge ratio

Abbreviations

ACN	Acetonitrile
A&D	Aspirate and dispense
AgTFA	Silver trifluoroacetate
ALSs	Acid-labile surfactants
AmBic	Ammonium Bicarbonate
ATT	6-Aza-2-thiothymine
CDCl3	Deuterated Chloroform
α-CHCA	α- Cyano-4-hydroxycinnamic acid (matrix for MALDI-MS)
CHEF	Chelation Enhanced Fluorescence
CID	Collision induced dissociation
DFT	Density funcional theory
2-DE	Two dimensional electrophoresis
1D-PAGE	One-dimensional polyacrylamide gel electrophoresis
2D-PAGE	Two-dimensional polyacrylamide gel electrophoresis
D&I	Direct and Inverse

DHB	2,5-Dihydroxibenzoic acid (matrix for MALDI-MS)
DMSO	Dimethyl sulfoxide
DNA	Deoxyribonucleic acid
DTT	DL-Dithiothreitol
EDTA	Ethylenediamine tetraacetic acid
Equiv.	Equivalent
ESI	Electrospay ionization
ESI-MS	Electrospray ionization mass spectrometry
FAB	Fast atom bombardment
Fig.	Figure
FD	Field desorption
FT	Fourier transform
GE	Gel elctrophoresis
GPC	Gel permeation chromatography
8-HQ	8-Hydroxyquinoline
HABA	2(4-Hydroxyphenylazo) benzoic acid (matrix for MALDI-MS)
3-HPA	3-Hydroxypicolinic acid (matrix for MALDI-MS)
HPLC	High performance liquid chromatography
IAA	Iodoacetamide
IEF	Isoelectric focusing
IR	Infrared
L	Ligand
LC	Liquid chromatography
LC/MS	Liquid chromatography coupled to mass spectrometry
LDI	Laser desorption/ionization
Lys-C	Lysine-C

MALDI	Matrix Assisted laser desorption/ionization
MALDI-TOF MS	Matrix Assisted laser desorption/ionization time-of-flight mass spectrometry
MeOH	Methanol
Milli-Q	Ultrapure water
Mn	Number-average molecular weight
MRM	Multiple reaction monitoring
MS	Mass spectrometry
MS/MS	mass spectrometry/mass spectrometry
Mw	Weight-average molecular weight
MW	Molecular weight
NMR	Nuclear magnetic resonance
PBS	Phosphate buffer solution
PDI	Polydispersity
PEG	Polyethylene glycol
PET	Photo-induced electron transfer
PFF	Peptide fragment fingerprint
pI	Isoeletric points
PMF	Peptide mass fingerprint
PPT	Photo-induced pronton transfer
PS	Polystyrene
PSD	Post-source decay
Q-TOF	Quadrupole time-of-flight (mass analyzer)
QIT	Quadrupole ion trap (mass analyzer)
RSD	Relative Standard Deviation
SDS	Sodium dodecyl sulfate
SDS-PAGE	Sodium dodecyl sulfate polyacrylamide gel electrophoresis

SIMS	Secondary ion mass spectrometry
S/N	Signal-to-noise ratio
Super-DHB	2,5-Dihydroxibenzoic acid and 2-hydroxy-5-methoxybenzoic acid (matrix for MALDI-MS)
TCA	Trichloroacetic acid
TFA	Trifluoroacetic acid
THAP	2,4,6-Trihydroxyacetophenone (matrix for MALDI-MS)
TDDFT	Time Dependent Density Functional Theory
TOF	Time-of-flight (mass analyzer)
UE	Ultrasonic energy
UP	Ultrasonic probe
USB	Ultrasonic bath
UTR	Sonoreactor
UV	Ultraviolet
UV-vis	Ultraviolet-visible

Chapter I

Introduction

I.1 Mass Spectrometry with matrix-assisted laser desorption ionization accomplished to time of flight analysers.

I.1.1 Basics on Mass Spectrometry approaches

The beginning of mass spectrometry can be traced back till the end of the XIX century, when Eugen Goldstein did the first experiments about canal rays in 1886. Later, in 1898, Wilhelm Wien and J. J. Thomson further developed the canal rays experiments using low pressure, being able of measuring the mass-to-charge ratio of electrons and protons [1], [2]. Currently, mass spectrometry is used to measure masses of molecules, to unravel their composition as well as for elucidating their chemical structure.

A mass spectrum is obtained from gaseous molecules or species desorbed from condensed phases that are first ionized, then accelerated by an electric field and finally separated according to their mass-to-charge ratio, m/z. Figure I.1 shows a matrix assisted laser desorption ionization, MALDI, mass spectrum of an enzymatic digest of BSA protein along with a comprehensive scheme of the working of a MALDI mass spectrometer. As a general role a mass spectrometer is build with three main components: an ion source, to convert in ions the molecules of the sample; a mass analyser, which separates the ions according to their mass-to-charge ratio using electromagnetic fields; and a detector, which transforms the current of ions in a measurable signal. Figure I.1 identifies those components for the case of a MALDI-TOF mass spectrometer, the most common interfaces is between a MALDI source and a time-of-flight (TOF) mass analyser.

The most intense peak in the spectrum (see Fig. I.1) is called the base peak and the intensities of other peaks are expressed as a percentage of the base peak intensity.

Mass spectrometry allows for the separation and identification of natural isotopes of elements and also allows for the separation and identification of isotopic distribution patterns of complex molecules, such as the case of the inset highlighted in Figure I.1, where the isotopic distribution of peptide m/z 927 from BSA is shown. Such patterns help to classify molecules. For instance the isotopic distribution patterns of one peptide is different from the one belonging to one lipid. Because the isotopic distributions of different molecules can be detected at the same time, if the spectrum is very complex,

isotopic distributions can be an additional headache for data interpretation, making data interpretation difficult [3].

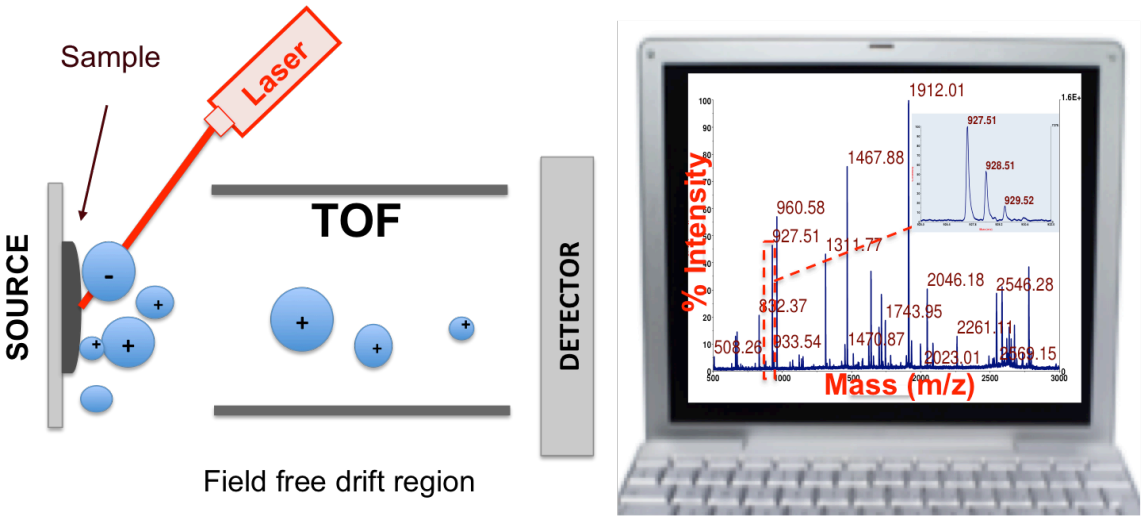

Figure I.1 The principle components of a MALDI time-of-flight mass spectrometry consisting of the ionization source followed by the mass analyser and detector. A computer is used to generate a spectrum with the data provided by the detector.

I.1.2 Matrix assisted laser desorption ionization.

I.1.2.1 The MALDI concept

It was believed during long time that molecules with large masses, e.g. 1000 Da, could not be measured by mass spectrometry in their intact form as they tend to get fragmented. Field desorption (FD), secondary ion mass spectrometry (SIMS) and fast atom bombardment (FAB) are techniques that precluded the advent of MALDI. It was during the development of FD, FAB and SIMS that the first attempts to desorb large molecules with laser irradiation began. It was during this time that the concept of "matrix" as a substance to help in the desorption process of large molecules and in enhancing ion yield was coined. The MALDI principle was first addressed in 1984 and the principle and acronyms were first published in 1985 [4], although the background to develop this technique existed since 1975 [5] and even earlier [6].

In brief, the sample containing the analyte of interest is mixed with a large excess of a small chemical compound, generally known as matrix. The matrix helps in the ionization of the sample favouring the absorption of the laser as well as promoting the protonation of the molecules of interest. Once into the apparatus, the sample is irradiated with a laser, which transfers energy to form a plume of molecules, which is transferred to a mass analyser, where the molecules are separated as a function of their mass-to-charge ratio. Finally, the molecules reach the detector, promoting a signal that is recorded and transformed in the characteristic mass spectrum [3], [7].

I.1.2.2 The Matrix

As it has been written above, the use of a chemical matrix in large excess over the analyte, with the main aim to help to promote ionization by absorbing the laser energy and/or transferring protons to the analyte is the core of MALDI principle. In addition to chemical matrices, other approaches to facilitate analyte ionization have been described in literature. For example, the use of nanoparticles as a matrix was first reported by Tanaka and co-workers in 1988 [8], and the use of dry carbon with the same purpose was first reported by Sunner and co-workers in 1995 [9]. Although the use of MALDI matrices can be traced back to more than 20 years ago, the complete physical and chemical processes involving the analyte-matrix-laser ionization process have not been yet fully understood [10]. Therefore, matrices have been matched analytes on a trial and error basis. A matrix can be found appropriate for an analyte whilst inappropriate for another one. As a matter of fact, the matrix used with peptides does not work properly with proteins and vice versa. Table I.1 presents the most common matrices for peptides, proteins, small molecules and polymers.

Table 1.1 Exemple of common matrices used in MALDI-MS. (Reproduces from references [2], [3])

Matrix	Structure	λ (nm)	Application
3-Amino-4-hydroxybenzoic acid	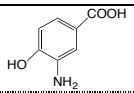	337	Oligosaccharides
2,5-Dihydroxibenzoic acid (DHB)	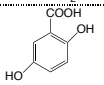	337, 353	Proteins, peptides, carbohydrates, synthetic polymers
5-Hydroxy-2-methoxybenzoic acid	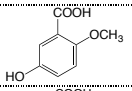	266, 337, 355	Lipids, Proteins,
2(4-Hydroxyphenylazo)benzoic acid (HABA)	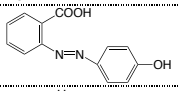	266, 337	Proteins, lipids
Cinnamic Acid	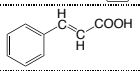	337	General
4-Methoxycinnamic acid	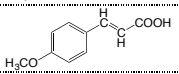	337	Proteins
Ferlulic acid	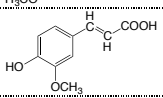	337, 266, 355	Proteins
Sinapinic acid	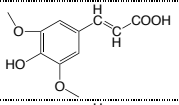	266, 337, 353, 355	Proteins, peptides,
α- Cyano-4-hydroxycinnamic acid (CHCA)	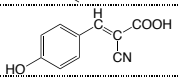	337, 353, 355	Peptides fragmentation
6,7-Dihydroxycoumarin	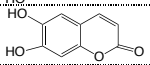	337	Lipids, peptides
3-Hydroxypicolinic acid (3-HPA)	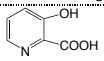	337, 353, 355	Oligonucleotides, Synthetic polymers
Nicitinic acid	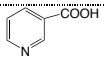	266	Proteins, peptides, adduct formation
Picolinic acid	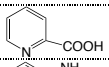	266	Oligonucleotides
3- Aminopicolinic acid	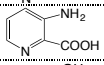	337, 355	Oligonucleotides
6-Aza-2-thiothymine	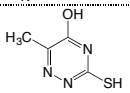	337, 353	Proteins, peptides, non-covalent complexes; near-neutral pH
2,6-Dihydroxyacetophenone		337, 353	Proteins, peptides, non-covalent complexes, Oligonucleotides
2,4,6-Trihydroxyacetophenone	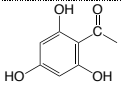	337, 353	Proteins, peptides, non-covalent complexes, Oligonucleotides
3-Aminoquinoline	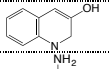	337	Oligosaccharides
1,5-Diaminonaphthalene	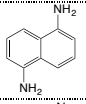	337	Lipids
Trans-3-indoleacrylic acid (IAA)	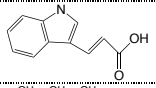	337	Synthetic polymers
Dithranol	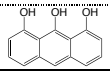	337	Synthetic polymers, Lipids, small molecules

I.1.2.3 Lasers for MALDI

The two main types of laser used in MALDI are based on infrared, IR, or ultraviolet, UV, wavelength [1], [10]. The absorption coefficient of common IR-matrices, such as glycerol, are high enough to guarantee a penetration depth of the laser beam of about 1 μm, more than 20-fold than a typical penetration achieved with an UV laser. As consequence, the mass of sample ablated for the same exposure time is 10 times higher for an IR laser than for an UV laser, being the sample consumption proportionally higher in IR-ablation as well [3].

I.1.2.4 The ionization process

The ionization process takes place after laser has ablated the surface of the matrix-analyte sample. However, it seems that the majority of the material that becomes part of the plume of molecules is present in neutral form. The ablation process itself is not well understood yet, although some interesting works have been done to this end. Such works suggest that ions are formed only within the first 300 ns after laser interaction with the material [11], [12]. However, the mechanism involved in the ion formation are even less understood that the laser ablation itself. Currently, two models are found in literature explaining the ionization process. The first model assumes two main steps for ion formation: (i) neutral analyte molecules and photoionization of the matrix molecules and (ii) charge transfer to the analyte molecules in the plume [13]. The second model assumes analytes as charges species within the matrix which becomes mostly neutralized during the ablation process due to interactions with the matrix [14].

Table I.2 Types of Ions in LDI and MALDI-MS. (Reproduced from reference [1])

Analytes	**Positive Ions**	**Negative Ions**
Non-polar	$M^{+\bullet}$	$M^{-\bullet}$
Medium polarity	$M^{+\bullet}$ and/or $[M+H]^+$, $[M+alkali]^+$, {*clusters* $[2M]^{+\bullet}$ and/or $[2M+H]^+$, $[2M+alkali]^+$, *adducts* $[M+Ma+H]^+$, $[M+Ma+alkali]^+$}[b]	$M^{-\bullet}$ and/or $[M-H]^-$, {*clusters* $[2M]^{-\bullet}$ and/or $[2M-H]^-$, *adducts* $[M+Ma]^{-\bullet}$, $[M+Ma-H]^-$}
Polar	$[M+H]^+$, $[M+alkali]^+$, *Exchange* $[M-H_n+alkali_{n+1}]^+$, *High-mass anal.* $[M+2H]^{2+}$, $[M+2alkali]^{2+}$, {*clusters* $[nM+H]^+$, $[nM+alkali]^+$, *adducts* $[M+Ma+H]^+$, $[M+Ma+alkali]^+$}	$[M-H]^-$, *Exchange* $[M-H_n+alkali_{n-1}]^-$, {*clusters* $[nM-H]^-$, *adducts* $[M+Ma-H]^-$}
Ionic[a]	C^+, $[C_n+A_{n-1}]^+$, $\{[CA]^{+\bullet}\}$	A^-, $[C_{n-1}+A_n]^-$, $\{[CA]^{-\bullet}\}$

[a] Comprising of catión C^+ and anion A^-. [b] Enclosure in parentheses denotes rarely observed species.

I.1.2.5 The Fragmentation process

The fragmentation process depends on many different variables, such as laser fluence and focus, ion extraction field strength and delay, as well as the choice of an adequate matrix [15]. Matrixes favouring high degree of fragmentation are classified as hard whilst matrixes that do not promote fragmentation are called “soft”. For instance α-cyano-4-hydroxycinnamic, the matrix of choice for peptide mass fingerprint, is one of the hardest matrices used whilst “super DHB” is one of the softest matrices, used for the measured of intact proteins [7].

Three different process account for fragmentation. First, ions absorb energy from the laser. Laser´s energy promotes collisions with the matrix molecules. Second, the electric field in the source will accelerate the ions make them crash within them and against other molecules present in the plume [7]. In addition to this processes, the plume is a very reactive medium where hydrogen and proton transfers between molecules takes place. All this factors contribute to the breaking of many molecules. Thus phosphor- or sulfo- peptides or glycolipids get dissociated before or during detection [3].

Tandem mass spectrometry is the process of selecting an ion, causing it to fragment and recording a mass spectrum of the fragments ions. Fragment ions carry information about the ion structure. One ion can be selected and isolated and then fragmented n times [1]–[3], [7], [16]. Through this method the amino acid sequence of one peptide can be elucidated.

Post-source decay (PSD) fragment ions correspond to the fragment ions formed between the ion source and reflectron in a reflectron TOF mass spectrometer [17]. Since PSD ions are unfocused or metastable, they appear as broad peaks at higher apparent mass than their focused counterparts. PSD ions can be focused by stepping the reflectron voltage and combining the resulting partial spectra. These methods were used extensively for the structural determination of carbohydrates [1]. PSD fragmentation is influenced by the matrix employed. Matrices such as 4-CHCA, classified as "hot", usually catalyze considerable fragmentation, whereas “cold” matrices such as DHB, SA, ATT or 1,3,5-THAP do not [18]–[20]. Using MALDI-PSD it is possible to obtain sequence information with the MALDI method by generating fragment ions [21]. However, the PSD

fragmentation is rather complex. The recent availability of MALDI sources for analyzers such as the Q-TOF, TOF/TOF, FT and QIT, enable far more efficient production and detection of product ions than is possible with PSD [3], [7].

I.1.2.6 Mass analysers: TOF mass spectrometer

I.1.2.6.1 Linear TOF mass spectrometer

Figure I.2 shows a typical linear TOF mass spectrometer. In this type of instruments all charged ions are first accelerated by a potential difference, between the sample support and a nearby grid. This accelerated the ions, which then travel down a field free path of variable length, generally 1m. This TOF render mass resolutions below 20 000.

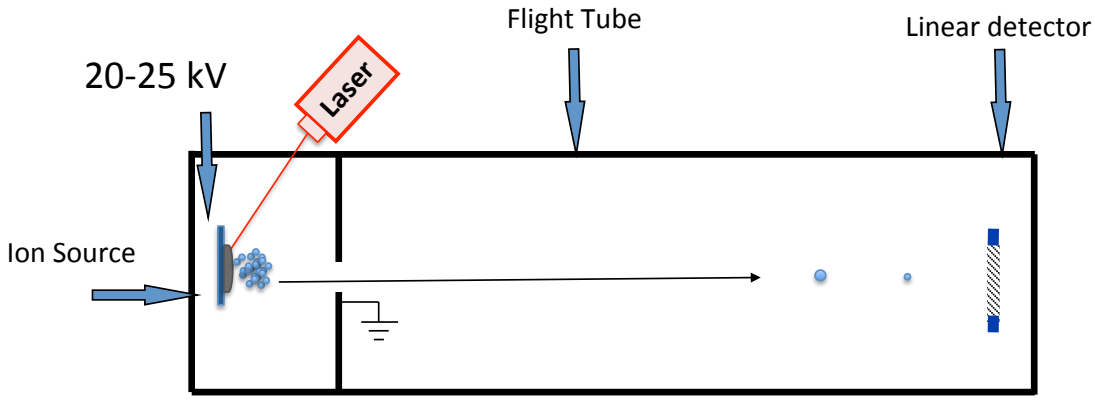

Figure I.2. Schematic representation of the linear time-of-flight mass analyser.

I.1.2.6.2 Reflectron TOF mass spectrometer

Figure I.3 shows a typical reflecton TOF Mass spectrometer. In this type of instruments the travel path distance is increased by using one reflector, also known as ion mirror, that reflects the ions from the first field free drift region to the second field free drift region. In addition, the reflector also compensates differences in ion travel energies, making the same m/z ions travel to more similar speeds. This type of TOF render mass resolutions higher than 20 000 and mass accuracy of 2-5 ppm [3].

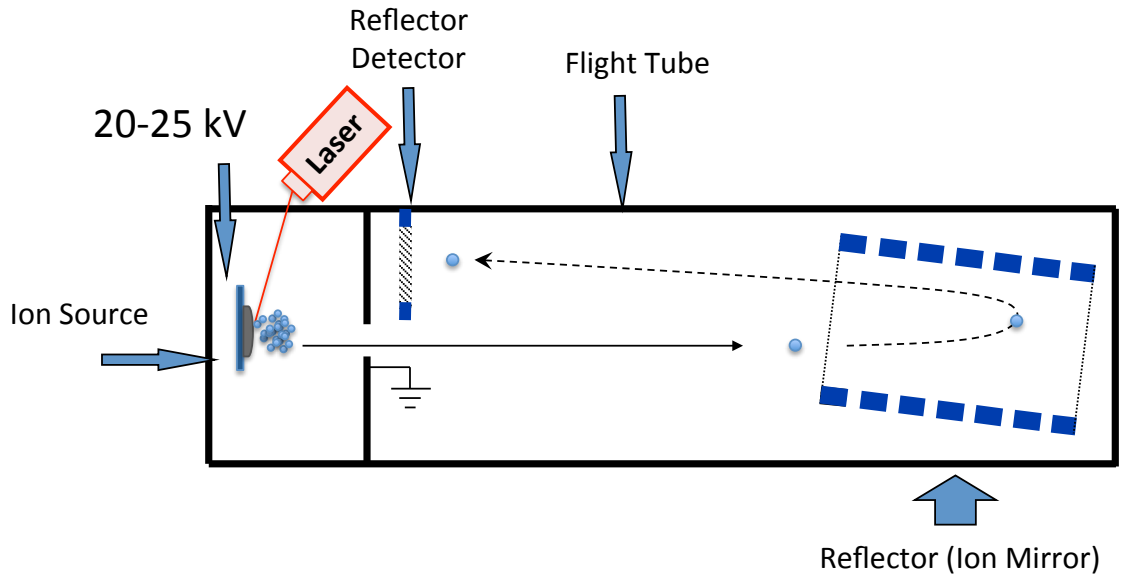

Figure I.3 Schematic representation of the reflectron time-of-flight mass analyser.

I.1.2.6.3 Tandem TOF mass spectrometer

Figure I.4 shows a typical tandem TOF mass spectrometry. Tandem procedure requires the selection of an ion, called precursor ion, fragmenting it, and the recording of the signal of all fragments in a single spectrum. This type of analysis reveals structural information. Fragmentation, for instance, allows knowing the sequence of a peptide, it allows determination of sites of deamidation, phosphorylation or sequence variation from mutation of the peptide´s parent DNA [3], [7].

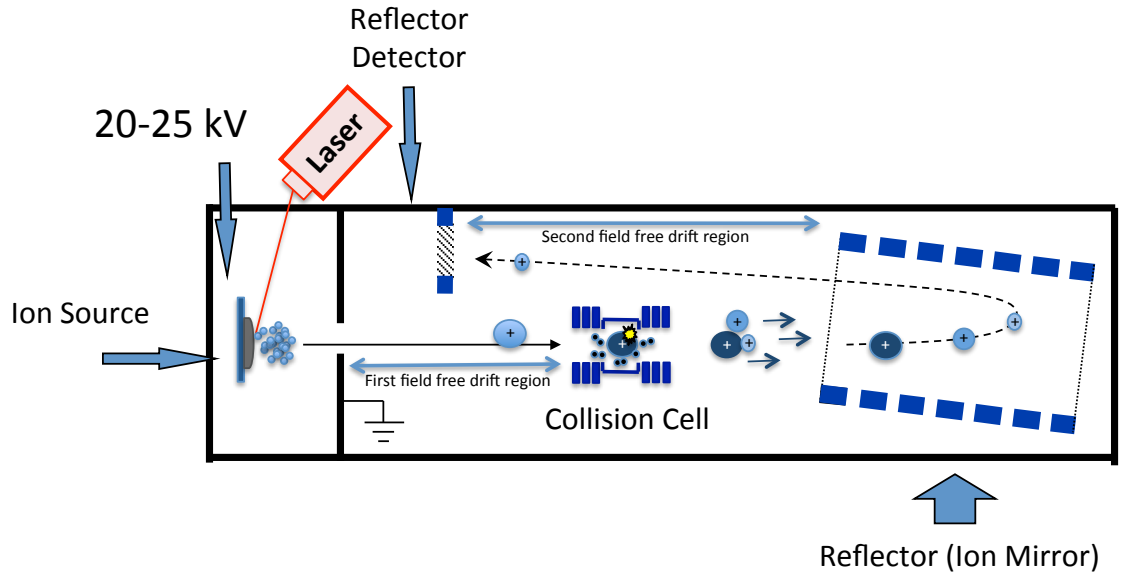

Figure I.4 Schematic representation of the tandem time-of-flight mass analyser.

I.2 MALDI-MS for proteomics

I.2.1 Basics on MALDI-MS for proteomics

MALDI-MS is a helpful tool in all type of studies involving proteins, from individual proteins to the analysis of large complex proteomes. It must be mind that proteins constitute the elemental block of the living organisms. Proteins are involved in all living processes and can be linked to diseases as well as to genetic mutations. Therefore the analysis of proteins using MALDI mass spectrometry is nowadays an important tool in many different fields of knowledge, such as biology, biomedicine or biotechnology.

Proteins can be studied using MALDI in three different ways. Intact proteins are studied using linear MALDI-TOF. Depending on the mass of the protein, the actual one may be obtained within and error of some Da. Figure I.5 shows a MALDI spectrum of a mixture of proteins. It may be noted that as the mass of the protein increases so it does the error in the mass determination.

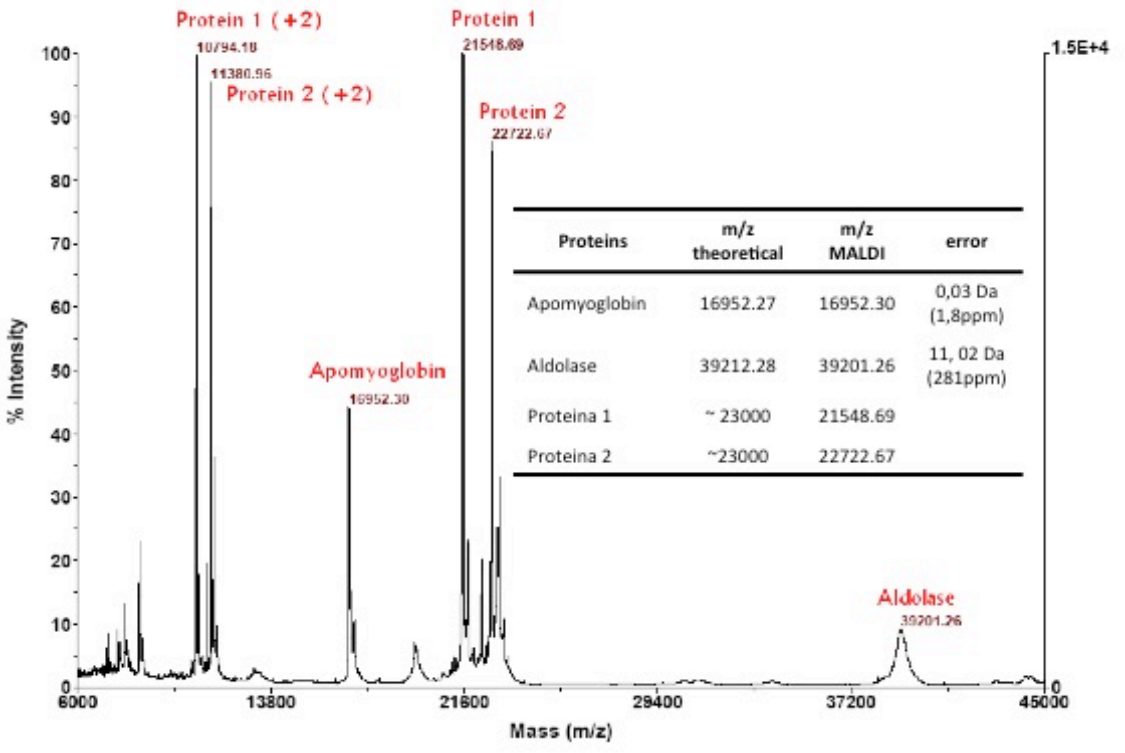

Figure I.5 MALDI spectrum of a proteins mixture.

Figure I.5 shows an example of this problem. If the mass of the protein changes from 17 kDA to 40 KDa the error vary from 0.03 Da to 11.02 Da.

The identification of a protein, and therefore its sequence, can be obtained using two different strategies. The first strategy entails the purification and isolation of the proteins by gel electrophoresis or by HPLC, and its subsequent digestion using one enzyme, generally trypsin. The digested protein is summited to MALDI-MS and one spectrum with a number of peptides is obtained. This spectrum is introduced in a searching engine (Generally MASCOT), which matches the experimental spectrum against a large database of millions of sequences of proteins "in silico" derived from genetical data. If the protein we are interested in is in the database, and the spectrum has enough quality, the protein and its sequence is retrieved. This methodology is known as peptide mass fingerprint, PMF. The second strategy uses tandem mass spectrometry over a peptide belonging to the protein, which is being identified. The peptide is sequenced by tandem mass spectrometry. The sequence of amino acids is introduced in the search engine (again, MASCOT) and then is matched against billions of sequences of peptides. Finally, the peptide is linked to one protein. This method is also called peptide fragment fingerprint, PFF or protein identification by MS/MS [3], [7], [22]–[24].

1.2.2 Peptide mass fingerprinting

The first step in peptide mass fingerprinting is the isolation and separation of proteins from complex mixtures. This is generally done using HPLC, gel electrophoresis (one dimension, 1D, or two dimensional, 2D) or a combination of both [7], [25]. Whatever the strategy used it must be ensured at this stage that there is only one protein in our sample before proceeding to the digestion step. The digestion step is addressed to obtain the peptides that constitute the protein. To obtain this set of peptides, enzymes that cleavage the proteins in a specific and reproducible manner are used. For instance, trypsin cleaves peptide chains mainly at the carboxyl side of the amino acids lysine or arginine, except when it is followed by proline. The peptide mass map produced by specific cleavage reagents or enzymes is unique for the protein and its post-translational modifications. In theory, after digestion, all peptides should be at the same concentration in the sample, and therefore the intensity of their signal should be the same in the MALDI mass spectrum. However, different mechanisms accounts for this not to happen [3], [7].

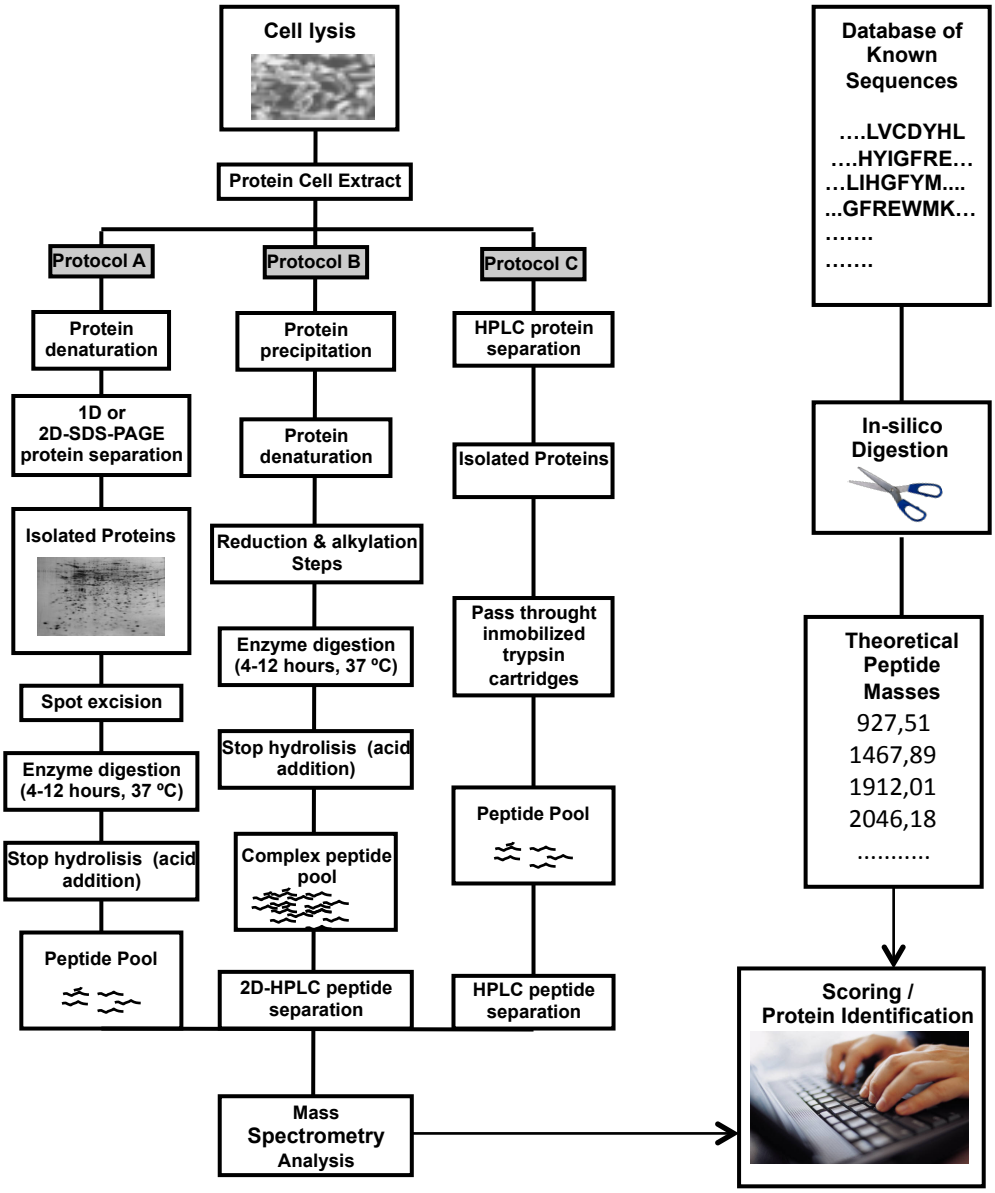

Figure I.6 Principle of protein identification by MALDI mass spectrometry-based peptide mass fingerprint. The experimentally determined MALDI-MS peptide mass map is compared to the "in-silico" (theoretical) peptide mass map of all proteins included in a biological database using computer-based search algorithms. A scoring scheme is used to retrieve the best match. Protocol A corresponds to the classical protein analysis, in which proteins are initially separated according to their isoelectric point and then according to their molecular weight. Protocol B corresponds to the typical gel-free approach, in which proteins are digested prior to any separation step and then the whole peptide pool is separated using multi-dimensional chromatography in tandem with mass spectrometry. Protocol C represents the new trends in protein digestion using immobilized trypsin. Firstly, proteins can be separated using different chromatography steps, and are then digested in-column, and, finally, the peptide pool is separated and analysed. (Adapted with permission from reference [24])

The ionization process is different for each peptide and this is reflected in the ionization efficiencies [7], which may vary over several orders of magnitude. For this reason, some peptides can be not detected in the spectrum [3]. The causes for those differences in the ionization efficiency are not well understood yet and they need to be elucidated. As an example, arginine containing peptides ionize very well as compared with peptides with a lack in arginine [7], [26]. This is the reason why an in-deep analysis by MALDI-MS of a mixture of peptides requires a previous separation using HPLC or Gel electrophoresis.

Table I.3 Computational services and tools for protein mass spectrometry. (Adapted from reference [3])

Name	Website	Purpose	References
ExPASy	www.expasy.org	Resource/software for protein sequence and mass analysis	Public
EBI	www.ebi.ac.uk	Biological databases and query tools	Public
NCBI	www.ncbi.nlm.nih.gov	Biological databases and query tools	Public
GPMAW	www.gpmaw.com	Protein sequence and mass analysis	Commercial
Mascot	www.matrixscience.com	Computational tool for protein identification by MS and MS/MS data. For links to more search engines, see ExPASy	Public/Commercial
X! Tandem	www.thegpm.org/TANDEM/	Computational tool for protein identification by MS/MS data	Public/Commercial
Phenyx	www.ionsource.com/functional_reviews/Phenyx/phenyx-web.htm	Computational tool for protein identification by MS/MS data, quantitation	Commercial
MSQuant	msquant.sourceforge.net	Tool for protein quantitation	Freeware
Protein-Prospector	Prospector.ucsf.edu/	Various tools for protein analysis and identification by MS and MS/MS data	Public
ProteinCenter	www.proxeon.com	Computational tool for analysis of large proteomic data sets	Commercial
NetPhos	Cbs.dtu.dk/services/NetPhos	Predictions for phosphorylation sites. For links to other predictors, see ExPASy	public

Protein identification using data retrieved from mass spectrometry in combination with protein sequence database searching was first proposed by a number of research groups [26]–[30]. Different methods of work are found to this end, which are summarized in Figure I.6. As stated above, the main aim of any PMF-based method consists in to obtain an experimental list of peptide masses belonging to the same protein. This list is compared with all the ones presented in a database. The protein whose theoretical, also known as in-silico, list of peptide masses best matched the experimental one is retrieved as the protein identified by the searching engine. A list of computational services and tools for protein mass spectrometry is presented in Table I.3.

I.2.2.1 Sample Treatment for protein identification through PMF

Proteins are cleavage on their constituents peptides by enzymatic digestion or chemical cleavage with acids [24], [31], [32]. The type of enzyme selected, or the type and concentration of acid depends on the protein and on the type of analysis to be done. For instance, the sample treatment to study phosphorylation is different from the sample treatment used to study glycosylation. The enzymes used to digest proteins for protein identification belongs to the family of proteases and comprises the following groups [32]: serine; aspartic; cysteine; or metalloproteases. Each enzyme cleaves the proteins at specific sites in a reproducible manner. As a general role for proteins identification the serine enzyme trypsin is used. This enzyme cleavages the protein at each arginine and lysine residue, each 10-12 aminoacids approximately, leading to the production of peptides with masses comprised between 800 to 2000 Da, which are very appropriated for mass spectrometry analysis [24]. Such peptides can be further fragmented in the mass spectrometer using different approaches, being the most frequent the named collision-induced dissociation, CID. This fragmentation allows the sequencing of peptides in a reproducible and fashion manner, allowing the identification of proteins trough the sequencing of peptides [7]. The variables affecting the protein cleavage performance are enzyme concentration, temperature and pH.

The sample treatment pipelines used for mass spectrometry-based protein identification are depicted in Figure I.6. Complex proteomes can be interrogated using protein separation and isolation by gel electrophoresis in the first and in the second dimension. The spots containing the protein(s) are submitted to the process named in-gel

protein digestion [33]. Other possibility entails the direct cleave of all the proteins present in a complex proteome by adding the enzyme to the sample. Thus, a highly complex solution of peptides is obtained which is subsequently separated by multi-dimensional chromatography [34]. Finally, the digestion of a protein or a complex proteome can be done in an automated mode using chromatography [25], [35], [36]. Table I.4 shows the advantages and drawbacks of the aforementioned approaches.

Table I.4 Analytical parameters for enzymatic protein digestion. (Reproduced with permission from reference [24].

Variable	**In gel digestion**	**In-solution digestion**	**In column digestion**
Treatment time	up to 12 h	up to 12 h	up to 10 min.
Handling	high	medium	low
Sample throughput	low	medium	high
On-line application	no	yes	yes
Protein digestion yield	low	medium	high
Robustness	low	high	medium
Protein/enzyme ratio	low	very low	medium
Cost	low	low	medium

I.2.3 Classic protocols

I.2.3.1 In-gel protein digestion

This methodology is time consuming, it requires operator skills and in handling intensive. However, it is not expensive if compared with the HPLC-based methods. The major advantages are its cost-effectiveness and that protein post-translational modifications can be seen at a glance. Figure I.7 shows how complicated the pipeline is for a Gel-based method. First proteins need to be purified and prepared to be separated using the gel [37]. Further preparation it requires protein concentration as well as the elimination of interfering substances with the electrophoretic separation. As an example, proteins can be precipitated using a mixture of trichloroacetic acid (TCA) / acetone [38].

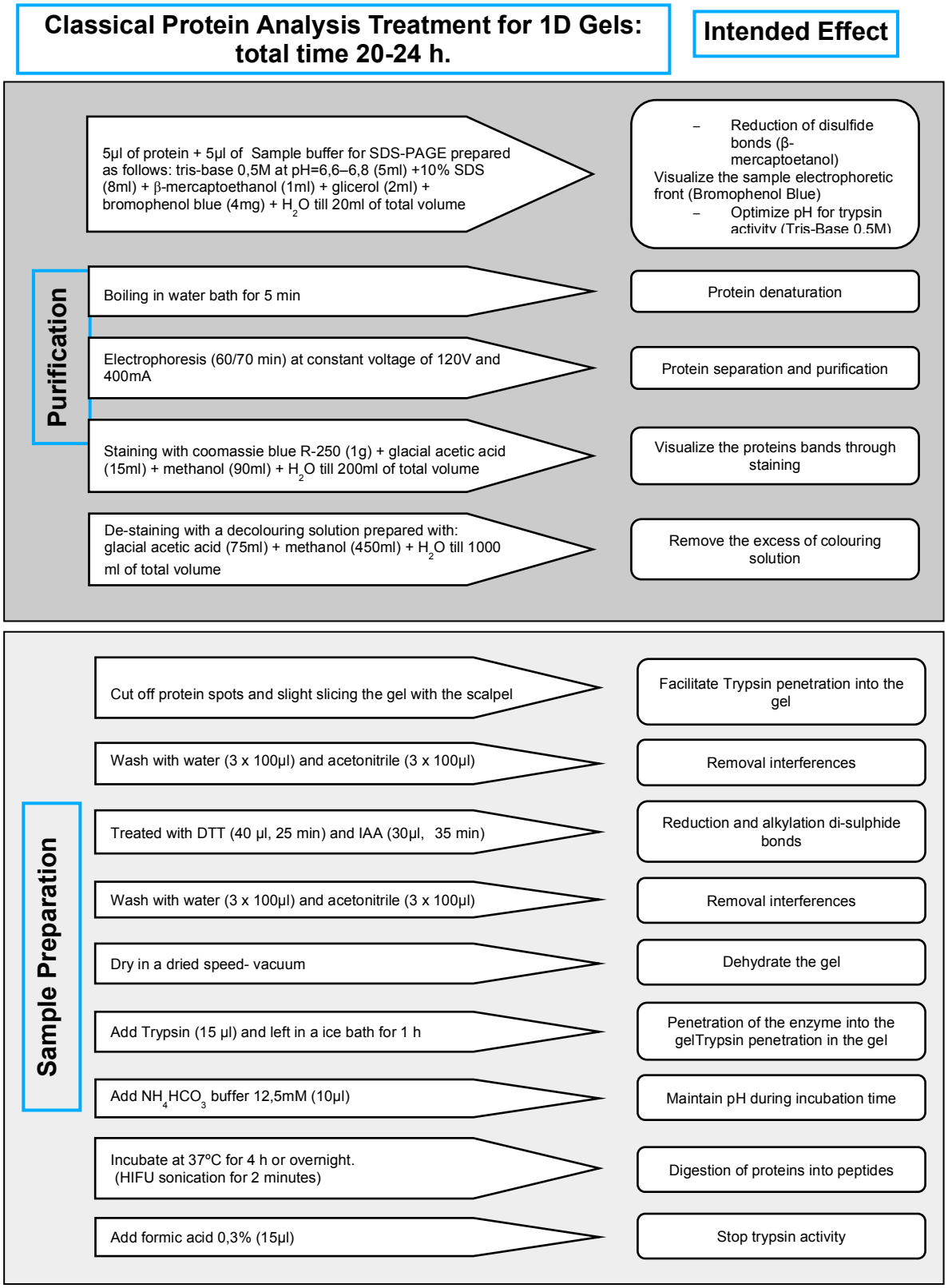

Figure I.7 Detailed description of an in-gel protein digestion protocol. (Figure reproduced with permission from reference [24])

Proteins are denatured and solubilized in urea/thiourea solutions at concentrations up to 9 M [39]. This helps to obtain a subsequent in-gel efficient separation of proteins. In a typical 2D gel electrophoresis experiment the proteins are first separated as a function of their isoelectric points, pI, (first dimension). After the completion of the first dimension, and in order to avoid further re-oxidation, it becomes necessary to reduce cystine residues using dithiothreitol (DTT). The resulting cysteines are then obstructed with iodoacetamide (IAA). Afterwards, proteins are then separated following their size (second dimension). [40]. Once the proteins have been separated, they need to be visualized. This is done using Coomassie Blue, fluorescent dyes, or with MS-compatible silver nitrate [41]. An example of a typical electrophoretic separation is given in Figure I.6, protocol A, where a gel corresponding to the second dimension is presented. Each dark spot corresponds to one or to some proteins, that can be extracted intact using (i) passive elution [42], (ii) electro elution [43], or (iii) the ultrasonic-assisted elution [44]. After elution, proteins are digested in solution, then analysed by PMF and finally, identified.

Protein elution from gels is troublesome, however, a faster and easiest approach is done where the protein is digested in the own gel, then the peptides are eluted from the gel into a solution, sometimes with the aid of ultrasonication. As a result, solid protocols have been developed for in-gel digestion [45], [46]. Furthermore, automated protein digestion is available in a large number of proteomic facilities.

Whatever the method of choice, the procedure is always the same. First, the bands (1D) or the spots (2D) are cut from the gel and then the staining chemicals are removed. For this, there are some specific protocols depending on the type of staining [47]. Then, an adequate amount of enzyme is introduced in the solution and the enzyme is allowed to reach the protein trapped in the gel, sometimes with the aid of microwave energy or ultrasonic energy. For this purpose, it is fundamental that the solvent composition inside the gel be rigorously controlled. Therefore, gel slides must firstly be dehydrated using acetonitrile and finally dried in a speed vacuum [36], [48], [49].

The pH and temperature are also controlled during all the procedure to ensure enzyme activity. Digestion is done in a couple of hours or during overnight incubation at 30 ºC or 37 ºC [24]. Lastly, the supernatant which contains the peptides is acidified in order to stop the digestion process and then submitted to MS analysis for protein identifications by PMF. A MALDI-TOF instrument is normally used in this process [50],

[51]. The in-gel digestion protocol presents, however, various disadvantages, as (i) inaccessibility of some peptide bonds to the enzyme as a result of the process of trapping protein substrates in the gel, and (ii) inability of some peptides produced during the digestion to be diffused freely from the gel. The aforementioned disadvantages clarify different results between in-gel and in- solution digestion methods [36].

I.2.3.2 In-solution protein digestion

In-solution protein digestion of complex proteomes and subsequent protein identification (shotgun proteomics), developed by Link et al. [34], is currently the most popular and powerful method to identify proteins in large scale. It is very simple: the whole proteome under study is cleavage at once. This produces a solution containing hundreds of thousands of peptides. Some precautions must be taken into consideration, namely (i) that the more abundant proteins are normally easier to identify; (ii) that some fractionation is needed in order to get the identification of less abundant proteins easier; and, (iii) that variation in the yield of digestion observed from sample to sample might happen due to the quantity and number of proteins, heterogeneity in the matrix, and its physical and chemical properties [7].

The in-solution procedure requires, first, the precipitation of the proteins with cold acetone or TCA, to separate them from other components, such as nucleic acid contaminants, lipids and salts from biological samples. Then, it is necessary to re-suspend the proteins again. To this end ammonium bicarbonate buffer supplemented with 8 M urea or another chaotropic agent (e.g., guanidine hydrochloride) is used. This solution helps to solubilise the proteins. Then, the disulphide bonds are reduced and alkylated with DTT and IAA respectively to avoid protein refolding [49]. Digestion is generally done with trypsin and because this enzyme is inactive if urea concentration is higher than 2 M, the solutions containing the 8-9 M urea must be diluted [45]. However, the enzyme Lysine-C is active at a concentration of 8 M and can be used to digest the protein [52], [53]. Protein digestion is usually performed overnight (12-24 hours), or it is speeded using microwave energy or ultrasonic energy [49], [54]. The cleavage is then stopped by adding an acid, to lower the solution´s pH to 2–3. Finally, the complex mixture of peptides is

separeted and desalted using Multi dimensional liquid chromatography and then analyzed by MS.

In-solution digestion has the advantage of being suitable for on-line applications and the sample treatment is easier than the in-gel approach stated earlier. Yet, there are still some disadvantages, such as time-consuming enzymatic digestion and the background noise in MS analysis introduced by enzyme autolysis products [24], [55].

A special mention is needed for membrane proteins, with low solubility in water. Cyanogen bromide, methanol or the use of acid labile surfactants are generally used to handle membrane proteins successfully [56], [57], [58]. Then, the complex mixture of peptides produced by the in-solution digestion procedure is separated using multi-dimensional chromatography coupled to tandem mass spectrometry [1], [7]. Proteins are then identified by the fragmentation spectra (amino acid sequence) of the peptides. This procedure is known as peptide fragment fingerprinting (PFF) [59].

1.2.3.3 In-column protein digestion

Several drawbacks can be pointed for the in-solution and in-gel digestion methods. First, long digestion time, typically overnight, is required. Second, the trypsin undergoes autolysis, what makes the solution reach in peptides of this enzyme, which may affect the analysis [7]. Third, if the protein concentration is low, in the micromolar range, low digestion yields are obtained. Fourth, they are time consuming and handling intensive and fifth, peptide losses by adsorption can occur [24].

To overcome these problems, columns filled with immobilized trypsin can be used to digest the samples on-line. Using this procedure lower digestion times, increased digestion ratios as well as the reduction of enzyme autolysis products are obtained. In addition, the columns can be incorporated in HPLC-based pipelines [60], as it is shown in Fig. I.8. This system shows the coupling of three HPLC pumps, two digestion columns, two separation columns and three injection valves [24].

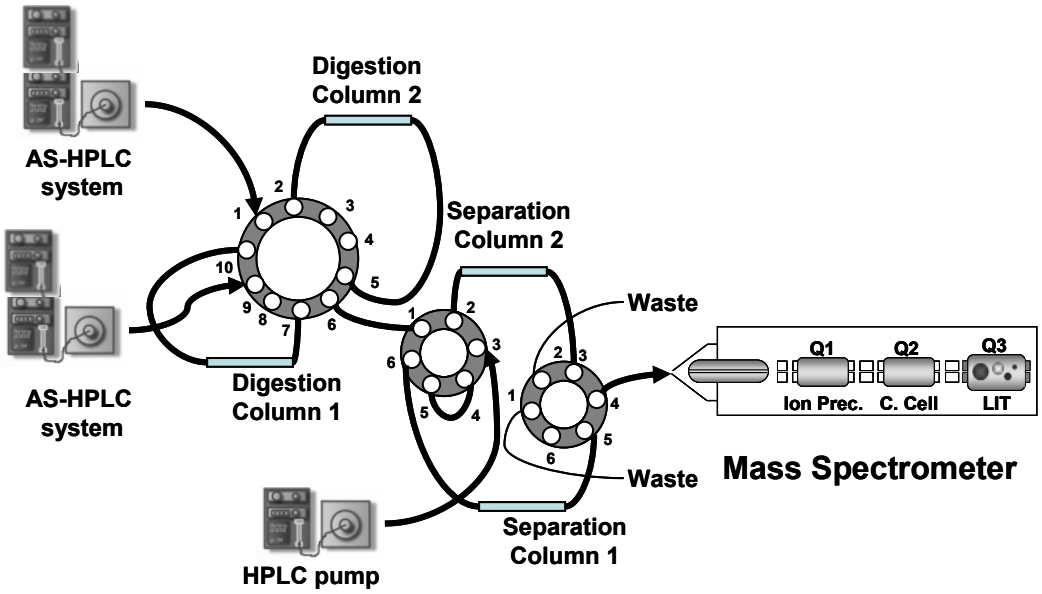

Figure I.8 An on-line protein digestion system. comprising three HPLC pumps (two gradient and one isocratic), three switching valves, and four columns (two used for protein digestion and two other for peptide separation). The whole system is connected on line to a mass spectrometer. To increase throughput of the analysis, each gradient HPLC pump is connected to one digestion column and one separation column through switching valves. These are synchronized to separate (separation-column 1) the digested peptides coming from digestion-column A using one of the gradient HPLC systems. In the meantime, the second gradient system delivers a protein mixture to digestion-column B, while separation-column 2 is being conditioned with the solvent delivered by the isocratic pump. (Figure reproduced with permission from reference [24])

I.2.4 Accelerated protocols

Modern approaches to boost or to enhance the performance of proteomics pipelines are currently consisted on the following approaches: (i) heating, (ii) microspin columns, (iii) ultrasonic energy, (iv) high pressure, (v) infrared energy, (vi) microwave energy, (vii) alternating electrical fields, and (viii) microreactors, are some examples of new methodologies developed to accelerate protein digestion. For a detailed description of those approaches the revision done by Capelo, et al., is recommend [49]. Below a detailed description of the application of ultrasonic energy to proteomics pipelines is provided.

1.2.4.1 Basics on Ultrasonics

The ultrasonic frequency range is normally divided into two principal zones, see Figure I.9, depending on the effects instigated by the ultrasonic wave on the liquid media during it's passage through it.

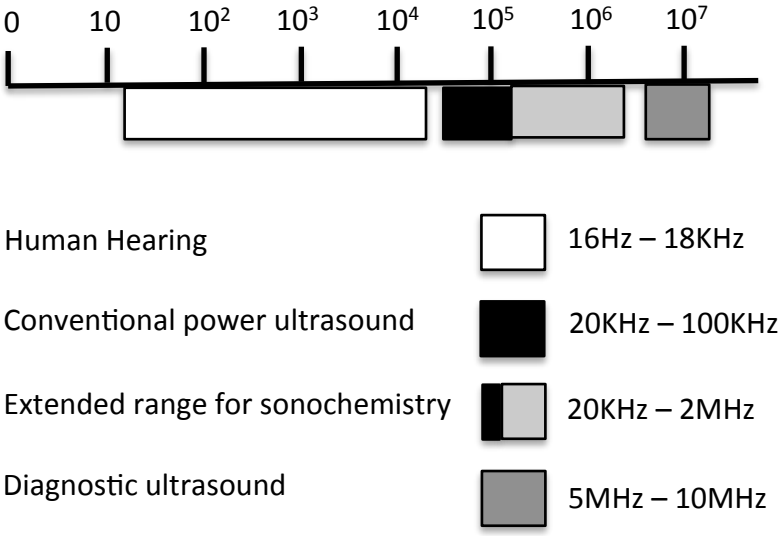

Figure I.9 Sound frequency ranges. (from Mason et al. [61])

High frequency ultrasound, with values comprised between 2Mhz and 10Mhz, or medical ultrasound, another designation for which is known, is largely used for medical purposes due to the immutability of the liquid media chemical and physical properties where the ultrasound is applied.

Low frequency ultrasound, is comprised within a range from 20Khz to 100Khz, and promotes several physical and chemical changes in the liquid media where they are used [62]. Low frequency ultrasound promotes in the liquid media a phenomenon known as cavitation (figure I.10).

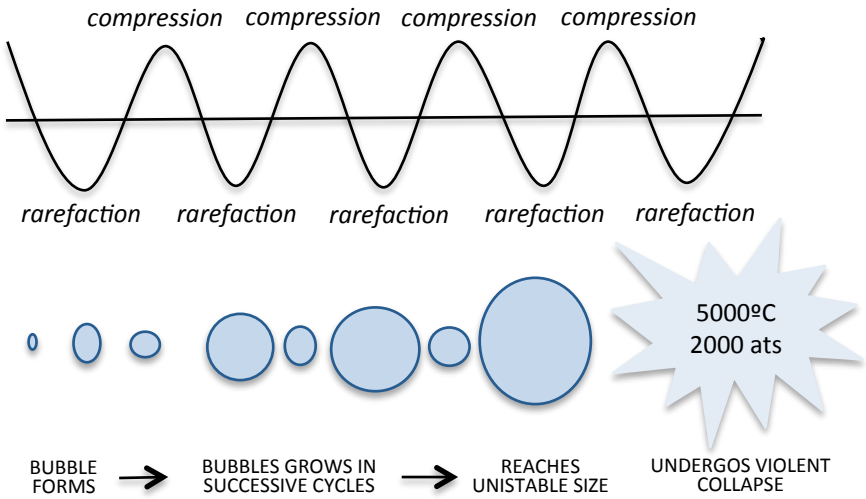

Figure I.10 Development and collapse of cavitation bubbles. (from Mason et al. [61])

Cavitation happens when waves cross the liquid with such a speed that liquid molecules can't follow the cycles of compression and decompression of the wavelength with the same speediness [54]. At some point the creation of cavities happens because the forces that keep liquid molecules together are broken. These formed cavities are named as cavitation bubbles. As more energy is supplied to the cavities in the form of ultrasound waves, the cavitation bubbles grow in size through the process called rectified diffusion [63]. Stable cavitation is defined by successive cycles of compression and decompression, as the wavelength passes through the liquid media. Yet, cavitation bubble never implodes [54]. Transient cavitation is defined by the impetuous collapse of the bubble, after it grow until reaching a maximum. In this implosion, temperatures and pressures of about 5000 $^{\circ}$C and 1000 atm, are reached respectively as indicated by the Hot-Spot theory [63]–[65]. The erosion and disruption of solid surfaces caused by the formation of micro-jets liquids during the implosion at c.a. 400 Km h^{-1} as well as the increase of mass transfer processes in heterogeneous systems constitute additional effects (see Fig. I.11). The formation of highly reactive radical species that can be used to enhance chemical reactions has been also described.

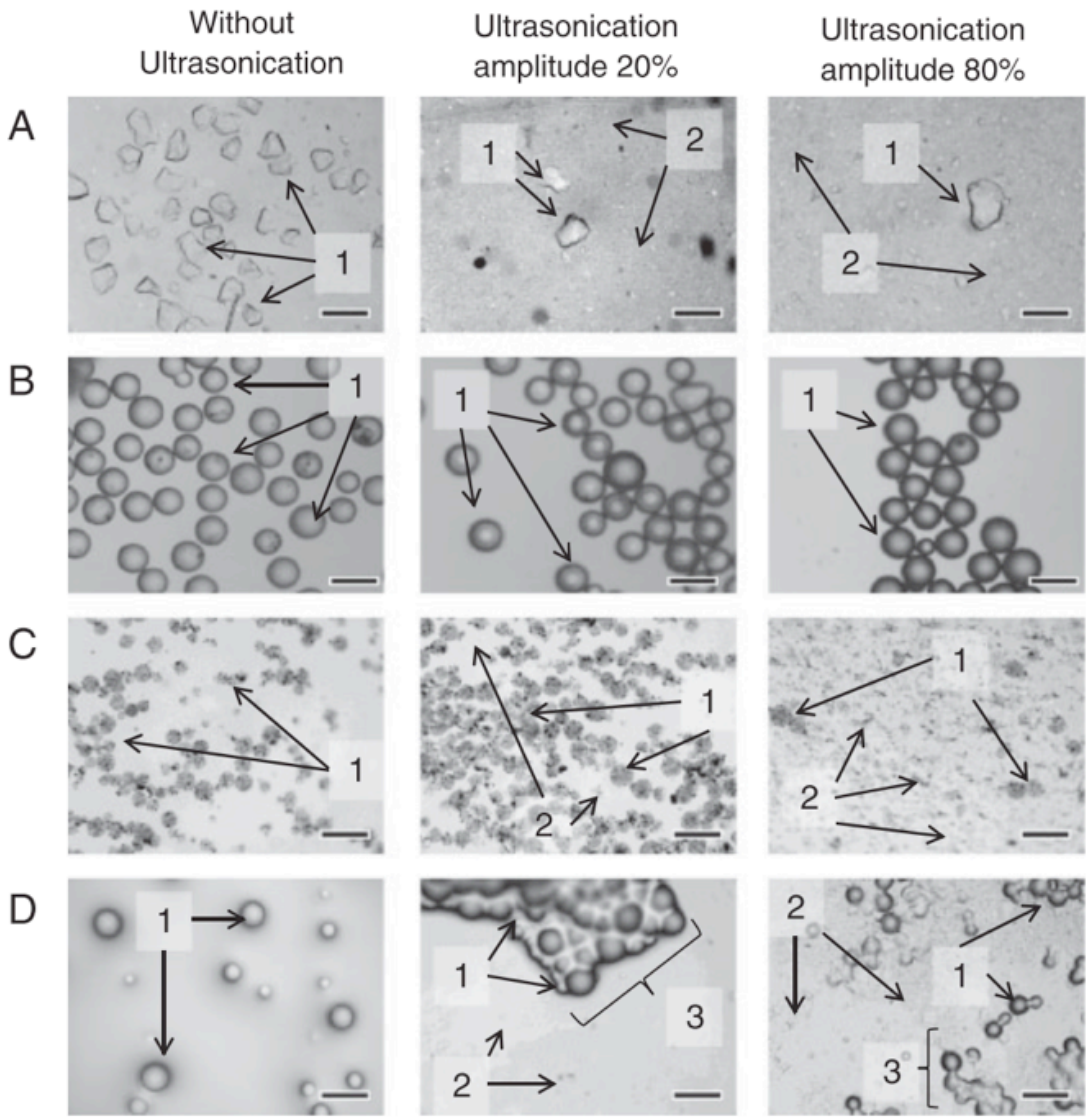

Figure I.11 Disruption effect of ultrasound in solid material. Different beads (200mg) were suspended in 1mL of Milli-Q water and ultrasonicated for 2min with an ultrasonic probe at different ultrasonic amplitudes. The microscopic pictures were taken with a magnification of 100 × and the scale corresponds to 200 mm. (A) silica particles; (B) glass particles; (C) magnetic particles; (D) sepharose particles; 1, intact particles; 2, disrupted particles; 3, aggregated particles. (Figure reproduced with permission from reference [66])

The right application of the ultrasonic energy is dependent of several variables, as listed in Figure I.12 [67]. Succinctly, the following can be pointed: ultrasound frequency, UF, ultrasound intensity, UI, ultrasound amplitude, UA, time of application, temperature, external pressure, type of liquid media, and type of gas present in the liquid media. These variables and the effects they cause, have been, to some extent, discussed in previous

publications from the Bioscope Group, concerning the ultrasonic-based sample treatment [16], [48], [66]–[82]. Nevertheless, it will be concisely exposed below.

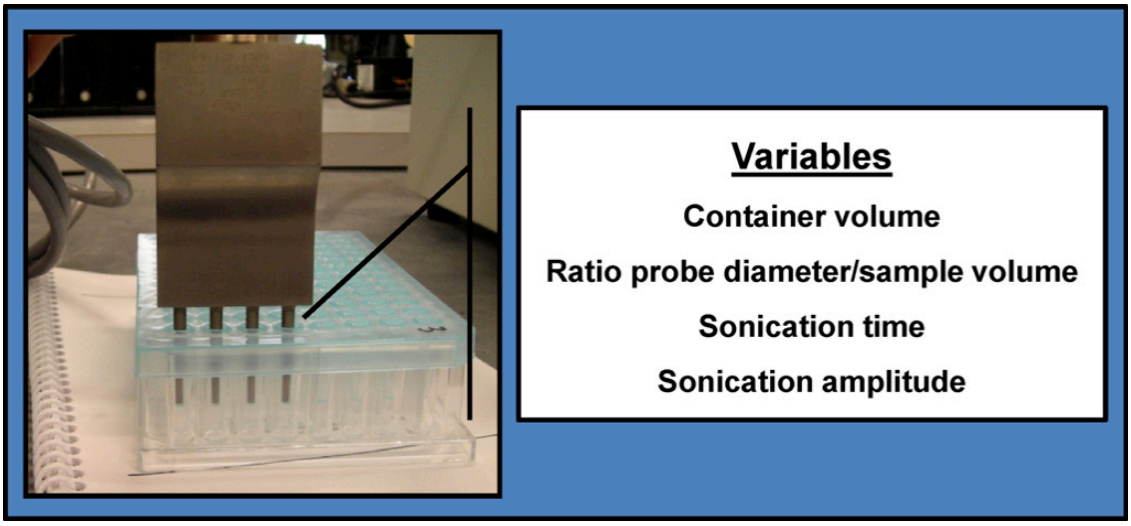

Figure I.12 This figure shows the new ultrasonic multiprobe coupled to the 96-well plate. (Figure reproduced with permission from reference [67])

Ordinary ultrasonic devices delivers a significant range of electrical energy, which is mentioned as the "power" of the ultrasonicator. It´s common to find ultrasonic apparatus classified according to the watts they deliver. The electrical energy is converted into mechanical (vibration) energy. This can be understood as a motion walking through the ultrasonic tip, inducing it to move up and down. The distance of the movement of vibration is called its amplitude. Depending on the power delivered by the ultrasonicator, there is the possibility to control vibration amplitude up to a maximum. Ultrasonic´s amplitude and intensity own a direct connection. As the intensity of an ultrasonic wave is proportional to the square of its amplitude, the highest is the amplitude the bigger will be the intensity [54].

For the same kind of sample, low amplitude and intensity will be achieved, if the output power is adjusted to low values. The effectiveness achieved with the ultrasonicator is directly proportional to amplitude and intensity. Therefore, the lower amplitude and intensity the lower effectiveness reached with the ultrasonicator. This is also valid for the opposite.

Current proteomics workflows using ultrasonic energy as a tool in sample treatment relay in short times of exposure, normally under 2 minutes time, and in the use of high intensity devices characterized for their capability of delivering frequencies

among 20KHz and 40KHz values. Ultrasound amplitudes are normally settled to 50%.The devices presently more used to deliver ultrasonic energy in proteomics are the ultrasonic probe (or multiprobe), the cup-horn and the sonoreactor. Modern ultrasonic devices can be used in the "pulse" mode. In this working mode, the amplifier switches the power on and off repeatedly, avoiding excessive warming of the bulk sample. External cooling can also be applied [16], [54], [68], [70].

The use of ultrasonic energy in proteomics, under atmospheric pressure, has been always done with success. Thus, this is a variable (external pressure) that should not be considered. With respect to liquid media, ultrasound has been applied with very good results to a large diversity of water or mixed organic-water solutions for both in-gel or in-solutions based approaches [16], [83], [82], [74], [81]. Due to the volatile nature of the organic solvents in the reaction mixture the possible changes in the reaction volume should be mind. Added gas in a reaction mixture will act as nucleation sites for the cavitation spots and thus will enhance the cavitation [16]. In the case of pressure, this particular variable appears to be of no importance, since the applications carried out so far have been successfully done with no need to add gas into the solutions.

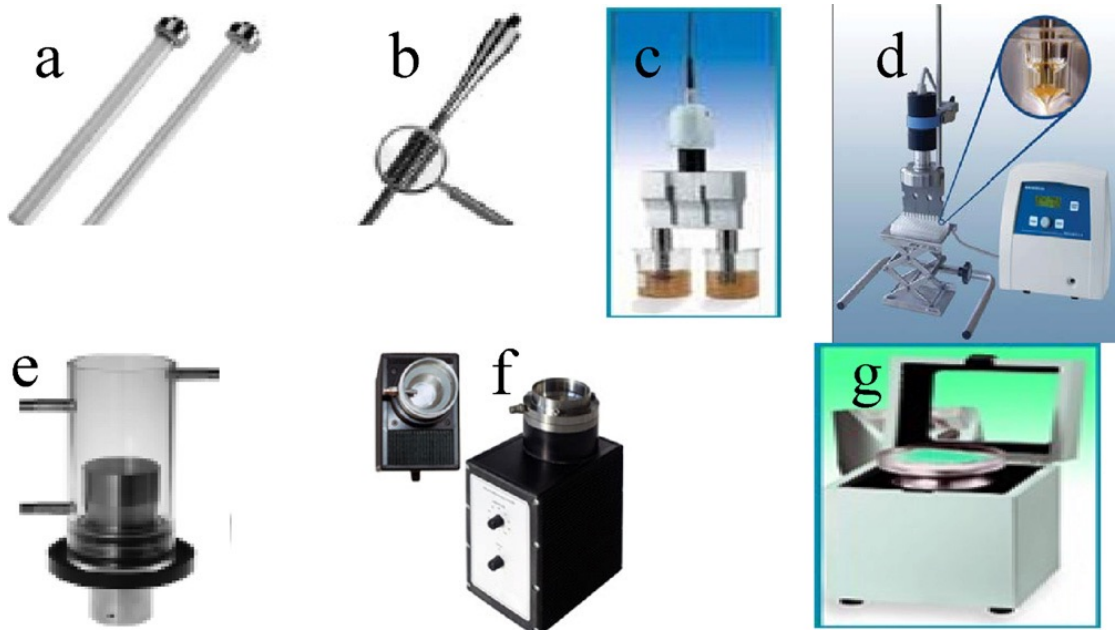

Figure I.13 Advances on ultrasonic probe technology: (a) silica glass probe; (b) spiral probe; (c) dual probe; (d) multi probe; (e) cup horns; (f) sonoreactor; (g) microplate horns. (a–d) are reproduced with permission of BandelinCompany; (e) and (g) are reproduced with permission of MisonixCompany; (e) is reproduced with permission of dr. Hielscher Company. (Figure reproduced with permission from reference [70])

Ultrasonic energy (UE) is frequently applied in proteomics in two diverse forms, in the following way: Direct ultrasonication (ultrasonic probe) is a term, which refers to the use of ultrasonic probes. Whenever this system is employed, a titanium tip is submerged into the sample. Indirect ultrasonication is a term referred to any system in which the sample is reached by the ultrasound though the walls of the sample container [70]. Modern ultrasonic devices are shown in Figure I.13.

Currently, indirect ultrasonication (cup-horns, sonoreactor) offers a number of advantages over the use of direct ultrasonication, as it follows. As no tip is inserted into the sample when indirect ultrasonication is applied, the risk of cross-contamination between samples is avoided. Also, samples can be treated in closed containers, which allow the treatment and safe handling of dangerous samples. Furthermore, some devices allow treating a considerable number of samples at once, thus opening high sample throughput for clinical purposes. Moreover, sample cooling is easily done.

1.2.4.2 The use of Ultrasonic energy in Proteomics

Ultrasonic energy is currently used to speed proteomics workflows addressed to identify proteins. Such workflows are mainly based on two different pipelines. The first one is gel-based, where proteins in complex mixtures are separated using gel electrophoresis in the first or in the second dimension. In this pipeline ultrasonication is used (i) to speed gel washing, (ii) to speed protein reduction and alkylation and (iii) to speed protein digestion. On the overall, the total time is reduced from 24 h to 4 minutes per sample, if a cup horn is used, where 6 samples can be treated at once. The second pipeline entails the use of in-solution approaches, this is, the proteins will be digested first, and then peptides are separated using off-gel based approaches, generally HPLC. For this case, (i) protein reduction, (ii) protein alkylation and (iii) protein digestion can be done also under the effects of an ultrasonic field, being time needed to handle a sample reduced from 12 h to merely 4 minutes [16], [70].

The use of ultrasound application in rapid sample treatment for protein identification will be further explored in chapter VI.

I.3 MALDI-MS for Polymer Characterization

I.3.1 Basics on polymer characterization using MALDI-MS

Characterize the chemical structure of a polymer is important because it can be directly linked to its function. A simple modification in the chemical structure of a polymer can have a deep impact in its macromolecular characteristics such as chemical reactivity, solubility and miscibility. Over the years, mass spectrometry, MS, has become a powerful tool in polymer characterization [1], [84], [85]. MS is used to detect and to identify minor polymer components or impurities, it helps to investigate by products of polymerization reactions and it can provide information to determine the average molecular mass and the molecular mass distribution of a polymer.

The following features can be considered the major advantages of polymer analysis by MALDI [3], [10], [86], [75]:

(i) Absolute molecular weights of narrowly distributed polymers (polydispersity< 1.2) can be determined as opposed to relative molecular weights obtained by chromatographic techniques.

(ii) The MALDI analysis of polymers does not require the use of polymer standards to assign molecular weights to oligomers.

(iii) Using submilligram amounts of sample material, the actual analysis can be accomplished in few minutes.

(iv) In addition, MALDI can determine the molecular weight independently of the polymer structure.

Because of these attributes, in many labs, MALDI MS has become a routine tool for polymer characterization.

As a general role, in MALDI-based polymer analysis, the sample (a polymer) is mixed with an adequate matrix and with a cationization reagent. The mixture is deposited in the MALDI target and then is analysed. The individual oligomer is ionized during the MALDI process by the attachment of a cation (cationization) which, in most cases, takes place in the gas phase [86], [75].

Polymer characteristics that can readily be determined by MALDI include the following [75]:

- The number-average molecular weight, **M**n. Which provides an average weight of a given polymer;
- The weight-average molecular weight, **M**w. Is another form to give the molecular weight of a polymer and is calculated as the arithmetic mean or average on the molecular weights of a certain number of molecules;
- The mass of repeat units;
- The polydispersity, PDI, which is the ratio **M**w to **M**n;
- The end-group mass structure.

Polymer distributions are typically characterized by **M**n and **M**w. The equations used for molecular mass determination and polydispersity calculation are [1]:

$$\boldsymbol{M}_n = \frac{\Sigma M_i I_i}{\Sigma I_i}$$

$$\boldsymbol{M}_w = \frac{\Sigma M_i^2 I_i}{\Sigma M_i I_i}$$

$$PDI = \frac{\boldsymbol{M}_w}{\boldsymbol{M}_n}$$

Where $\boldsymbol{M}_i$ and $\boldsymbol{I}_i$ represent the molecular weights of the oligomeric components and their signal intensities, respectively. It is assumed a linear relationship between number of ions and signal intensity [1], [3], [75].

Sample preparation is a key issue to obtain reliable results and this subject is discussed below.

I.4.2 Sample Treatment for polymer characterization using MALDI-MS

The type of polymer to be studied dictates the type of matrix, the cationization reagent and the solvents to be chosen to perform MALDI-MS-based studies. In fact the knowledge accumulated during the last decades has been developed in an empiric way, following the strategy of trial-and-error. This is because there is no universal matrix to be used for MALDI analysis of polymers. For an unknown polymer this strategy begins with a screening process, where some known matrices are checked for its MALDI suitability with the targeted polymer. The matrix or matrices for which the best results are obtained are then selected for further studies. From one matrix to another, variables such as sensitivity, mass working range and oligomer resolution can vary dramatically. The reasons for these differences remain unclear. For instance, over the same polymer, the matrix DHB required twice the laser power used for matrixes HABA and IAA, Furthermore, the shot-to-shot reproducibility, sensitivity and resolution was poorer using DHB [1], [84]–[86].

In addition to these problems, the ionization of polymers requires the presence of a cationization reagent. To this end, Na^+, K^+, and Ag^+ are generally the cations screened in first place. The use of one cation or another influences, for instance, the mass range of analysis and the uniformity of detection from oligomer to oligomer [84], [85].

Another problem to consider when dealing with polymer characterization by MALDI is the solvent or solvents used to prepare the samples and the matrix [87]. The solvent greatly influences the size and shape of the crystals formed as well as crystal density. In addition, the solvent selected also determines the incorporation and distribution of the polymer in the crystal. As consequence, the reproducibility, the detection sensitivity and relative intensities of components of a mixture greatly depend upon the solvent used. Besides the aforementioned issue, problems dealing with the polymer and matrix compatibility with the solvent must be taken into consideration. Very often the solvent that dissolves the polymer cannot dissolve the matrix and vice versa. Whenever possible, a single solvent should be used, but if it is necessary to use one mixture, then both solvents must be compatible. For this reason care in the selection of the solvents is recommend when a new polymer is going to be analysed. It is rather obvious that a complete mixing of the polymer with the matrix is a key issue, especially if, as mentioned above, problems related to solubility are found during the experimental. To

this end, the effects of ultrasonic-based mixing of matrices and polymers to form more homogeneous mixtures has not been systematically studied for sample preparation of polymers for MALDI characterization yet [88]–[90].

The chapter III is devoted to assess the effects of ultrasonication in sample treatment for polymer characterization. Thus, the mixing of different matrices to form more homogeneous samples, has not been systematically studied in literature for sample preparation of polymers for MALDI characterization yet, despite of the advantages of high throughput and simplicity allowed by ultrasonication. To overcome this drawback, an ultrasonic bath with dual frequency, a sonoreactor, and an ultrasonic probe, were used to study the influence of the following ultrasonic parameters in the sample treatment of polymers:(i) frequency of sonication, (ii) amplitude of sonication and (iii) time of sonication on the Mn and Mw values obtained using MALDI analysis. Vortex mixing was used for comparative purposes and it was considered the reference procedure for polymer/matrix homogenization. Poly(styrene) (PS) and poly(ethylene glycol) (PEG) polymers were used as target analytes.

I.4 MALDI-MS for small molecules

I.4.1 Introduction

MALDI technology was originally developed with the main aim to investigate on molecules of high molecular mass. Such molecules, as proteins, used to fragment when they were analysed by electrospray-based mass spectrometry, ESI-MS. However, MALDI offers the advantage of tolerance for contamination and buffers, spectra of easy interpretation, as most ions are singly charged ions and rapid analysis compared to ESI-MS [7]. Such advantages have led to a slow but constant development of MALDI applications in the study of small molecules [3].

I.4.2 Type of matrices for small molecule analysis using MALDI-MS

A good practice in the studying of small molecules by MALDI consists in to dissolve the molecule of interest in an adequate solvent to make an ultra violet spectrum of the solution. If the molecule absorbs in the wavelength range at which the MALDI laser works is a good signal, because the molecule will absorb the laser energy efficiently, thus facilitating the formation of the plume. In fact, for some molecules the addition of matrix becomes not necessary. However, even for molecules absorbing in the laser´s working wavelength, the use of matrix can be advantageous. As a general role, the matrix must match the following requirements: (i) to provide an efficient ionization and (ii) to produce minimal or non-interfering fragmentation. A way to overcome matrix interferences in the study of small molecules is to use a higher molecular weight matrix, which does not interfere in the low-mass region [3]. For instance, porphyrins have been used with this purpose [91].

Matrices used in the analysis of small molecules are generally classified in two main groups, organic and inorganic matrices. Organic matrices are mainly derived from cinnamic acid and from aromatic carbonyls. Two of the most frequently used molecules are α-cyano-4-hydroxycinnamic acid (α-CHCA) and 2,5-dihydroxy benzoic acid (DHB). It must be mind that the matrix-to-analyte molar ratio is much lower when studying low molecular weight compounds by MALDI, typically 10^{-1}:1 to 10^{3}:1, than when studying high molecular weight compounds, typically 10^{3} to 10^{5}:1 [3].

Tanaka et al. first introduced the use of inorganic matrices in 1988. They used an ultra fine metal powder (cobalt powder of about 300 Å diameter) suspended in glycerol to analyse polyethylene glycol 200 [8]. Following this approach soon it was introduced the use of graphite particles suspended in a mixture of glycerol, sucrose and methanol [92]. Many other approaches have been reported in literature since the firs communication done by Tanaka et al [93]. For instance, the use of carbon nanotubes has been also cited [94], [95].

In addition to organic and inorganic matrices, the use of liquid matrices has been also reported [96], [97]. The use of these matrices brings a number of benefits, such as higher signal reproducibility and the possibility to dissolve both polar and non-polar analytes. A number of drawbacks must be also reported for the use of liquid matrices, such as high chemical background, potential instrument contamination and poor ionization efficiency.

As it was written above, some matrix-free approaches are also possible, taking advantage of the own molecular structure of the target analyte. Other approaches introduce technical modification on the surface of the MALDI target. Such is the case for the desorption ionization on silicon mass spectrometry [98], [99]. In this technique the molecules of interest are deposited onto a porous silicon surface. This methodology enables the analysis of compounds with little or no fragmentation.

I.4.3 Sample Treatment for small molecule analysis using MALDI-MS

The method of matrix-to-sample mixing is very important as it influences the performance of the analysis. The most common method of work is the dried droplet method. In this method the analyte solution is mixed with the matrix, previously dissolved in an organic solvent/water mixture, with an appropriate matrix: analyte ratio, generally higher than 10:1 [2]. The mixture is deposited in the MALDI target and air-drying. Electrospray deposition has also been cited [100], [88], [101]. However others sample treatment methodologies as layer by layer technique can be also explored. In this case, several layers of the organic molecule with the inorganic or organic analyte are superimposing in the MALDI plate.

I.4.4 The Derivatization of the matrix: Towards new Active matrices.

The derivatization of the matrix is an alternative to improve the performance of the analysis. It allows increment the ionization efficiency, and also helps to observe interactions in the gas phase between the matrix and the analytes [102], [103]. Signals due to the increment in the mass of the analyte as consequence of the derivatized matrix must be observed. In some cases, for specific analysis (steroids) the introduction of isotopic labels allows for analyte quantification [78], [77], [104].

In chapters IV and V, MALDI is applied to measure the masses as well as to retrieve structural information of new in-situ formed inorganic complexes and adducts. Furthermore, MALDI is used to follow titrations of the aforementioned organic derivatized molecules used as Active Matrices in the presence of metal ions and inorganic or organic anions.

I.5 Bibliography

[1] J. H. Gross, Mass Spectrometry: A Textbook. Springer-Verlag, 2004.

[2] D. M. Desiderio and N. M. Nibbering, Fundamentals of Contemporary Mass Spectrometry. New Jersey: John Wiley & Sons, Inc., Publication, 2007.

[3] F. Hillenkamp and J. Peter-Katalinic, Eds., MALDI MS - A Pratical guide to Instrumentation Methods and Applications. WILEY-VCH, 2007.

[4] M. Karas, D. Bachmann, and F. Hillenkamp, "Influence of the wavelength in high-irradiance ultraviolet laser desorption mass spectrometry of organic molecules," Anal. Chem., vol. 57, no. 14, pp. 2935–2939, 1985.

[5] F. Hillenkamp, R. Kaufmann, R. Nitsche, E. Remy, and E. Unsold, "Laser micropobe mass analysis of organic materials nature," Nature, vol. 256, pp. 119–120, 1975.

[6] N. C. Fenner and N. R. Daly, "Laser used for mass analysis," Rev. Sci. Instrum., vol. 37, pp. 1068–1072, 1966.

[7] R. Matthiesen, Mass Spectrometry Data Analysis in Proteomics, Second Edi. Humana Press, 2013.

[8] K. Tanaka, H. Waki, Y. Ido, S. Akita, Y. Yosida, and T. Yoshida, "Protein and polymer analyses up to m/z 100 000 by laser ionization time-of-flight mass spectrometry," Rapid Commun. Mass Spectrom.Spectrom, vol. 2, pp. 151–153, 1988.

[9] J. Sunner, E. Dratz, and Y. C. Chen, "Graphite surface-assisted laser desorption/ionization time-of-flight mass spectrometry of peptides and proteins from liquid solutions.," Anal. Chem., vol. 67, no. 23, pp. 4335–4342, 1995.

[10] L. Li, MALDI : Mass Spectrometry for Synthetic Polymer Analysis, Wiley. New Jersey: John Wiley & Sons, Inc., Publication, 2010.

[11] C. Menzel, K. Dreisewerd, S. Berkenkamp, and F. Hillenkamp, "The role of the laser pulse duration in infrared matrix-assisted laser desorption/ionization mass spectrometry," J Am Soc Mass Spectrom, vol. 13, no. 8, pp. 975–984, 2002.

[12] A. Vogel and V. Venugopalan, "Mechanisms of Pulsed Laser Ablation of Biological Tissues," Chem. Rev., vol. 103, no. 2, pp. 577–644, 2003.

[13] M. Karas, D. Bachmann, U. Bahr, and F. Hillenkamp, "Matrix-assisted ultraviolet laser desorption of non-volatile compounds," Int. J. MassSpectrom. Ion. Proc., vol. 78, pp. 53–68, 1987.

[14] M. Karas, M. Glückmann, and J. Schäfer, "Ionization in matrix-assisted laser desorption/ionization: Singly charged molecular ions are the lucky survivors," J. Mass Spectrom., vol. 35, no. 1, pp. 1–12, 2000.

[15] V. Gabelica, E. Schulz, and M. Karas, "Internal energy build-up in matrix-assisted laser desorption/ionization," J. Mass Spectrom., vol. 39, no. 6, pp. 579–593, 2004.

[16] J.-L. Capelo-Martínez, Ultrasound in Chemistry. WILEY-VCH VERLAG GMBH, 2009.

[17] A. I. Mallet and S. Down, Dictionary of Mass Spectrometry, Wiley. A John Wiley and Sons, Ltd, Publication, 2009.

[18] M. Mann, R. C. Hendrickson, and A. Pandey, "Analysis of proteins and proteomes by mass spectrometry.," Annu. Rev. Biochem., vol. 70, pp. 437–473, 2001.

[19] K. Dreisewerd, "The Desorption Process in MALDI," Chem. Rev., vol. 103, pp. 395–425, 2003.

[20] R. Zenobi and R. Knochenmuss, "Ion formation in MALDI mass spectrometry," Mass Spectrom. Rev., vol. 17, pp. 337–366, 1998.

[21] B. Spengler, D. Kirsch, and R. Kaufmann, "Metastable Decay of peptides and proteins in matrix-assited desorption mass spectrometry," Rapid Communications in Mass Spectrometry, vol. 5. pp. 198–202, 1991.

[22] T. Wehr, "Top-Down versus Bottom-Up Approaches in Proteomics," LCGC North Am., vol. 24, no. 9, pp. 1004–1010, 2006.

[23] A. Speers and C. C. Wu, "Proteomics of Integral Membrane ProteinsTheory and Application," Chem. Rev., vol. 107, no. 8, pp. 3687–3714, 2007.

[24] D. López-Ferrer, B. Cañas, J. Vázquez, C. Lodeiro, R. Rial-Otero, I. Moura, and J. L. Capelo, "Sample treatment for protein identification by mass spectrometry-based techniques," TrAC Trends Anal. Chem., vol. 25, no. 10, pp. 996–1005, 2006.

[25] B. Thiede, W. Höhenwarter, A. Krah, J. Mattow, M. Schmid, F. Schmidt, and P. R. Jungblut, "Peptide mass fingerprinting," Methods, vol. 35, no. 3 SPEC.ISS., pp. 237–247, 2005.

[26] D. J. C. Pappin, P. Hojrup, and A. J. Bleasby, “Rapid identification of proteins by peptide-mass fingerprinting,” Curr. Biol., vol. 3, no. 6, pp. 327–332, Jun. 1993.

[27] P. James, M. Quadroni, E. Carafoli, and G. Gonnet, “Protein identification by mass profile fingerprinting.,” Biochemical and biophysical research communications, vol. 195, no. 1. pp. 58–64, 1993.

[28] W. J. Henzel, T. M. Billeci, J. T. Stults, S. C. Wong, C. Grimley, and C. Watanabe, “Identifying proteins from two-dimensional gels by molecular mass searching of peptide fragments in protein sequence databases.,” Proc. Natl. Acad. Sci. U. S. A., vol. 90, no. 11, pp. 5011–5, 1993.

[29] J. R. Yates, S. Speicher, P. R. Griffin, and T. Hunkapiller, “Peptide Mass Maps: A Highly Informative Approach to Protein Identification,” Analytical Biochemistry, vol. 214, no. 2. pp. 397–408, 1993.

[30] M. Mann and O. N. Jensen, “Proteomic analysis of post-translational modifications,” Nat Biotech, vol. 21, no. 3, pp. 255–261, Mar. 2003.

[31] R. G. Krishna and F. Wold, “Proteins, Analysis and Design,” AcademicPr., R. . Angeletti, Ed. Oxford: AcademicPress, 1998.

[32] P. Giansanti, L. Tsiatsiani, T. Y. Low, and A. J. R. Heck, “Six alternative proteases for mass spectrometry-based proteomics beyond trypsin,” Nat. Protoc., vol. 11, no. 5, pp. 993–1006, 2016.

[33] J. Rosenfeld, J. Capdevielle, J. C. Guillemot, and P. Ferrara, “In-gel digestion of proteins for internal sequence analysis after one- or two-dimensional gel electrophoresis,” Anal. Biochem., vol. 203, no. 1, pp. 173–179, 1992.

[34] A. J. Link, J. Eng, D. M. Schieltz, E. Carmack, G. J. Mize, D. R. Morris, B. M. Garvik, and J. R. Yates, “Direct analysis of protein complexes using mass spectrometry,” Nat Biotech, vol. 17, no. 7, pp. 676–682, Jul. 1999.

[35] Y. L. F. Hsieh, H. Q. Wang, C. Elicone, J. Mark, S. Martin, and F. Regnier, “Automated analytical system for the examination of protein primary structure.,” Anal. Chem., vol. 68, p. 455, 1996.

[36] B. Cañas, C. Piñeiro, E. Calvo, D. López-Ferrer, and J. M. Gallardo, “Trends in sample preparation for classical and second generation proteomics,” Journal of Chromatography A, vol. 1153, no. 1–2. pp. 235–258, 2007.

[37] A. Görg, W. Weiss, and M. J. Dunn, "Current two-dimensional electrophoresis technology for proteomics," Proteomics, vol. 4, no. 12, pp. 3665–3685, 2004.

[38] L. Jiang, L. He, and M. Fountoulakis, "Comparison of protein precipitation methods for sample preparation prior to proteomic analysis," J. Chromatogr. A, vol. 1023, no. 2, pp. 317–320, 2004.

[39] T. Rabilloud, "Use of thiourea to increase the solubility of membrane proteins in two-dimensional electrophoresis," Electrophoresis, vol. 19, no. 5, pp. 758–760, 1998.

[40] B. Bjellqvist, K. Ek, P. G. Righetti, E. Gianazza, A. Gorg, R. Westermeier, and W. Postel, "Isoelectric focusing in immobilized pH gradients: principle, methodology and some applications.," J Biochem Biophys Methods., vol. 6, pp. 317–39, 1982.

[41] W. M. Lauber, J. A. Carroll, D. R. Dufield, J. R. Kiesel, M. R. Radabaugh, and J. P. Malone, "Mass spectrometry compatibility of two-dimensional gel protein stains.," Electrophoresis, vol. 22, pp. 906–18, 2001.

[42] L. D. Adams and K. M. Weaver, "Detection and recovery of proteins from gels following zinc chloride staining.," Appl Theor Electrophor., vol. 1, pp. 279–82, 1990.

[43] M. J. Dunn, "Electroelution of proteins from polyacrylamide gels.," Methods Mol Biol., vol. 244, pp. 339–43, 2004.

[44] C. A. Retamal, P. Thiebaut, and E. W. Alves, "Protein purification from polyacrylamide gels by sonication extraction.," Anal Biochem., vol. 268, pp. 15–20, 1999.

[45] M. Wilm, A. Shevchenko, T. Houthaeve, S. Breit, L. Schweigerer, T. Fotsis, and M. Mann, "Femtomole sequencing of proteins from polyacrylamide gels by nano-electrospray mass spectrometry," Nature, vol. 379, pp. 466–9, 1996.

[46] P. Kumarathasan, S. Mohottalage, P. Goegan, and R. Vincent, "An optimized protein in-gel digest method for reliable proteome characterization by MALDI–TOF–MS analysis," Anal. Biochem., vol. 346, no. 1, pp. 85–89, 2005.

[47] F. Gharahdaghi, C. R. Weinberg, D. A. Meagher, B. S. Imai, and S. M. Mische, "Mass spectrometric identification of proteins from silver-stained polyacrylamide gel: a method for the removal of silver ions to enhance sensitivity," Electrophoresis, vol. 20, pp. 601–605, 1999.

[48] R. Rial-Otero, R. J. Carreira, F. M. Cordeiro, A. J. Moro, H. M. Santos, G. Vale, I. Moura, and J. L. Capelo, "Ultrasonic assisted protein enzymatic digestion for fast protein identification by matrix-assisted laser desorption/ionization time-of-flight mass spectrometry: Sonoreactor versus ultrasonic probe," J. Chromatogr. A, vol. 1166, no. 1, pp. 101–107, 2007.

[49] J. L. Capelo, R. Carreira, M. Diniz, L. Fernandes, M. Galesio, C. Lodeiro, H. M. Santos, and G. Vale, "Overview on modern approaches to speed up protein identification workflows relying on enzymatic cleavage and mass spectrometry-based techniques," Anal. Chim. Acta, vol. 650, no. 2, pp. 151–159, 2009.

[50] F. Hillenkamp and M. Karas, "Matrix-assisted laser desorption / ionization mass spectrometry of biopolymers," Anal. Chem., vol. 63, no. 24, pp. 1193–1203, 1991.

[51] J. K. Lewis, J. Wei, and G. Siuzdak, "Matrix-assisted Laser Desorption / Ionization Mass Spectrometry in Peptide and Protein Analysis," Encycl. Anal. Chem., pp. 5880–5894, 2000.

[52] P. A. Nielsen, J. V. Olsen, A. V. Podtelejnikov, J. R. Andersen, M. Mann, and J. R. Wisniewski, "Proteomic mapping of brain plasma membrane proteins," Mol Cell Proteomics, vol. 4, pp. 402–8, 2005.

[53] M. P. Washburn, D. Wolters, and J. R. Yates, "Large-scale analysis of the yeast proteome by multidimensional protein identification technology," Nat Biotechnol, vol. 19, pp. 242–7, 2001.

[54] J. E. Araújo, E. Oliveira, P. Kouvonen, G. L. Corthals, C. Lodeiro, H. M. Santos, and J. L. Capelo, "A journey through PROTEOSONICS," Talanta, vol. 121, pp. 71–80, 2014.

[55] B. Cañasa, C. Piñeirob, E. Calvoc, D. López-Ferrerd, and J. M. Gallardo, "Trends in sample preparation for classical and second generation proteomics," J. Chromatogr. A, vol. 1153, 2007.

[56] C. C. Wu and J. R. Yates, "The application of mass spectrometry to membrane proteomics," Nat Biotechnol, vol. 21, pp. 262–7, 2003.

[57] J. Blonder, T. P. Conrads, L. R. Yu, A. Terunuma, G. M. Janini, H. J. Issaq, J. C. Vogel, and T. D. Veenstra, "A detergent- and cyanogen bromide-free method for integral membrane proteomics: Application to Halobacterium purple membranes and the human epidermal membrane proteome," Proteomics, vol. 4, no. 1, pp. 31–45, 2004.

[58] A. R. Ross, P. J. Lee, D. L. Smith, J. I. Langridge, A. D. Whetton, and S. J. Gaskell, "Identification of proteins from two-dimensional polyacrylamide gels using a novel acid-labile surfactant," Proteomics, vol. 2, pp. 928–36, 2002.

[59] R. G. Sadygov, D. Cociorva, and J. R. Yates, "Large-scale database searching using tandem mass spectra: looking up the answer in the back of the book," Nat. Methods, vol. 1, pp. 195–202, 2004.

[60] D. Craft and L. Li, "Integrated sample processing system involving on-column protein adsorption, sample washing, and enzyme digestion for protein identification by LC-ESI MS/MS," Anal Chem., vol. 77, pp. 2649–55, 2005.

[61] J. T. Mason, Sonochemistry. Oxford University Press, 1999.

[62] K. S. Suslick, "Sonochemistry," Science (80-.)., vol. 247, no. 4949, pp. 1439–45, 1990.

[63] Y. Hsieh and M. S. Plesset, "Theory of rectified diffusion of massin to gas bubbles," J. Acoust. Soc. Am., vol. 33, pp. 206–215, 1961.

[64] T. S. Hot, "The Sonochemical Hot," Am. Chem. Soc., vol. 108, no. 18, pp. 5641–5642, 1986.

[65] Y. D. K.S. Suslick, W.B. McNamara III, "Hot Spot Conditions During Multi-Bubble Cavitation," eds. Kluwer Publ. Dordrecht, Netherlands, no. 16, pp. 191–204, 1999.

[66] G. Vale, H. M. Santos, R. J. Carreira, L. Fonseca, M. Miró, V. Cerdà, M. Reboiro-Jato, and J. L. Capelo, "An assessment of the ultrasonic probe-based enhancement of protein cleavage with immobilized trypsin," Proteomics, vol. 11, no. 19, pp. 3866–3876, 2011.

[67] H. M. Santos, R. Carreira, M. S. Diniz, M. G. Rivas, C. Lodeiro, J. J. G. Moura, and J. L. Capelo, "Ultrasonic multiprobe as a new tool to overcome the bottleneck of throughput in workflows for protein identification relaying on ultrasonic energy," Talanta, vol. 81, no. 1–2, pp. 55–62, 2010.

[68] J. L. Capelo Martínez, "Can enzymatic protein digests assists in E. coli discrimination at the strain level using mass spectrometry?," J. Integr. OMICS, vol. 3, no. 1, pp. 44–50, 2013.

[69] J. L. Capelo, C. Maduro, and C. Vilhena, “Discussion of parameters associated with the ultrasonic solid-liquid extraction for elemental analysis (total content) by electrothermal atomic absorption spectrometry. An overview,” Ultrason. Sonochem., vol. 12, no. 3, pp. 225–232, 2005.

[70] H. M. Santos and J. L. Capelo, “Trends in ultrasonic-based equipment for analytical sample treatment,” Talanta, vol. 73, no. 5, pp. 795–802, 2007.

[71] J. E. Araújo, S. Jorge, R. Magriço, T. e Costa, A. Ramos, M. Reboiro-Jato, F. Fdez-Riverola, C. Lodeiro, J. L. Capelo, and H. M. Santos, “Classifying patients in peritoneal dialysis by mass spectrometry-based profiling,” Talanta, vol. 152, pp. 364–370, 2016.

[72] R. J. Carreira, C. Lodeiro, M. Reboiro-Jato, D. Glez-Peña, F. Fdez-Riverola, and J. L. Capelo, “Indirect ultrasonication for protein quantification and peptide mass mapping through mass spectrometry-based techniques,” Talanta, vol. 82, no. 2, pp. 587–593, 2010.

[73] R. J. Carreira, F. M. Cordeiro, A. J. Moro, M. G. Rivas, R. Rial-Otero, E. M. Gaspar, I. Moura, and J. L. Capelo, “New findings for in-gel digestion accelerated by high-intensity focused ultrasound for protein identification by matrix-assisted laser desorption ionization time-of-flight mass spectrometry,” J. Chromatogr. A, vol. 1153, no. 1, pp. 291–299, 2007.

[74] F. M. Cordeiro, R. J. Carreira, R. Rial-Otero, M. G. Rivas, I. Moura, and J.-L. Capelo, “Simplifying sample handling for protein identification by peptide mass fingerprint using matrix-assisted laser desorption/ionization time-of-flight mass spectrometry.,” Rapid Commun. Mass Spectrom., vol. 21, pp. 3269–3278, 2007.

[75] L. Fernandes, R. Rial-Otero, M. Temtem, C. Veiga de Macedo, A. Aguiar-Ricardo, and J. L. Capelo, “Ultrasonic energy as a tool in the sample treatment for polymer characterization through matrix-assisted laser desorption ionization time-of-flight mass spectrometry,” Talanta, vol. 77, no. 2, pp. 882–888, 2008.

[76] M. Galesio, H. López-Fdez, M. Reboiro-Jato, S. Gómez-Meire, D. Glez-Peña, F. Fdez-Riverola, C. Lodeiro, M. E. Diniz, and J. L. Capelo, “Speeding up the screening of steroids in urine: Development of a user-friendly library,” 2013.

[77] M. Galesio, M. Mazzarino, X. De La Torre, F. Botrè, and J. L. Capelo, "Accelerated sample treatment for screening of banned doping substances by GC-MS: Ultrasonication versus microwave energy," Anal. Bioanal. Chem., vol. 399, no. 2, pp. 861–875, 2011.

[78] M. Galesio, R. Rial-Otero, J. Simal-Gándara, X. Torre, F. Botre, and J. L. Capelo-Martínez, "Improved ultrasonic-based sample treatment for the screening of anabolic steroids by gas chromatography/ mass spectrometry," Rapid Commun. mass Spectrom., vol. 24, no. 24, pp. 2375–2385, 2010.

[79] M. Galesio, C. Núñez, M. S. Diniz, R. Welter, C. Lodeiro, and J. Luis Capelo, "Matrix-assisted laser desorption/ionisation time of flight spectrometry for the fast screening of oxosteroids using aromatic hydrated hydrazines as versatile probes," Talanta, vol. 100, pp. 262–269, 2012.

[80] M. Larguinho, J. L. Capelo, and P. V. Baptista, "Fast nucleotide identification through fingerprinting using gold nanoparticle-based surface-assisted laser desorption/ionisation," 2013.

[81] R. Rial-Otero, R. J. Carreira, F. M. Cordeiro, A. J. Moro, L. Fernandes, I. Moura, and J. L. Capelo, "Sonoreactor-based technology for fast high-throughput proteolytic digestion of proteins," J. Proteome Res., vol. 6, no. 2, pp. 909–912, 2007.

[82] H. M. Santos, C. Mota, C. Lodeiro, I. Moura, I. Isaac, and J. L. Capelo, "An improved clean sonoreactor-based method for protein identification by mass spectrometry-based techniques," Talanta, vol. 77, no. 2, pp. 870–875, 2008.

[83] J. Matthijnssens, M. Ciarlet, M. Rahman, H. Attoui, M. K. Estes, J. R. Gentsch, M. Iturriza-gómara, C. Kirkwood, P. P. C. Mertens, O. Nakagomi, J. T. Patton, and M. Franco, "NIH Public Access," vol. 153, no. 8, pp. 1621–1629, 2009.

[84] S. F. Macha and P. a Limbach, "M atrix-assisted laser desorption / ionization (MALDI) mass spectrometry of polymers," Solid State Mater. Sci., vol. 6, pp. 213–220, 2002.

[85] H. Pasch and W. Schrepp, MALDI-TOF mass Spectrometry of Synthetic Polymers, Springer. Germany, 2003.

[86] K. J. Wu and R. W. Odom, "Characterizing Synthetic Polymers by MALDI MS," 1998.

[87] T. Yalcin, Y. Dai, and L. Li, “Matrix-Assisted Laser Desorption/Ionization Time-of-Flight Mass Spectrometry for Polymer Analysis : Solvent Effect in Sample Preparation,” Am. Soc. Mass Spectrom., vol. 9, no. 98, pp. 1303–1310, 1998.

[88] J. Axelsson, A. M. Hoberg, C. Waterson, P. Myatt, G. L. Shield, J. Varney, D. M. Haddleton, and P. J. Derrick, “Improved reproducibility and increased signal intensity in matrix-assisted laser desorption/ionization as a result of electrospray sample preparation,” Rapid Commun. Mass Spectrom., vol. 11, no. 2, pp. 209–213, 1997.

[89] D. C. Schriemer and L. Li, “Detection of High Molecular Weight Narrow Polydisperse Polymers up to 1.5 Million Daltons by MALDI Mass Spectrometry.,” Anal. Chem., vol. 68, no. 17, pp. 2721–2725, 1996.

[90] S. J. Wetzel, C. M. Guttman, and J. E. Girard, “The influence of matrix and laser energy on the molecular mass distribution of synthetic polymers obtained by MALDI-TOF-MS,” Int. J. Mass Spectrom., vol. 238, no. 3, pp. 215–225, 2004.

[91] F. Ayorinde, P. Hambright, T. N. Porter, and Q. L. Keith, “Use of meso-tetrakis(pentafluorophenyl)porphyrin as a matrix for low molecular weight alkylphenol ethoxylates in laser desorption/ ionization time-of-flight mass spectrometry,” Rapid Commun. Mass Spectrom., vol. 13, pp. 2474–2479, 1999.

[92] J. Sunner, E. Dratz, and Y. C. Chen, “Graphite surface-assisted laser desorption/ionization time-of-flight mass spectrometry of peptides and proteins from liquid solutions,” Anal Chem., vol. 67, pp. 4335–42, 1995.

[93] X. Li, X. Wu, J. M. Kim, S. S. Kim, M. Jin, and D. Li, “MALDI-TOF-MS Analysis of Small Molecules Using Modified Mesoporous Material SBA-15 as Assisted Matrix,” J. Am. Soc. Mass Spectrom., vol. 20, no. 11, pp. 2167–2173, 2009.

[94] S. Xu, Y. Li, H. Zou, J. Qiu, Z. Guo, and B. Guo, “Carbon nanotubes as assisted matrix for laser desorption/ionization time-of-flight mass spectrometry,” Anal. Chem., vol. 75, no. 22, pp. 6191–6195, 2003.

[95] C. Pan, S. Xu, L. Hu, X. Su, J. Ou, H. Zou, Z. Guo, Y. Zhang, and B. Guo, “Using oxidized carbon nanotubes as matrix for analysis of small molecules by MALDI-TOF MS,” J. Am. Soc. Mass Spectrom., vol. 16, no. 6, pp. 883–892, 2005.

[96] T. W. Dominic Chan, I. Thomas, A. W. Colburn, and P. J. Derrick, "Initial velocities of positive and negative protein molecule-ions produced in matrix-assisted ultraviolet laser desorption using a liquid matrix," Chem. Phys. Lett., vol. 222, no. 6, pp. 579–585, 1994.

[97] D. S. Cornett, M. A. Duncan, and I. J. Amster, "Liquid mixtures for matrix-assisted laser desorption," Anal. Chem., vol. 65, no. 19, pp. 2608–2613, 1993.

[98] J. Wei, J. M. Buriak, and G. Siuzdak, "Desorption-ionization mass spectrometry on porous silicon.," Nature, vol. 399, no. 6733, pp. 243–246, 1999.

[99] Z. Shen, J. J. Thomas, C. Averbuj, K. M. Broo, M. Engelhard, J. E. Crowell, M. G. Finn, and G. Siuzdak, "Porous silicon as a versatile platform for laser desorption/ionization mass spectrometry," Anal Chem., vol. 73, pp. 612–9, 2001.

[100] M. W. F. Nielen, "Maldi time-of-flight mass spectrometry of synthetic polymer," Mass Spectrom. Rev., vol. 18, no. 5, pp. 309–344, 1999.

[101] R. R. Hensel, R. C. King, and K. G. Owens, "Electrospray sample preparation for improved quantitation in matrix-assisted laser desorption/ionization time-of-flight mass spectrometry," Rapid Commun. Mass Spectrom., vol. 11, no. 16, pp. 1785–1793, 1997.

[102] B. Pedras, E. Oliveira, H. Santos, L. Rodríguez, R. Crehuet, T. Avilés, J. L. Capelo, and C. Lodeiro, "A new tripodal poly-imine indole-containing ligand: Synthesis, complexation, spectroscopic and theoretical studies," Inorganica Chim. Acta, vol. 362, no. 8, pp. 2627–2635, 2009.

[103] B. Pedras, H. M. Santos, L. Fernandes, B. Covelo, A. Tamayo, E. Bértolo, J. L. Capelo, T. Avilés, and C. Lodeiro, "Sensing metal ions with two new azomethine–thiophene pincer ligands (NSN): Fluorescence and MALDI-TOF-MS applications," 2007.

[104] E. P. Go, Z. Shen, K. Harris, and G. Siuzdak, "Quantitative Analysis with Desorption/Ionization on Silicon Mass Spectrometry Using Electrospray Deposition," Anal. Chem., vol. 75, no. 20, pp. 5475–5479, 2003.

Chapter II

Objectives, Working Plan and Thesis Output

II.1 Objectives

This thesis is developed with the goal to aid the mass spectrometry service of the Department of Chemistry of the Faculty of Sciences and Technology of the New University of Lisbon, DQ-FCT-UNL, to provide a service as good and modern as possible in the analysis of different types of molecules. To achieve this commitment a number of molecules have been selected following the criteria of utility, pursuing always to serve the research interests of the members of the DQ-FCT-UNL. Therefore, the objectives were:

1. To establish a routine protocol for protein identification in a large set of samples. The protocol must be ideally, fast, clean, and should match the analytical minimalisms roles[1].

2. To establish a routine protocol for the characterization of polymers, focusing in the values of number-average molecular weight, Mn, and weight-average molecular weight, Mw.

3. To establish a routine protocol for the characterization of small molecules.

4. To assemble matrix laser assisted desorption ionization as a tool to characterize the structure of molecules in conjunction with other analytical techniques.

5. To assess the effectiveness of ultrasonic energy as a tool to reduce the handling, time and complexity of current protocols for sample treatment for protein identification.

6. To study the effects of ultrasonic energy in the values of number-average molecular weight, Mn, and weight-average molecular weight, Mw, for polymers when ultrasound is used as a tool to simplify and speed the procedures for polymer characterization using MALDI.

1 D. J. Halls, "Analytical minimalism applied to the determination of trace elements by atomic spectrometry. Invited lecture," *J. Anal. At. Spectrom*, vol. 10, pp. 169–175, 1995.

II.2 Working Plan

In order to achieve the objectives described above, whenever possible while executing the experiments, the expertise of the Bioscope research group related with the simplification of sample treatments using ultrasonic energy will be considered to achieve better results, particularly those related with proteins and polymers.

The first part is dedicated to test and to evaluate the effect of three ultrasonic devices: ultrasonic probe, ultrasonic bath and sonoreactor in the sample treatment for polymers characterization. The evaluation is done using three standard polymers. In addition two different MALDI matrixes were assayed. The influence on the following ultrasonic variables over the sample treatment are studied: i) sonication amplitude, ii) sonication frequency and iii) sonication time.

The second part is focused in small molecules, and in their sensing capability of new compounds that readily ionize in MALDI, with and without the use of a matrix. New methodologies for sample preparation will be established using *in situ* titrations. This methodology allows testing the sensor capability of these molecules in the presence of metal ions and anions, evaluating their selectivity for a particular ion, and subsequently it will define its potential use as an active complexed matrix to detect these ions by MALDI-TOF MS.

In the final part of the work involved in this thesis, ultrasonic energy will be evaluated as a tool to develop a fast protocol to cleavage proteins of complex proteomes for subsequent protein identification using MALDI. An ultrasonic multiprobe of four tips will be used, along with a 96-well plate, for the treatment of proteins separated in gel, that will be used also to study, based on labeling ^{18}O, the type of peptides extracted from the gels when the extraction is carried out with the help of ultrasonic energy. The proteins are firstly separated using gel electrophoresis, and then the ultrasonic energy is applied to the key steps of the sample treatment for proteins identification by protein mass fingerprint in order to speed up and simplify the following steps: (i) the washing steps (ii) alkylation, (iii) reduction, (iv) gel bands digestion and (v) extraction of peptides. The influence on the following ultrasonic variables over the sample treatment are studied: i) sonication amplitude, ii) sonication frequency and iii) sonication time.

II.3 Thesis Output

II.3.1 Papers published in international scientific journals

4 – "Ultrasonic Enhanced Applications in Proteomics Workflows: single probe versus multiprobe" Luz Fernandes, Hugo. M. Santos, J. D. Nunes-Miranda, Carlos Lodeiro and José Luís Capelo Martínez Capelo JL. Journal of Integrated OMICS, Vol 1, No 1, Feb 2011, Pages 144-150.
(DOI: 10.5584/jiomics.vlil.55).

3 – "Exploiting anionic and cationic interactions with a new emissive imine-based b-naphthol molecular probe" Luz Fernandes, Maxime Boucher, Javier Fernández-Lodeiro, Elisabete Oliveira, Cristina Nuñez, Hugo M. Santos, Jose Luis Capelo, Olalla Nieto Faza, Emilia Bértolo, Carlos Lodeiro. *Inorganic Chemistry Communications* 12 (2009), *Pages* 905–912.
(DOI: 10.1016/j.inoche.2009.07.011).

2 – "Synthesis, characterization, and fluorescence behavior of four novel macrocyclic emissive ligands containing a flexible 8-hydroxyquinoline unit", Nunez C., Bastida R., Macias A., Bértolo E., Fernandes L., Capelo J.L. and Lodeiro C. *Tetrahedron, 65 (2009), Pages 6179-6188.*
(DOI: 10.1016/j.tet.2009.05.046).

1 – "Ultrasonic energy as a tool in the sample treatment for polymers characterization through matrix-assisted laser desorption ionization time-of-flight mass spectrometry", L. Fernandes, R. Rial-Otero, M. Temtem, C. Veiga de Macedo, A. Aguiar-Ricardo, J. L. Capelo. *Talanta*, *Volume 77, Issue 2*, *15 December 2008, Pages 882-888*.
(DOI: 10.1016/j.talanta.2008.07.049).

II.3.2 Participation in national and international conferences

3 - L. Fernandes, H. M. Santos, A. Rodrigues, M. S. Diniz, C. Lodeiro, J. L. Capelo. Speeding up enzymatic digestion of proteins: Ultrasonication versus microwave energy. CONGRESS: 3rd EuPA Congress (European Proteomics Association) Stockholm, Sweden 14-17 June 2009.

2 - L. Fernandes, A. Rodrigues, H. M. Santos, C. Lodeiro, J. L. Capelo. Proteins Digestion: Microwave versus Ultrasonication. Poster P-TUE-113, HUPO 2008, 7th World Congress, 16th-20th August, Amsterdam, Netherland.

1 – Luz Fernandes, M.C.Macedo, R.Rial-Otero, M.Temtem, A.Aguiar-Ricardo, J.L Capelo. The influence of ultrasounds for sample treatment in polymers analyses by MALDI-TOF-MS. pag. 198, XX Encontro Nacional SPQ, FCT/UNL, 14 a 16 de Dezembro de 2006, Portugal.

Chapter III

Ultrasonic energy as a tool in the sample treatment for polymers characterization through matrix-assisted laser desorption ionization time-of-flight mass spectrometry

---

Published in:

Talanta, 77 (2008) 882-888

L. Fernandes, R. Rial-Otero, M. Temtem, C. Veiga de Macedo, A. Aguiar-Ricardo, J. L.Capelo.

(DOI: 10.1016/j.talanta.2008.07.049)

III.1 Abstract

Different ultrasonic devices including ultrasonic bath with dual frequency, sonoreactor and ultrasonic probe, were tested for their viability in the sample treatment for polymer characterization by matrix-assisted laser desorption/ionization time of flight mass spectrometry analysis. The effect of sonication frequency (35 kHz, 40 kHz and 130 kHz), sonication amplitude, and sonication time on the polymer's number-average molecular weight (M_n) and weight-average molecular weight (M_w) were investigated. The effect of those variables in the molecular mass distribution of three polymer standards, poly(styrene) 2000 Da and 10,000 Da and poly(ethylene glycol) 1000 Da, was evaluated. In addition, the influence of ultrasonic energy on the sample treatment as a function of the MALDI matrix was also studied through two common standard matrices, dithranol and 2,5-dihydroxybenzoic acid. The results obtained show that the ultrasonic bath at 35 kHz is the best option for the purpose of fast sample treatment for polymer characterization. The M_n and M_w values obtained for this ultrasonic device and for the three polymers tested using Dithranol as MALDI matrix, were not statistically different from the ones acquired with vortex mixing and also were in concordance with the values recommended by the polymer manufacturers.

Keywords: Polymers, Ultrasound, Molecular mass distribution, MALDI-TOF-MS

My contribution to this work was the optimization of all experimental variables, MALDI-TOF MS analysis and interpretation.

III.2 Introduction

Synthetic polymers today find application in nearly every industry and area of life. They are used as adhesives, lubricants, structural components for many different materials, from computers to satellites. The most recent applications are found in the bioscience area, from artificial components for the human body to drug delivery.

The way in which monomers are distributed to form the structure of the polymer will dictate the polymer's properties, such as solubility, durability, resistibility, crystallinity or tensile strength.

The characterization of a polymer is mandatory to define its properties, since the monomers are distributed statistically in chains of variable lengths which originate differences in terms of polymer's physical and chemical characteristic.

Different analytical techniques can be used to define a polymer, including wide Fourier transform infrared spectroscopy, angle X-ray scattering, scattering, small angle neutron scattering, gel permeation chromatography (GPC), Raman, small angle X-ray, nuclear magnetic resonance, polydispersity and mass spectrometry-based techniques. Furthermore, matrix-assisted laser desorption/ionization time-of-flight mass spectrometry, MALDI-TOF-MS, referred in this manuscript as MALDI, is a well-established rapid instrumental technique for polymer characterization [1], [2].

Polymer characteristics that can readily be determined by MALDI include the following: (i) the number-average molecular weight, M_n, which provides an average weight of a given polymer; (ii) the weight-average molecular weight, M_w, is another form of to give the molecular weight of a polymer and is calculated as the arithmetic mean or average on the molecular weights of a certain number of molecules; (iii) the mass of repeat units; (iv) the polydispersity, PDI, which is the ratio M_w to M_n; and (v) the end-group mass structure [3], [4]. Polymer distributions are typically characterized by M_n and M_w, which are calculated as follows [5]:

$$M_n = \sum[(M_i I_i)/I_i]$$

$$M_w = \sum[(M_i^2 I_i)/M_i I_i]$$

$$PDI = M_w/M_n$$

Where M_i and I_i are the molecular weights of the oligomeric components and their signal intensities, respectively. It is assumed a linear relationship between number of ions and signal intensity [5].

The following features can be considered the major advantages of polymer analysis by MALDI [2], [6], [7]:

(i) Absolute molecular weights of narrowly distributed polymers (polydispersity < 1.2) can be determined as opposed to relative molecular weights obtained by chromatographic techniques.
(ii) Analysis does not require polymer standards to assign molecular weights to oligomers.
(iii) Using submilligram amounts of sample material, the actual analysis can be accomplished in few minutes.
(iv) In addition, MALDI can determine the molecular weight independently of the polymer structure.

Therefore, the speed and information obtained by MALDI are significantly greater than with other conventional molecular-weight-determination techniques, such as gel permeation chromatography (GPC) [2], [6]. The following drawbacks, that can also be extended to other type of analysis by MALDI, limit widespread application of MALDI for polymer analysis [3], [4], [7]-[9]:

(i) The availability of proper matrices for specific polymers.
(ii) The availability of proper cationization reagents.
(iii) The availability of common solvents for both analyte and matrix.
(iv) The polymer distribution is affected by (1) matrix type; and (2) polymer and matrix salt concentrations used to prepare the sample.
(v) The following MALDI instrumental parameters affect polymer distribution: (1) detector voltage; (2) laser energy; (3) delay time; (4) extraction voltage; and (5) lens voltage.

In addition to the above mentioned drawbacks, it must be emphasized that the M_n and M_w of polymers determined by MALDI often differ from those moments determined by other methods of polymer characterization such as GPC, overall for polymers with

high polydispersity (PDI >1.2). As an example, when data obtained through MALDI are compared with data obtained by GPC, larger discrepancies in the values for M_n and M_w are observed for polymers of high polydispersity. On the other hand, when polymers of narrow polydispersities (PDI < 1.2) are compared, the GPC and MALDI values for M_n ans M_w tend to have better agreement [4].

MALDI analysis consists of three steps: sample preparation, sample deposition on the MALDI sample plate and mass spectral analysis. Regarding sample preparation, one of the keys to a successful MALDI analysis depends primarily on uniformly mixing the matrix and the analyte. Samples are typically prepared in an analyte/matrix concentration ratio comprised between $1:10^3$ to $1:10^5$ in a suitable solvent such as water, acetone, or tetrahydrofuran. However, for high molecular weight samples much higher ratios ($1:8x10^6$) have been used [10]. Matrices used for polymer analysis by MALDI include dithranol, 2,5-dihydroxybenzoic acid (DHB), trans-3-indoleacrylic acid (IAA), and 2-(4-hydroxyphenylazo) benzoic acid (HABA). These matrices are often used in conjunction with alkali metal salts (LiCl, NaCl, KCl) or silver salts such as silver trifluoroacetate (AgTFA) to form matrix-cationization agent mixtures in order to promote polymer ionization [3], [4], [6]-[8].

Concerning sample deposition on the MALDI sample plate, hand-spotting and electrospray are the techniques of choice. The aforementioned deposition methods can lead to different results as a function of the matrix used in the sample preparation process [6], [7].

As far as MALDI analysis concerns, as written above, the instrumental parameters must be carefully chosen and controlled since variations can arise from those sources [4], [7], [8].

Ultrasonication has been used for sample treatment for analytical chemistry for decades [9], [11]. Ultrasonication has also become a tool in polymer research with two main aims. On the one hand, ultrasonication has been used for long in the synthesis of polymers, as a initiator or to obtain a homogeneous distribution of the monomers. On the other hand, it has been also used to study polymer degradation mechanisms. However, one of its multiple applications, the mixing of different matrices to form more homogeneous samples, has not been systematically studied for sample preparation of

polymers for MALDI characterization yet, despite of the advantages of high throughput and simplicity allowed by ultrasonication.

In this work an ultrasonic bath with dual frequency, a sonoreactor, and an ultrasonic probe, were used to study the influence frequency of sonication, amplitude of sonication and time of sonication on the M_n and M_w values, when the aforementioned devices are used in the sample treatment for mixing polymers and matrices previous to MALDI analysis. Vortex mixing was used for comparative purposes and it was considered the reference procedure for polymer/matrix homogeneization. Poly(styrene) (PS) and poly(ethylene glycol) (PEG) polymers were used as target analytes because both have been systematically studied by MALDI by numerous authors and there is a huge amount of information available in literature regarding these polymers [4], [10], [12], [13].

III.3 Experimental

III.3.1 Chemicals, solvents, disposables and apparatus

MALDI-TOF-MS analysis was performed on the following synthetic polymers purchased from Fluka (Buchs, Switzerland): (1) a 2000 Da poly(styrene) sample (M_n = 2140, M_w = 2250 and PDI = 1.05); (2) a 10000 Da poly(styrene) sample (M_n = 8650, M_w = 8900 and PDI = 1.03); and (3) a 1000 Da poly(ethylene glycol) sample (M_n = 970, M_w = 940 and PDI = 1.05). All of them were standards for GPC certified according to DIN, the German Institute for Standardization [14]. Matrices used in this work were dithranol and 2,5-dihydroxybenzoic acid (DHB), both with quality for MALDI-MS (> 98.5 %) purchased from Fluka and used as received. Silver trifluoroacetate (AgTFA) (> 98 %) from Fluka was used to increase the polymer ionization and to minimize the formation of adducts with Na^+ and K^+. Acetone Pestanal® grade from Fluka was used as solvent for MALDI matrices and samples.

Polymer-matrix solutions were prepared in safe-lock tubes of 0.5 ml from Eppendorf (Hamburg, Germany) and were homogenized with a vortex, model Sky Line, from ELMI (Riga, Latvia) or using the following ultrasonic devices: an ultrasonic bath

with dual frequency (35 and 130 kHz), model Transsonic TI-H-5, from Elma (Singen, Germany); a sonoreactor model UTR200, from dr. Hielsher (Teltow, Switzerland); and an ultrasonic probe, model UP 200S (dr. Hielscher).

III.3.2 Sample preparation

Stock solutions of PS and PEG were prepared by dissolving the polymer samples in acetone to a final concentration of c.a. 2 x 10^{-4} M. MALDI matrices (dithranol and DHB) were also dissolved in acetone to a final concentration of 10 mg/ml, and AgTFA was added to the matrix solution to enhance polymer ionization. An aliquot of 20 µl of the polymer stock solution was mixed with 20 µl of the MALDI matrix solution. Polymer-matrix mixing and homogenization was done through one of the following processes:

(i) homogeneization in vortex for 30 s.
(ii) homogeneization in an ultrasonic bath: 100 % sonication amplitude, continuous mode, 130 kHz sonication frequency, 120 s sonication time.
(iii) homogeneization in an ultrasonic bath: 100 % sonication amplitude, continuous mode, 35 kHz sonication frequency, 30 s sonication time.
(iv) homogeneization in a sonoreactor: 20 % sonication amplitude, continuous mode, 10 s sonication time.
(v) homogeneization in a sonoreactor: 20 % sonication amplitude, continuous mode, 30 s sonication time.
(vi) homogeneization with an ultrasonic probe: 20 % sonication amplitude, continuous mode, 10 s sonication time.
(vii) homogeneization with an ultrasonic probe: 20 % sonication amplitude, continuous mode, 30 s sonication time.

Finally, the samples were hand-spotted onto the MALDI sample plate. Three replicates were done for each sample preparation mode (n=3).

The sonication amplitudes and the sonication times were selected based on our expertise with ultrasonication for sample treatment [9], [11]. Briefly, to avoid polymer degradation due to ultrasonication, short sonication times were generally used. For the same reason, for the sonoreactor and ultrasonic probe, both having high sonication intensity, the lower amplitude of sonication was selected.

III.3.3 MALDI analysis

A MALDI-TOF-MS system, model Voyager DE-PRO Biospectrometry Workstation, equipped with a nitrogen laser radiating at 337 nm and 3 ns pulse from Applied Biosystems (Foster City, USA) was used to obtain the polymer mass spectra following the instructions of the manufacturer. The polymers with molecular weight of 1000 and 2000 Da were analysed in the ion reflector mode in order to enhance peak resolution. Analysis of the 10000 Da PS sample was done in the linear mode, due to the low sensitivity obtained in the reflector mode for high molecular weight polymers. Measurements were done in the positive ion mode, with the following parameter settings: an accelerating voltage of 20 kV, a grid voltage of 77 %, a guide wire of 0.01 % and a mirror voltage ratio of 1.12. Delayed extraction was optimized for signal-to-noise for the necessary mass range. Matrix type has a large influence on the laser energy required to obtain a MALDI mass spectrum. As recommended by Wetzel *et al.* [7], for each matrix data were obtained at randomized laser energy intervals within that range, not in order of increasing or decreasing laser energy. The polymer mass spectra were collected at laser energies of 5.9-6.3 $\mu J/cm^2$ for dithranol; and 6.9-7.1 $\mu J/cm^2$ for DHB. The resolution of the peaks near the molecular mass, for 500 laser shots, was 6500 in the reflector mode and 600 in the linear mode.

MALDI mass spectra were obtained in a manner designed to minimize bias due to sample preparation and application. Each mass spectrum represents the accumulated data from 500 laser shots as the laser spot was moved over a sample site on a stainless steel MALDI sample plate. The mass spectra were obtained from different sites on the 100-site MALDI sample plate to reduce the possibility of bias.

III.3.4 Data analysis methods

M_n and M_w values were calculated from each polymer mass spectrum obtained by MALDI-MS. Polymerix (Sierra Analytics, Modesto, CA, USA) analysis software was used to integrate the M_n and M_w, and to obtain the moments and separate the different peak series. When necessary, the secondary and tertiary peaks series were used to obtain an estimate of extent of fragmentation through the polymerix program. Analysis of variance (ANOVA) was used to determine whether the measured polymer M_n and M_w were influenced by the sample treatment applied or not. The significance level of the ANOVA was chosen to be 0.05. ANOVA compares the variance at a given parameter value with the variance among parameter values to determine if there is a significant influence of the parameter on the polymer distribution. A parameter has a significant variation when the variance between parameter values is greater than a multiple (depending of the significant level) of the variance within parameter values. When significant variations were detected a Multiple Range test was done to determine which means were significantly different from which others. This test uses the Fisher's least significant difference (LSD) procedure to discriminate among the means. With this method, there is a 5.0 % risk of calling each pair of means significantly different when the actual difference equals zero [15].

III.4 Results and discussion

III.4.1 Poly(styrene), PS, 2000Da

III.4.1.1 MALDI spectra

Poly(styrene), PS, (2000 Da) was analyzed in dithranol and DHB matrices using AgTFA to enhance polymer ionization during MALDI analysis [1]. Figure III.1(A) shows the MALDI mass spectrum obtained for the 2000 Da PS sample, for the 35 kHz ultrasonic bath, UB, in dithranol, where peaks can be seen with mass differences of 104 Da, corresponding to the PS monomer mass (C_8H_8).

Regarding PS in dithranol (Figure III.1(A)) the mass spectra showed good repeatability regardless of the polymer/matrix mixing process used. A matrix made of

dithranol (10 mg/ml) and AgTFA (1 mg/ml) was used. The average PS MALDI mass spectrum (500 laser shots) showed in Figure III.1(A) was easily obtained thought the accumulation of 5 spectra with a total of 100 laser shots/spectrum. In addition, no fragmentation was observed during the ionization process. Therefore, no fragmentation due to ultrasonication sample pretreatment neither to MALDI ionization was observed. These results are in agreement with previous data described in literature [7], and can be related to the thermal stability of PS, which has a high ceiling temperature, and as such, no fragmentation is expected during a typical MALDI analysis.

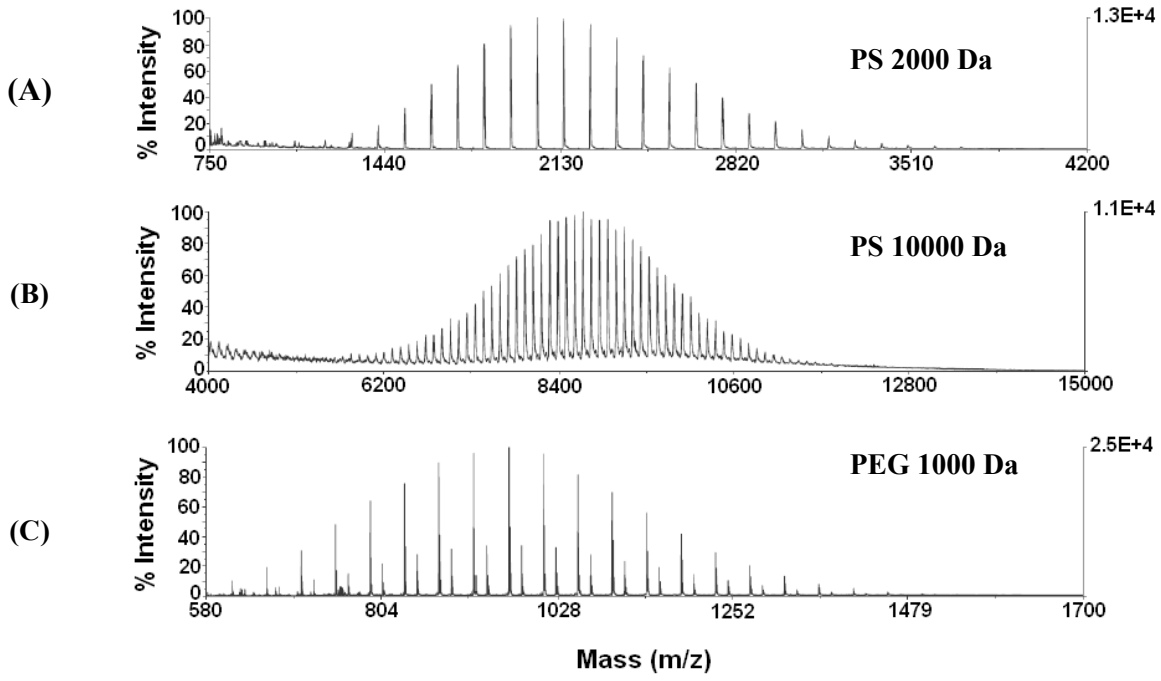

Figure III.1 MALDI mass spectra in dithranol matrix with sample treatment done with the ultrasonic bath at 35 kHz sonication frequency of poly(styrene) standard 2000 Da (A); poly(styrene) standard 10,000 Da (B) and poly(ethylene glycol) standard 1000 Da (C).

Concerning PS in DHB matrix, a higher amount of AgTFA (6 mg/ml) was necessary to obtain good polymer ionization, thus confirming that the choice of the MALDI matrix is critical when performing polymer analysis by MALDI, as previously reported by different authors [3], [4]. The MALDI mass spectra acquisition was more difficult than with dithranol. In fact, to achieve similar results in terms of intensity to those obtained with PS in dithranol, we needed to reduce the laser shots/spectrum ratio to 50 and also we needed to impact the laser twice in the same point of the sample spot, so the first 50 shots were discarded and the following 50 shots were accumulated. Sample

preparations containing high salts concentrations often yield increased signal intensity after an initial period of low intensity at the top layer of sample spot, suggesting the formation of a layer of salt over the polymer during the sample drying in the MALDI sample plate [16]. The poor performance of the DHB as matrix for PS is directly linked with its chemical properties: the DHB is recommended for polar polymers and PS is an aromatic one. The different ultrasonic conditions tested for sample treatment did not help to improve results when DHB matrix was used.

Table III.1 M_n and M_w values ± standard deviations of the three polymers in dithranol and DHB matrices for each one of the seven sample treatments tested.

Sample treatment	Polymer									
	PS 2000				PS 10000		PEG 1000			
	Dithranol		DHB		Dithranol		Dithranol		DHB	
	Mn	*Mw*	*Mn*	*Mw*	*Mn*	*Mw*	*Mn*	*Mw*	*Mn*	*Mw*
US bath 130 KHz, 120s	2246±24	2382±29	1755±71	1855±75	8711±47	8828±41	1009±8	1037±8	1028±1	1058±1
US bath 35 KHz, 30s	2250±42	2371±57	1826±22	1930±25	8681±38	8795±28	1001±11	1033±10	1003±20	1033±21
US Probe 10s	2234±26	2378±23	1922±70	2028±66	8524±146	8638±145	1024±7	1054±9	997±5	1031±3
US Probe 30s	2245±70	2392±71	1876±10	1993±11	8625±72	8743±70	1024±6	1053±4	1010±14	1045±14
Sonoreactor 10s	2156±81	2312±98	1921±25	2029±31	8726±63	8837±64	1014±11	1043±8	1029±8	1058±9
Sonoreactor 30s	2176±35	2313±20	1954±60	2059±52	8646±95	8757±94	1029±12	1056±11	1039±2	1069±1
Vortex	2198±39	2352±56	1888±95	2004±92	8615±72	8727±67	1003±7	1035±5	1014±4	1044±6
Theorical value	2140	2250	2140	2250	8650	8900	900	940	900	940

Mn and Mw values are averages of the data obtained for three samples (n=3).

III.4.1.2 Polymer characterization

As far as M_n and M_w values concerns, data regarding PS in dithranol and DHB for the seven sample treatments tested are shown in Table III.1. As it can be seen, results obtained for both matrices were different. On the one hand, M_n values obtained in dithranol (ranging from 2156 to 2250 Da) were similar to the theoretical M_n value for this polymer recommended by the manufacturer (2140 Da). Results closest to the theoretical value were obtained with the sonoreactor for either 10 s or 30 s of sonication time. In the same way, equivalent conclusions were drawn for the M_w values. ANOVA analysis of the M_n and M_w values obtained using dithranol revealed no significant variation among the

different sample treatments studied. In addition, sample sonication time, in the range studied in this work, was also found non significant. On the other hand, as it can be seen in Table III.1, M_n and M_w values obtained in DHB were ca. 200-500 Da lower than those obtained with dithranol.

This finding has been previously reported in literature and can be related to analyte-matrix interactions rather than to the mixing procedure [4]. In addition, M_n and M_w values for PS 2000 Da in DHB were also lower than its recommended mass values. ANOVA analysis of the M_n and M_w values for DHB showed statistically significant differences at 95 % confidence level (P = 0.05). To determine which means were significantly different, a multiple range test was done. In Figure III.2, a plot of the ANOVA analysis of means at 95 % confidence level for the M_n and M_w values obtained for PS 2000 Da in DHB is showed. As it can be seen in this figure, statistical differences were found between the vortex mixing and the sample/matrix homogenization using the ultrasonic bath at 130 kHz for 120 s. This sample treatment displayed the lowest M_n and M_w values (1755 and 1855, respectively).

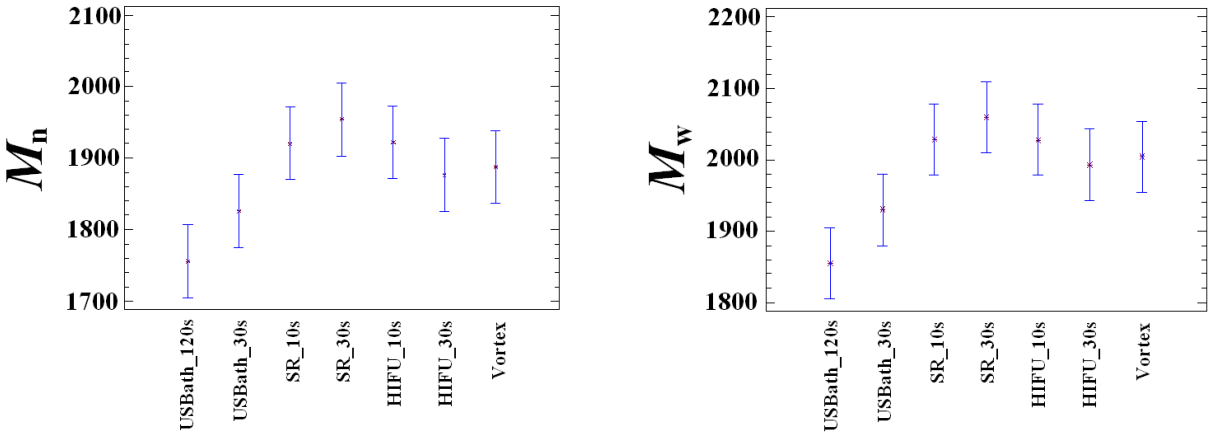

Figure III.2 Statistical analysis of means at 95% confidence level for the *M*n and *M*w values obtained for the poly(styrene) standard 2000 Da in DHB. LSD intervals display the least significant difference intervals for the two-factor interactions.

III.4.2 Poly(styrene), 10,000Da

III.4.2.1 MALDI spectra

As descrived above for the PS 2000, good MALDI spectra were obtained using dithranol (10 mg/ml) and AgTFA (1 mg/ml) as matrix for the PS 10000 Da. It must be pointed out that it was impossible to analyze this polymer with DHB even after increasing the amount of silver to 6 mg/ml. The mass spectrum of PS 10000 in dithranol is shown in Figure III.1(B), where it can be seen peaks with mass differences of 104 Da, corresponding to the PS monomer mass (C_8H_8). No fragmentation peaks were noted.

III.4.2.2. Polymer characterization

M_n and M_w values for PS 10000 Da in dithranol are shown in Table III.1. As it can be seen in this table, M_n and M_w values were very similar to the recommended values certified by the manufacturer for this polymer (8650 Da and 8900 Da, respectively). In addition, ANOVA analysis of the M_n and M_w values revealed no significant variations as a result of the sample treatments done with the different apparatus tested (vortex, ultrasonic bath, ultrasonic cell disruptor and sonoreactor), regardless of the sonication times applied. Differences observed in the M_n values for the different sample treatments are comprised between ± 1.5 % of the theoretical value.

III.4.3 Poly(ethylene glycol), PEG, 1000Da

III.4.3.1 MALDI spectra

Polyethylene glycol, PEG, was analyzed in dithranol and DHB using AgTFA (1mg/ml). The mass spectra of PEG obtained in dithranol is shown in Figure III.1(C), where it can be seen main peaks with mass differences of 44 Da, corresponding to the PEG monomer mass (C_2H_4O).

Regarding analysis done in dithranol, either for ultrasonication or vortex, a secondary peak series shifted about 16 Da to lower masses from the main series was observed (see Fig III.1(C)). The peak series shifted by about 16 Da to lower masses from the main series can be attributed to the fragmentation at the carbon-oxygen bond as

referred in literature [7], [13]. This fragmentation series was obtained independently of the mixing process used, thus indicating that ultrasonication was not the cause of the fragmentation. The percentage of the peak area represented by the secondary peak series was comprised between 15% and 25%. It must be stressed that there was not a link between the areas of the secondary fragmentation and the sample treatment used, thus showing that no extra fragmentation due to ultrasonication was observed.

Concerning DHB matrix, a secondary and tertiary peak series were observed shifted by about 4 and 16 Da, respectively, to lower masses from the main series (data not shown). Those series indicate fragmentation. The terciary peak series shifted 16 Da can be attributed to the fragmentation at the carbon-oxygen bond as commented above. To the best of our knowledge, the secondary peak series shifted 4 Da has not been cited in literature previously. In any case, for the purposes of this study, it is unnecessary to fully characterize the fragments, since the apparent molecular mass distribution was close to the theoretical one given as reference for PEG by the manufacturer of the polymer. The pattern of fragmentation is not linked to ultrasonication since the same series of peaks were obtained after mixing the PEG and matrix with vortex. For DHB matrix the secondary peak series represented the principal contribution to the polymer distribution with an area percentage of about 50-65 %, being the contribution of the main series of about 35-50 % and the percentage of the tertiary series lower than 9 %. Those data suggest that for DHB matrix the polymer fragmentation during the MALDI ionization process is higher than for dithranol matrix.

The best resolution with the highest intensity was obtained for the PEG/dithranol mixture in the clear zone, situated in the outer zones of the sample spot. In this position the matrix peaks are less intense and have no influence in the mass spectra. On the other hand, when DHB was used, the best MALDI mass spectra were obtained in the dark region of the sample spot because in the clear region more interferences of the matrix were found. This can be explained because hand-spotting usually causes large matrix crystals to form, the polymer sample being not homogeneously distributed throughout the matrix. Hand-spotted samples can have large signal variations across the sample plate; in some regions, it can be obtained large polymer signals (‘sweet spots’), whilst in other regions no polymer signal is obtained [7].

III.4.3.2. Polymer characterization

M_n and M_w values obtained for PEG in dithranol and DHB, for all sample treatments studied are summarized in Table III.1. As it can be seen in this table, results for both matrices were similar, for the same sample treatment. In addition, similar standard deviations were observed. Finally, depending on the sample treatment, a slight increment comprised between 3 % and 7 % for the M_n value and between 10 % and 14 % for the M_w value was obtained when comparing it with the recommended value given for the manufacturer.

The ANOVA analysis of M_n and M_w values obtained for PEG in dithranol and DHB revealed statistically significant differences, at 95 % confidence level (P = 0.05), among the different sample treatments used. As consequence, a multiple range test was performed to find out which treatments were significantly different. Results are given in Figure III.3, where it can be seen that:

(i) for dithranol, the M_n value obtained with the vortex sample/matrix mixing was statistically different from the M_n values obtained after sample/matrix mixing with the sonoreactor with a sonication time of 30 seconds and the ultrasonic probe, with a sonication time of 10 s or 30 s (Figure III.3(A)). Similar conclusions can be obtained for the M_w values (Figure III.3(B)). Consequently, for this polymer and dithranol, vortex homogenization can not be substituted for the sonoreactor or the ultrasonic probe.

(ii) for DHB, M_n and M_w values obtained for vortex and sonoreactor with a sonication time of 30 s were statistically different (Figures III.3(C) and III.3(D)). Accordingly, for this polymer and DHB, vortex homogenization can not be substituted for the sonoreactor.

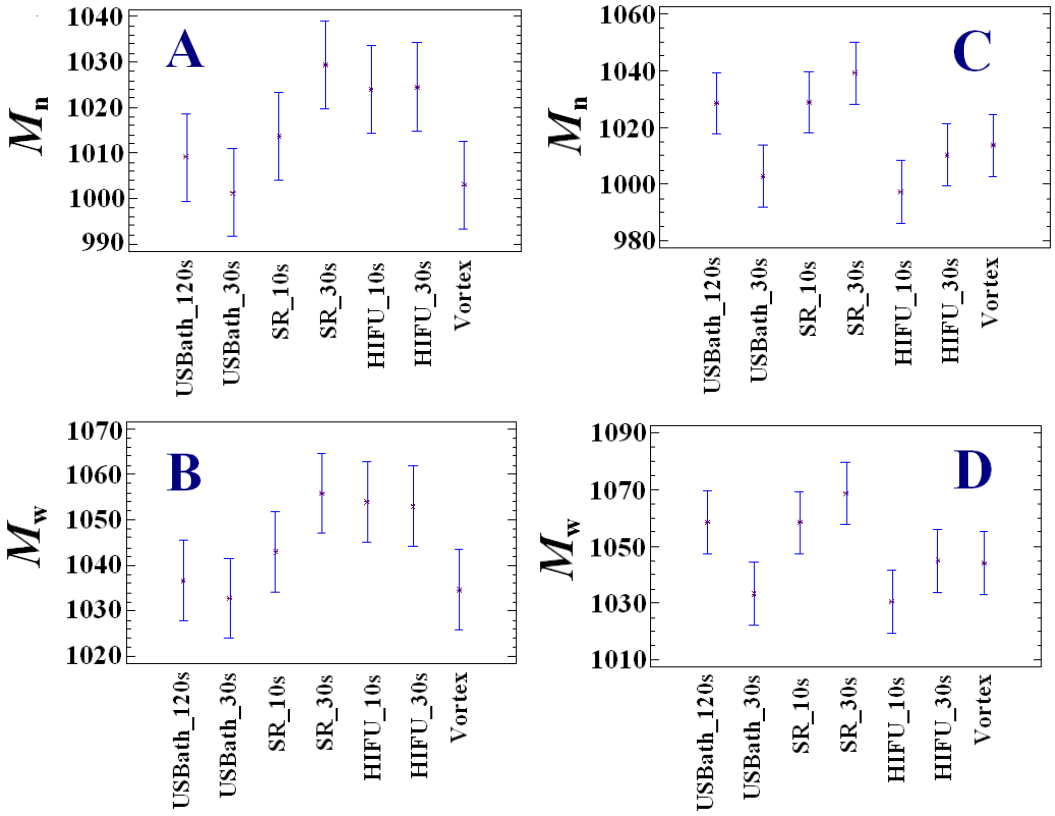

Figure III.3 Statistical analysis of means at 95% confidence level for the *M*n and *M*w values obtained for the poly(ethylene glycol) standard 1000 Da in dithranol (A and B) and DHB (C and D).

III.5 Conclusions

The most promising device for sample treatment for polymer characterization by MALDI seems to be the ultrasonic bath. With this system it was assayed two different frequencies of sonication 35 and 130 kHz. The homogenization process with the last frequency for the PS 2000 Da in DHB matrix during 120s, led to low $\overline{M}_w$ and $\overline{M}_n$ values, that were found statistically different from the values obtained for the sample homogenization using vortex and from the values giving by the polymer manufacturer. Despite of this results, when UB at a sonication frequency of 35 kHz was used, the values for $\overline{M}_w$ and $\overline{M}_n$ obtained for PS and PEG in dithranol matrix were not statistically different from the ones acquired with vortex mixing or from the values recommended by the manufacturers.

As a general role, the sonoreactor and the ultrasonic probe can be also used, but firstly needs to be clearly established by comparison with a regular mixing procedure, such as vortex, that they can be used without troubles in the sample preparation of a given polymer, since in this work the applicability of such devices was shown to be dependant of a series of factors such as the type of matrix used and the sonication time employed.

For PS analysis by MALDI the DHB matrix should not be used. This matrix needs six times more Ag as cationic reagent than dithranol, for the analysis of PS 2000 Da, making necessary to discard the spectrum of the first 50 shots due to the high saline content of the mixture. In addition, it was found a high dependence on the analyte/matrix mixing procedure for this matrix. For instance, PS 2000 in DHB can not be mixed with the ultrasonic bath at 130 kHz with a sonication time of 120 s. Moreover, when the mass of the poly(styrene) was increased from 2000 Da to 10000 Da, analysis with DHB matrix was not possible for any of the sample mixing procedures studied, even increasing the cationic agent 6 times more than the amount needed for the analysis of PS 10000 Da in dithranol.

For PEG analysis in dithranol, significant differences were found for M_n and M_w values, between vortex mixing and the sonoreactor (30 s of sonication time) and the sonication probe (10 s or 30 s of sonication time), the most intense sonication devices. When the matrix for PEG was DHB, M_n and M_w values obtained with vortex mixing were statistically different than those obtained with the sonoreactor (30 s of sonication time).

This pioneer work thus suggests that the UB with a sonication frequency of 35 kHz could be used for fast and high throughput sample treatment of polymers for their characterization. Nevertheless, this methodology needs of further confirmation and to be extended to more polymers, and for this reason more works dealing with this subject are anticipated.

III.6 Acknowledgments

R. Rial-Otero acknowledges the post-doctoral grant given by the FCT (Science and Technical Foundation) from Portugal (SFRH/BPD/23072/2005). C. Veiga de Macedo and M. Temtem acknowledge the doctoral grants SFRH/BD/19055/2004 and SFRH/BD/16908/2004, respectively, from FCT (Portugal).

III.7 References

[1] J. A. Castro, C. Koster, C.Wilkins, Rapid Commun. Mass Spectrom. 6 (1992) 239.

[2] S. F. Macha, P. A. Limbach, Curr. Opin. Solid State Mat. Sci. 6 (2002) 213.

[3] S. J. Wetzel, C. M. Guttman, K. M. Flynn, J. J. Filliben, J. Am. Soc. Mass spectrum. 17 (2006) 246.

[4] S. J Wetzel, C. M. Guttman, J. E. Girard, Int. J. Mass Spectrom. 238 (2004) 215.

[5] J. H. Gross. Mass spectrometry. A text book. Ed. Springer –Verlag. 2004; p. 425.

[6] K. J. Wu, R. W. Odom, Anal. Chem. 70 (1998) 456A.

[7] S. J. Wetzel, C. M. Guttman, K. M. Flynn, Rapid Commun. Mass Spectrom. 18 (2004) 1139.

[8] C. M. Guttman, S. J. Wetzel, J. E. Girard, W. R. Blair, B. M. Fanconi, R. J. Goldschmidt, W. E. Wallace, D. L. Van der Hart, Anal. Chem. 773 (2001) 1252.

[9] H. M. Santos, J. L. Capelo, Talanta 73 (2007) 795.

[10] D. C. Schriemer, L. Li, Anal. Chem. 68 (1996) 2721.

[11] J. L. Capelo, A. M. Mota, Curr. Anal. Chem. 1 (2005) 193.

[12] J. Axelsson, A. Hoberg, C. Waterson, P. Myatt, G. L. Shiel, J. Varney, D. M. Haddleton, P.J. Derrick, Rapid Commun. Mass Spectrom. 11 (1997) 209.

[13] R. P. Lattimer, J. Anal. Appl. Pyrolysis. 56 (2000) 61.

[14] German Institute for Standardization, http://www.din.de (last access Dezember 2007).

[15] J. N. Miller, J. C. Miller, Statistics and Chemometrics for Analytical Chemsitry. 4th edition. Chapter 4. Prentice Hall, 1999.

[16] Voyager Biospectrometry Workstation. User Guide. Applied Biosystems. USA, 2001; p.8-67.

Chapter IV

Exploiting anionic and cationic interactions with a new emissive imine-based β-naphthol molecular probe

Published in:

Inorganic Chemistry Communications, 12 (2009) 905-912

Luz Fernandes, Maxime Boucher, Javier Fernández-Lodeiro, Elisabete Oliveira, Cristina Nuñez, Hugo M. Santos, Tiago Silva, Jose Luis Capelo, Olalla Nieto Faza, Emilia Bertolo, Carlos Lodeiro.

(DOI: 10.1016/j.inoche.2009.07.011)

IV.1 Abstract

A new emissive molecular probe derived from 1,7-bis(2'-formylphenyl)-1,4,7-trioxaheptane and 2-hydroxy-1-naphthaldehyde has been synthesized by a Schiff-base condensation method. Its sensor capability towards cations such as Cu^{2+}, Zn^{2+}, Cd^{2+} and Hg^{2+}, and anions such as halides (F^-, Cl^-, Br^- and I^-) and CN^- was explored in DMSO solution. The geometry was optimized using Density Functional Theory (DFT). The probe showed remarkable selectivity for Cu^{2+} and interaction with the more basic anions CN^- and F^-.

Keywords: Molecular Probe; β-naphthol Emission; Anion; Density Functional Theory; DFT; Schiff-base

My contribution to this work was the optimization of sample treatment preparation for MALDI-TOF MS analysis, data acquisition and characterization, MALDI titrations and interpretation.

IV.2 Introduction and discussion

The development of new molecules whose properties can be modulated by interaction with anions [1] and cations [2] has received considerable attention in recent years. A fluorescence chemosensor or molecular probe is a system that exhibits changes in its properties upon interaction with an analyte. A fluorescence chemosensor is composed of receptor, chromophore and spacers. The receptor acts as a recognition unit for the target analyte. The chromophore exhibits changes in its optical signal (fluorescence or color) when the sensing takes place. The spacer links chemically receptor and chromophore units [3].

Schiff-base compounds incorporating a phenol or β-naphthol units have been reported as successful sensors due to their strong ability to detect metal ions and/or anions [4]. The presence of a hydroxyl group, potentially proton donor, can be used to modulate the fluorescence emission or colorimetric properties upon deprotonation, using PPT (Photoinduced Proton Transfer) or ESIPT (Excited State Intramolecular Proton Transfer) mechanisms [4]. Some of these compounds have been reported as selective sensors for Hg^{2+} or Cu^{2+}; these sensing effects can be determined using fluorescent (Hg^{2+}) or electrochemical (Cu^{2+}) measurements [4c], [5].

The synthesis of selective fluorescence chemosensors for soft-transition and post-transition metal ions with toxic effects in the environment (e.g. Cu^{2+}, Hg^{2+}, Cd^{2+} and Pb^{2+} has attracted considerable attention, due to the need of finding new methods for the rapid determination of these metals in environmental analysis and industrial wastewater treatment [6]. It is also important to detect anions such as cyanide, hydroxide, phosphate or halides, due to their extensive use in areas such as metallurgy, the plastic industry, photography and lithography processes, as well as medicine [7]. These anions have important negative impacts in the environment: cyanide, for example, is extremely toxic even in very low concentrations, being lethal to humans. Efforts are now focused on the synthesis of multifunctional molecular probes capable of recognizing both metal ions and anions.

As a part of our ongoing research in the design and synthesis of new fluorescence chemosensors [8] and matrix assisted laser desorption/ionization time-of-flight mass

spectrometry (MALDI-TOF MS) active probes, we present a new fluorescence ligand **L**, containing two emissive β-naphthol units as chromophores. Compound **L**, whose absorption and emission spectra are in the visible region, has been synthesized following a one-pot method using a Schiff-base condensation reaction. The presence of a complex chelating unit formed by two hydroxyl groups, two imine nitrogens, and the three oxygen atoms of a poly-oxa chain, gives the molecule strong recognition capability towards metal ions through formation of coordination compounds. Moreover, when the receptor has the hydroxyl groups protonated, it also allows the recognition of anions through the formation of hydrogen bonds.

The effect of cations such as Cu^{2+}, Zn^{2+}, Cd^{2+} and Hg^{2+}, and anions such as Cl^-, F^-, Br^-, I^- and CN^-, on the absorption, fluorescence and MALDI-TOF MS spectra has been studied. To conduct the analyses, the ligand was dissolved in DMSO or acetone and titrated with the analytes. A remarkable selectivity towards Cu^{2+}, and strong interaction with F^- and CN^- was observed. Moreover, metal complexes with Cu^{2+}, Zn^{2+} and Cd^{2+} were synthesized, in order to confirm the stoichiometry observed in solution by absorption and fluorescence spectroscopy.

Ligand **L** was synthesized following a one-pot method, by direct condensation of 1,7-bis(2'-formylphenyl)-1,4,7-trioxaheptane (**1**) [9] and the commercial carbonyl precursor and 2-hydroxy-1-naphthaldehyde. The reaction pathway is shown in Figure IV.1; details of the synthesis are given in note 10 (Reference section). **L** was isolated as an air-stable yellow solid, *ca*. 70% yield.

Elemental analysis data confirm that the Schiff-base **L** was isolated pure. The infrared spectrum (in KBr) shows a band at 1620 cm^{-1} corresponding to the imine bond, and no peaks attributable to unreacted amine or carbonyl groups were present. The absorption bands corresponding to the ν(C=C) vibrations of the phenyl groups appear at 1456 cm^{-1}. A band attributable to the C-O-C chain can be observed at 1158 cm^{-1}. The MALDI-TOF MS spectrum of **L** shows a parent peak at 597.2 *m/z*, corresponding to the protonated form of the ligand $[\mathbf{L}H]^+$. The ^1H NMR spectrum shows a peak at ca. 9.68 ppm, corresponding to the imine protons, and no signals corresponding to the amine protons are present. All the experimental data are summarized as a note [10].

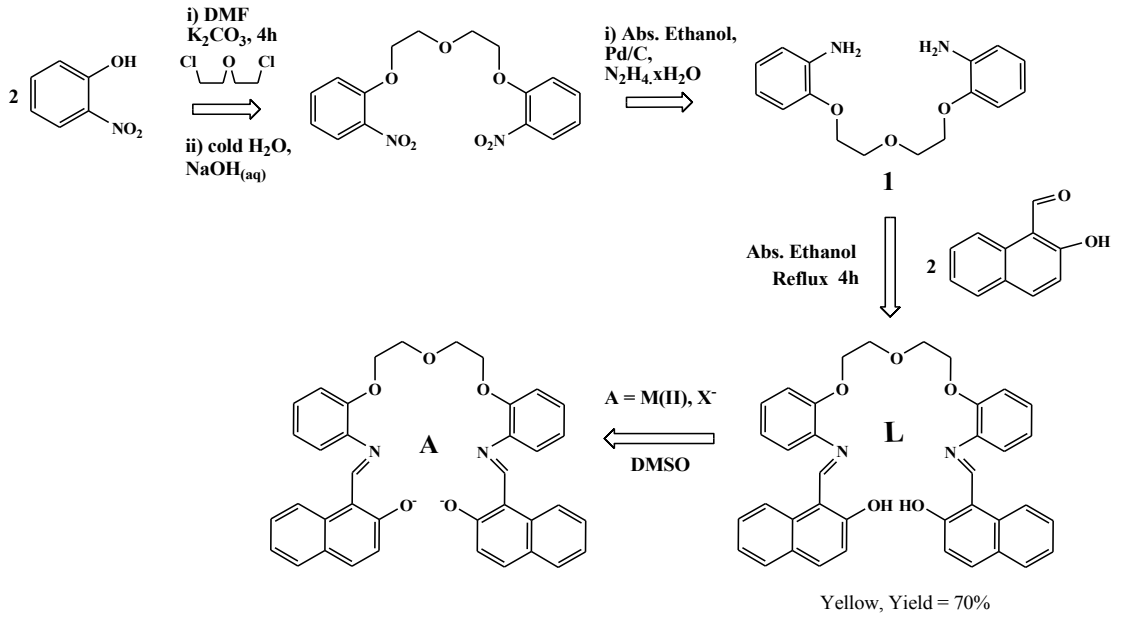

Figure IV.1 ChemDraw reaction-pathway of compound **L** and its complexes.

Density Functional Theory (DFT) calculations have been used to evaluate the stability of the proposed copper (II) complexes and provide structural information [11]. Several conformations have been considered for each compound, with special consideration to the sampling of both extended and coiled structures. The extended conformations for the free ligand, in which the tether between the chelating groups adopt an antiperiplanar conformation at every bond, are stable in solution; **L_a**, in which the most polarized regions are accessible by the solvent, is the lowest in energy. However, this trend is inverted if we consider the gas phase structures: a structure in which the ether oxygen atoms are in gauche is then the preferred conformation.

In this framework, copper (II) coordinates to a doubly deprotonated **L** to yield a neutral, covalently bonded 1:1 complex (**L** : Cu), with square planar geometry. The calculated Cu-O and Cu-N distances are very similar to those observed in the crystal structures of copper (II) complexes of the hydroxynaphtalenic Schiff bases published by Fernández-G. [12]. Our values of 1.94 Å for copper-oxygen bonds and 2.03 Å for copper-nitrogen bonds match the 1.9 and 2.0 Å reported by Fernández-G. Moreover, as in the case of their non-tethered ligands, both the two copper-nitrogen and the two copper-oxygen bonds are collinear in our complex. Other possible geometries for the coordination site that we have studied either converged to the structure of **L** : Cu, or led to structures considerably higher in energy.

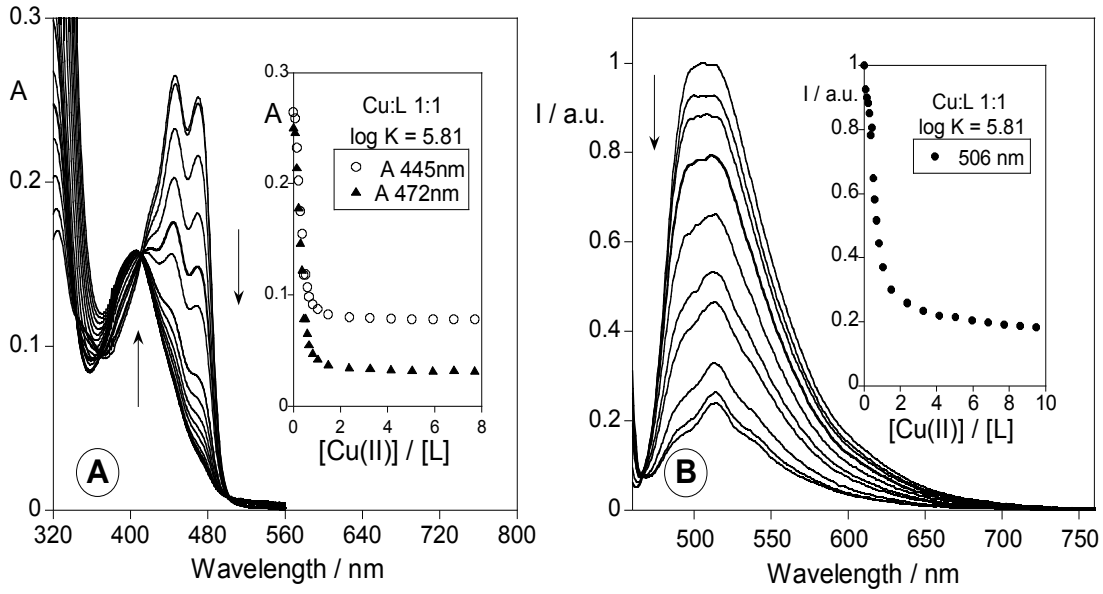

Figure IV.2 Spectrophometric (A) and spectrofluorimetric (B) titrations of ligand L in DMSO as a function of increasing amounts of $Cu(CF_3SO_3)_2$. The insets show the absorption at 445 and 472 nm, and the normalized fluorescence intensity at 506 nm. [L] = 1.00E^{-5}M ; λ_{exc}= 445nm.

When considering the structure of **L**, it is reasonable to expect that the polyether chain might play a role in the ligand's coordination to copper (II). Thus, several of the starting structures considered a helical conformation of **L** in which all its heteroatoms were at bonding distance from the central metal cation (about the actual bond distance for the naphtol oxygens and imine nitrogens and 2.5 Å for the ether oxygens). During the corresponding geometry optimizations the polyether chain relaxed away from the copper (II) ion, and the structures converged to **L_a**. We have also considered the possibility of copper (II) coordination to the non-deprotonated naphtol oxygens: this resulted in a structure not dissimilar to the neutral complex, with slightly shortened Cu-N bonds (2.0 Å) and elongated Cu-O bonds (2.0-2.1Å). In this case, the metal site is slightly less planar; this loss of planarity is more evident on the ligand, in which the extended conjugation seems to be broken at the nitrogen sites.

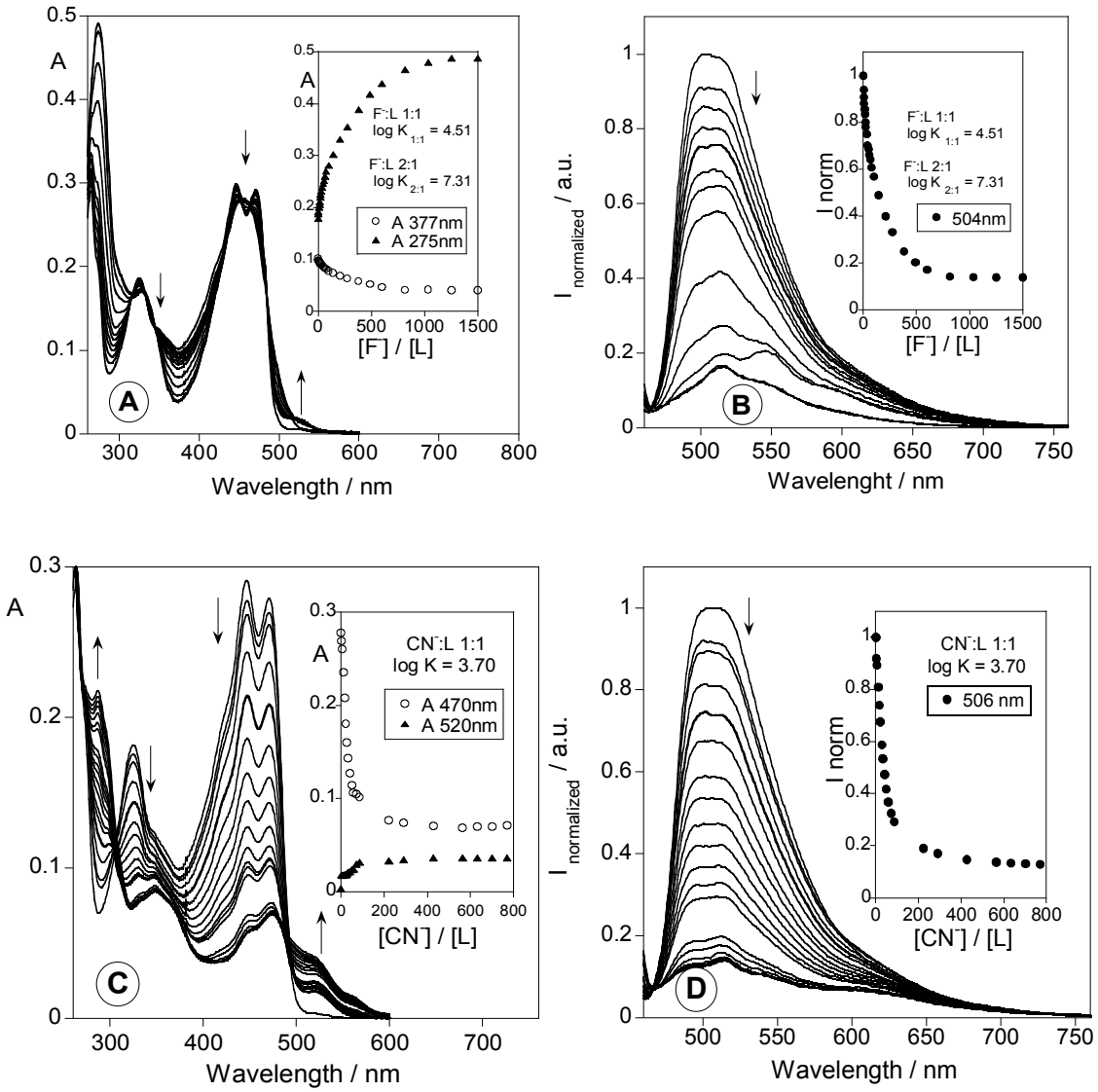

Figure IV.3 Spectrophometric (A) and (C) and spectrofluorimetric (B) and (D) titrations of ligand L in DMSO as a function of added $(Bu_4N)F$ and $(Bu_4N)CN$ respectively. The insets show the absorption at 275 and 377 nm for fluoride and at 470 and 520 nm for cyanide additions; and the normalized fluorescence intensity at 504 nm (F^-) and at 506 nm (CN^-) [L] = 1.00E^{-5}M ;λ_{exc}= 445nm.

To confirm the results obtained in solution by absorption and emission spectroscopy when studying the interaction of the ligand with the metal ions studied, some solid metal complexes were prepared by direct reaction between **L** and

$Cu(CF_3SO_3)_2$, $Zn(CF_3SO_3)_2$, and $Cd(ClO_4)_2.6H_2O$, by addition of the metal salt dissolved in absolute ethanol to a hot stirred solution of L in DMSO. In all cases, pure mononuclear complexes have been characterized [13]. The synthesis was also attempted using $Hg(CF_3SO_3)_2$; however, no analytical pure product was recovered on this case. The number of metal ions in each complex has been determined by atomic absorption spectrometry following methods reported previously [14]; all compounds were characterized by the usual techniques [15].

Ligands with absorption and emission spectral bands located in the visible region open up multiple possibilities in a variety of fields, from environmental analysis to biomedical research. The absorption spectrum of ligand L in DMSO (neutral pH) exhibits three bands at 328, 450 and 472 nm. The band at 328 nm corresponds to the π-π* transitions of the benzyl rings, and the last two bands to the π-π* transitions associated with the naphthol groups. The ligand exhibits a broad emission band centered at 508 nm (also in DMSO) with a relative fluorescence quantum yield of $\phi = 0.025$, when excited at 445 nm. The fluorescence quantum yielded was determined using as the reference a solution of $Ru(bpy)_3^{2+}$ with $\phi_f = 0.06$ in acetonitrile [16].

Upon addition of $Cu(CF_3SO_3)_2$ dissolved in absolute ethanol, the bands at 450 and 472 nm disappear. (see Figure IV.2A). The presence of a well-defined isosbestic point at 414 nm indicates that only two species are in equilibrium, the free ligand and the metal complex. The association constant of the Cu^{2+}-**L** complex, calculated with the program SPECFIT-32, is log K = 5.81 ± 0.10 [17]. This value was obtained from the absorption and fluorescence emission titrations, and it is slightly higher than the value previously reported by Duan and co-workers for a similar 2-hydroxyl-naphthalene derivative [4c]. Upon addition of one equivalent of Cu^{2+}, the fluorescence emission was quenched in ca. 80% (See Figure IV.2B). The molar ratio obtained was 1:1 M:**L**. This quenching of the emission upon complexation reflects the dissociation of the hydroxyl group of the naphthol moiety, which leads to the formation of the less emissive naphtholate anion. [4a].

The behavior of **L** in the presence of increasing amounts of Zn^{2+}, Cd^{2+} and Hg^{2+} was studied by absorption and emission spectroscopy. Even after addition of up to 30 equivalents of each metal ion, no significant changes in absorption or emission were observed. Competitive experiments were also carried out: only when Cu^{2+} was added to

the solution a remarkable interaction was observed. There is a strong interaction with the copper ion through coordination between the metal and the hydroxyl groups of the β-naphthol units. Zn^{2+}, Cd^{2+} and Hg^{2+}, cannot remove the protons by coordination and thus do not affect the native fluorescence emission.

The solid metal complexes were synthesized (see note 13) in order to check the ligand-metal molar ratio. Only for the Cu^{2+} complex the analytical data fit well with what would be expected for a neutral complex, suggesting coordination through the deprotonated hydroxyl groups. However, solid Zn^{2+} and Cd^{2+} complexes have been isolated with two counter ions. This could explain why these two metals, as well as Hg^{2+}, do not affect the fluorescence emission of the β-naphthyl groups; it is likely that the coordination takes place through the imine bonds and the poly-oxa chain, too far from the emissive chromophore units. In the solid state all complexes show a very low fluorescence emission centered at ca. 524 nm, ten nm blue-shifted from the free ligand.

We have also studied the interaction of **L** in DMSO with the anions F^-, Cl^-, Br^-, I^- and CN^-. Compounds containing OH or NH binding groups can be used to study anionic interactions: it is the formation of $X^{-\cdots}H$-O hydrogen interactions which leads to the recognition event. Excess of these anions can also cause deprotonation, resulting in a classical Bronsted acid-base reaction [2d,18]. The deprotonation usually results in a dramatic change in the color of the solution, or an intense modification of the fluorescence spectra. Addition of negative charged anions can deprotonate both hydroxyl groups of the β-naphthyl units.

In our case, these interactions were observed only for CN^- and F^-. Absorption and emission titrations are represented in Figures IV.3A-D. In the absorption spectrum, the bands at 450 and 472 nm disappear; this decrease is more intense for the case of cyanide. At the same time, a small band centered at 521 (CN^-) or 535 nm (F^-) can be observed. The association constants obtained from the absorption spectra, calculated with the SPECFIT-32 program [17], point towards the formation of one molecular species with stoichiometry of 1:1 (CN:L) in the case of cyanide, and two species for fluoride, with 1:1 and 2:1 stoichiometry (F:L). The values for the constants are log K = 3.70 ± 0.05 (CN^-), log K = 4.51 ± 0.20 (1:1 F^-) and log K = 7.31 ± 0.23 (2:1 F^-) respectively. Figures IV.3B and IV.3D shows the fluorescence emission titration upon addition of $(Bu_4N)F$ and $(Bu_4N)CN$ respectively. A strong quenching effect was observed for both anions, with the interaction

constant for fluoride being larger than for cyanide. The association constants obtained from the fluorescence spectra agree with those obtained from the absorption ones, which again confirms the formation of the less emissive naphtholate species.

In order to discard an acid-base reaction between **L** and the basic anions, instead of a supramolecular interaction, several DFT studies were performed. In contrast with its coordination to metal cations, the complexation of **L** with the anionic ligands CN^- and F^- takes place through non-covalent interactions, making use of the polar naphtol groups to stabilize the negative charge in the anions with hydrogen bonds. We have optimized the geometry of the 1:1 complexes with CN^- and F^-: in both cases, the most stable structure is that in which two hydrogen bonds are formed with the anion. In the case of CN^-, the interaction gave a linear structure, as expected from the available orbitals, with a N-H bond of 1.6 Å N-H bond and a C-H bond of 1.7 Å. For F^-, the most stable structure displays a 90º H-F-H angle (the F-H-O angles are still linear), with F-H distances of 1.4 Å, even if another linear minimum is found to be only 2.9 kcal/mol less stable. Somewhat higher in energy for both anions (about 14 kcal/mol), however, lie the other complexes where the anion has abstracted one of the protons (which then forms a hydrogen bond with the resultant naphtolate) and interacts with the other through a hydrogen bond. TDDFT has been used to simulate the UV-visible spectra of all the computed structures, and the results, together with further thermodynamic and structural information can be found in the Supporting Information.

Several MALDI-TOF MS mass spectra were obtained, using the free ligand **L** dissolved in acetone without any matrix, and upon titration with Cu^{2+} and cyanide. The ligand peak in the MALDI-TOF MS positive mode appears at 597.1 m/z; this peak can be attributed to the protonated species $[LH]^+$. In negative mode the peak appears at 595.1 m/z, corresponding to the species [L]. (See Figure IV.4, panels A and B).

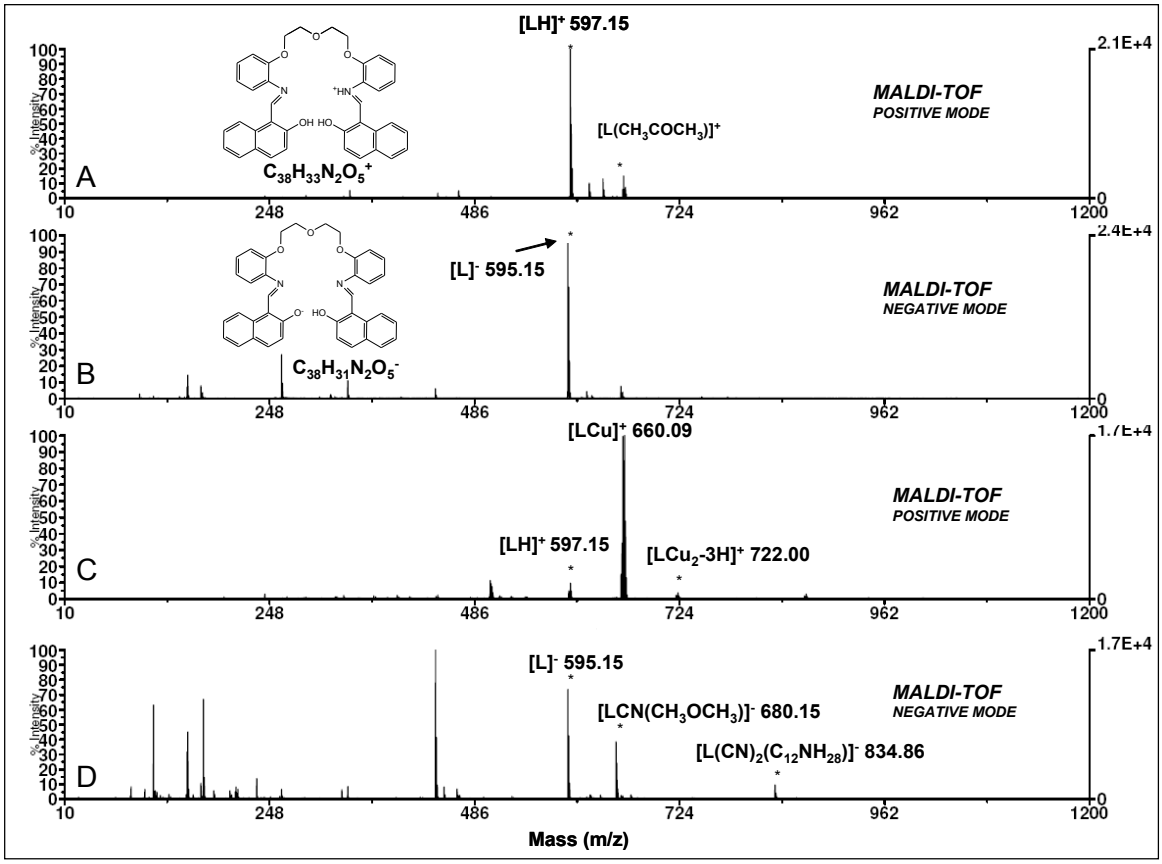

Figure IV.4 MALDI-TOF mass spectra of ligand L in positive (A) and negative (B) modes in acetone. Panel C shows the spectrum (positive mode) after titration with Cu(CF3SO3)2 (one equivalent of metal). Panel D shows the spectrum (negative mode) after the addition of ten equivalents of (Bu4N)CN solution.

In positive mode, upon addition of one equivalent of Cu^{2+}, the peak attributable to the ligand disappears, and a new peak with 100% of intensity appears at 660.09; this peak corresponds to the mononuclear species $[LCu]^+$. A second small peak at 722.0 m/z, attributable to the dinuclear species also was formed. (See also Figure IV.4, panel C). The pattern of the mononuclear peak observed at 660.09 m/z fits well with a complex isotopic model obtained using the program from the DATA EXPLORER instrument (see Figure IV.5). This model takes into account several species with formula $C_{38}H_{32}CuN_2O_5$ $[LCu]^+$, $C_{38}H_{31}CuN_2O_5$ $[LCu\text{-}H]^+$, $C_{38}H_{30}CuN_2O_5$ $[LCu\text{-}2H]^+$ and $C_{38}H_{29}CuN_2O_5$ $[LCu\text{-}3H]^+$. This suggests the formation in gas phase of several protonated complexes, by losing one hydroxyl protons, two and tree protons in the ligand. The most intense signals corresponded to isotope model 2, attributable to the species $[LCu]^+$. As it can be seen in Figure IV.5, the sum of the four isotopic models suggested fits well with the experimental

peak obtained. The same model can be applied for the dinuclear peak at 722.0 m/z , formed only in the gas phase.

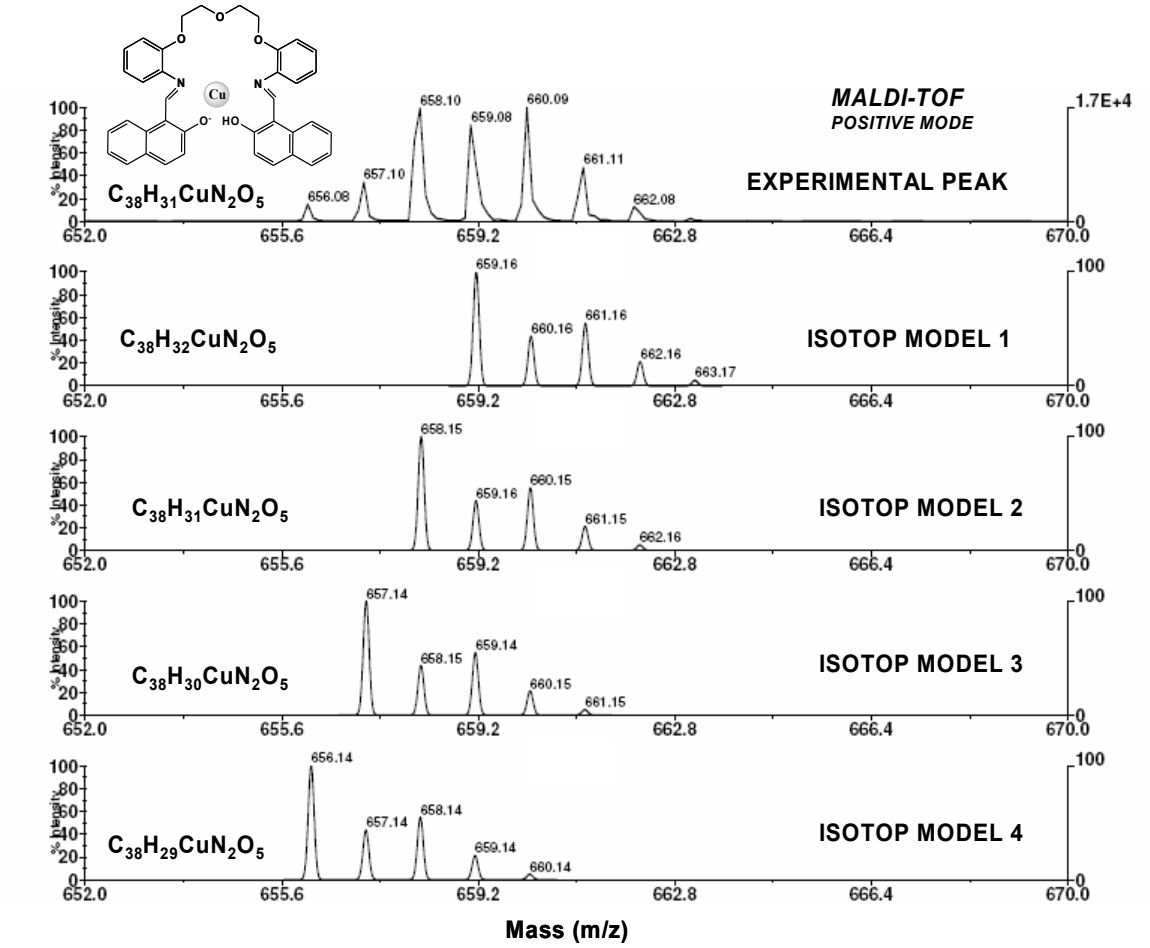

Figure IV.5 ISOTOP model for the peak at 660.09 m/z observed in the MALDI-TOF mass spectrum of ligand **L** upon addition of one equivalent of Cu(II); the peak can be attributed to the $[\mathbf{L}Cu]^+$ complex.

In the negative MALDI-TOF MS mode, addition of ten equivalents of CN^- induced the formation of two peaks at 680.15 m/z and 834.86 m/z, attributable to the formation of the species $[LCN(CH_3COCH_3)]^-$ and $[L(CN)_2(C_{12}NH_{28})]^-$ respectively (See figure IV.4, panel D). Unfortunately, no peak was observed when the ligand was titrated with a stoichiometrical quantity of fluoride anion; for higher concentrations of fluoride (ten equivalents) the peak corresponding with the $[\mathbf{L}F]^-$ species was observed. The results from these experiments suggest that **L** can be used to sense Cu^{2+} in positive MALDI-TOF MS mode, and cyanide by MALDI-TOF MS negative mode.

In conclusion a new fluorescence β-naphtol derivative **L**, containing an N_2O_5 donor set has been synthesised in excellent yield by a simple Schiff-base condensation reaction, and its photophysical properties have been evaluated in solution by absorption and fluorescence emission spectroscopy and by MALDI-TOF MS spectrometry. Its capacity to act as a potential sensor for Cu^{2+}, Zn^{2+}, Cd^{2+} and Hg^{2+}, and the basic anions such as F^-, Cl^-, Br^-, I^- and CN^-, was carried out in DMSO solution. Among the cations and anions studied, the probe has shown a remarkable selectivity for Cu^{2+}, CN^- and F^-. This selectivity means that the new ligand could find an application as the building block to design a more complex chemosensor for these three ions.

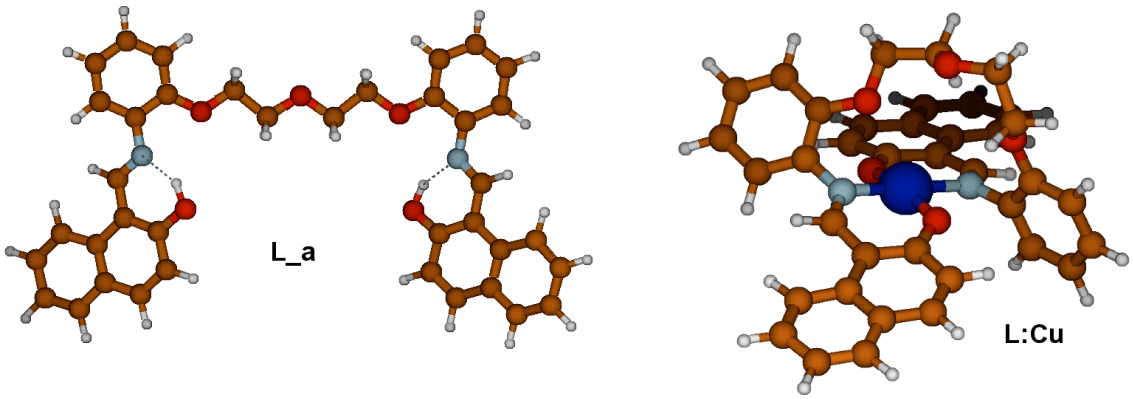

Figure IV.6 Ball-and-stick representation of the structure of the free ligand (L) and its copper(II) complex optimized at the B3LYP/6-31G(d), LANL2DZ level.

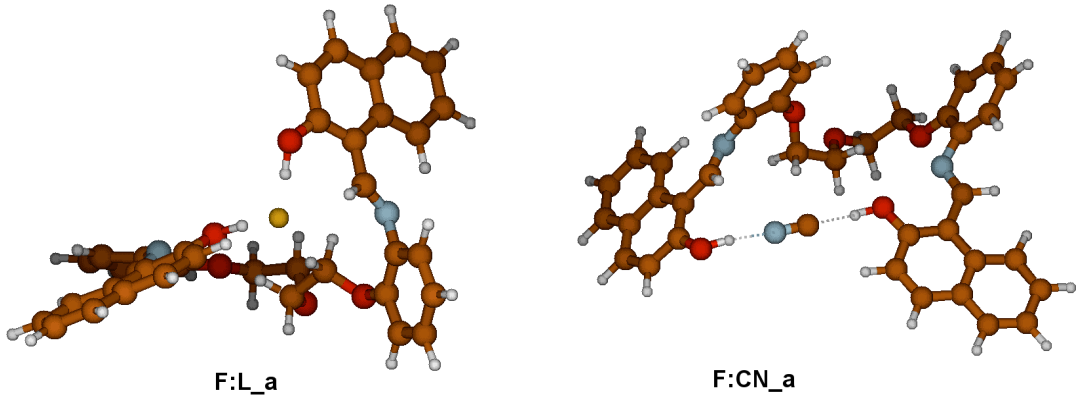

Figure IV.7 Ball-and-stick representation of the most stable CN^- and F^- complexes of **L** optimized at the B3LYP/6-31G(d), LANL2DZ level.

The interaction of **L** with Cu (II), CN^- and F^- was also studied using MALDI-TOF mass spectrometry (both in positive and negative mode). No peak was observed when the ligand was titrated with fluoride anion in stoichiometry concentrations appearing a peak assigned to $[\mathbf{L}F]^-$ when the concentration of F^- was increased. In the other hand, noteworthy changes in the mass spectrum of the ligand (either in the positive or negative mode) were observed upon titration with Cu^{2+} and CN^-. The results from the MALDI-TOF MS studies suggest that **L** can be used to sense Cu^{2+} in positive mode, and cyanide in negative mode. DFT studies showed that the Copper (II) complex is formed by the unprotonated $\mathbf{L}^{2-}$ species as was predicted experimentally. However, the anionic complexes with fluoride and cyanide take places via supramolecular interactions with the diprotonated **L** form. This clearly demonstrated that **L** is not deprotonated upon anion interaction.

IV.3 Acknowledgments

The authors are grateful to *FCT-MCTES Portugal by* project PTDC/QUI/66250/2006, InOu 2009-UVIGO and *Canterbury Christ Church University* Research Fund for financial support. E. B, J. L. C. and C. L thank bilateral program "Acções integradas Luso-Británicas 2006", agreement numbers B-16/06 and B-61/07. E. O. and H. S. acknowledge the FCT/Portugal PhD grants (SFRH/BD/35905/2007) and (SFRH/BD/38509/2007) respectively. C.N. thanks Xunta de Galicia (Spain) for her *Maria Barbeito* pre-doctoral contract. J. L. C. and C. L. thank Xunta de Galicia for the Isidro Parga Pondal Research Program. We also thank the CESGA (Centro de Supercomputación de Galicia) for generous allocation of computational resources.

IV.4 Appendix A. Supplementary material

Supplementary data associated with this article can be found, in the online version, at doi:10.1016/j.inoche.2009.07.011.

IV.5 References

[1] (a) H. Tong, G. Zhou, L. X. Wang, X. B. Jing, F. S. Wang, J. P. Zhang, Tetrahedron Lett., 44 (2003) 131; (b) T. Gunnlaugsson, P. E. Kruger, T. C. Lee, R. Parkesh, F. M. Pfeffer, G. M. Hussey, Tetrahedron Lett. 44 (2003) 6575; (c) C. F. Chen, Q. Y. Chem, Tetrahedron Lett., *45* (2004) 3957; (d) R. M. F. Batista, E. Oliveira, C. Nunez, S. P. G. Costa, C. Lodeiro, M. M. M. Raposo, J. Phys. Org. Chem., (2009), DOI 10.1002/poc.1440; (e) M. P. Clares, C. Lodeiro, D. Fernández, A. J. Parola, F. Pina, E. García-España, C. Soriano, R. Tejero, Chem. Commun., (2006) 3824; (f) E. Arturoni, C. Bazzicalupi, A. Bencini, C. Caltagirone, A. Danesi, A. Garau, C. Giorgi, V. Lippolis, B. Valtancoli, *Inorg. Chem*., *47* (2008), 6551.

[2] (a) M. Beltramello, M. Gatos, F. Macin, P. Tecilla, U. Tonellato, Tetrahedron Lett., 42 (2001) 9143; (b) P. Kele, T. L. Calhoun, R. E. Gawley, R.M. Leblanc, Tetrahedron Lett., 43 (2002) 4413; (c) C. F. Chen, Q. Y. Chem, Tetrahedron Lett., *46* (2005), 165; (d). R. M. F. Batista, E. Oliveira, S. P. G. Costa, C. Lodeiro, M. M. M. Raposo, Org. Lett., *9* (2007) 3201; (e) N. H. Lee, H. N. Kim, K. M. K. Swamy, M. S. Park, J. Kim, H. Lee, K. H. Lee, S. Park, J. Yoon, Tetrahedron Lett., 49 (2008) 1261; (f) A. Tamayo, C. Lodeiro, L. Escriche, J. Casabó, B. Covelo, P. González, Inorg. Chem., 44 (2005) 8105; (g) A. Tamayo, B. Pedras, C. Lodeiro, L. Escriche, J. Casabó, J. L. Capelo, B. Covelo, R. Kivekäs, R. Sillampäa, Inorg. Chem., 46 (2007) 7618; (h) G. Farrugia, S. Iotti, L. Prodi, M. Montalti, N. Zaccheroni, P. B. Savage, V. Trapani, P. Sale, F.I. Wolf, J. Am. Chem. Soc., 128 (2006) 344.

[3] (a) A. W. Czarnik, Acc. Chem. Res., 27 (1994) 302; (b) C. Lodeiro, F. Pina, Coord. Chem. Rev. 253 (2009) 1353.

[4] (a) K-C. Wu, Y-S. Lin, Y-S. Yeh, C-Y. Chen, M. O. Ahmed, P-T. Chou, Y-S. Hon, Tetrahedron, 60 (2004) 11861; (b) J. Ren, W. Zhu, H. Tian, *Talanta*, 75 (2008) 760; (c) C. He, Y. Zhao, C. He, Y. Liu, C. Duan, Inorg.

Chem., 47 (2008) 5169; (d) T. C. Chien, L. G. Dias, G. M. Arantes, L. G. C. Santos, E. R. Triboni, E. L. Bastos, M. J. Politi, J. Photochem. Photobiol. A. Chem., 194 (2008) 37.

[5] N. Alizadeh, S. Ershad, H. Naeimi, H. Sharghi, M. Shamsipur, Fresenius J. Anal. Chem., 365 (1999) 511.

[6] (a) M. C. Aragoni, M. Arca, F. Devillanova, F. Isaia, A. Garau, V. Lippolis, U. Papke, M. Shamsipur, A. Yari, G. Verani, Inorg. Chem., 41 (2002) 6623; (b) F. Y. Wu, S. W. Bae, J. I. Hong, Tetrahedron Lett., 47 (2006) 8851.; (c) F. Zapata, A. Caballero, A. Espinosa, A. Tarraga, P. Molina, Org. Lett., 10, (2008) 41.; (d) R. Shunmugan, G. J. Gabriel, C. E. Smith, K. A. Aamer, G. N. Tew., Chem. Eur. J., 14 (2008) 3904.; (e) E. W. Miller, Q. W. He, C. J. Chang, Nat. Prot., 3 (2008) 777.

[7] (a) B. C. Tzeng, Y. F. Chen, C. C. Wu, C. C. Hu, Y. T. Chang, C. K. Cheng., New J. Chem., 31 (2007) 202.; (b) T. P. Lin, C. Y. Chen, Y. S. Wen, S. S. Sun., Inorg. Chem., 46 (2007) 9201. (c) N. Singh, D. O. Jang, Org. Lett., 9 (2007) 1991.; (d) V. Thiagarajan, P. Ramamurthy, Spec. Acta A., 67 (2007) 772.

[8] (a) S. P. G. Costa, E. Oliveira, C. Lodeiro, M. M. M. Raposo, Tetrahedron Let. 49 (2008) 5258; (b) C. Nuñez, L. Valencia, A. Macias, R. Bastida, E. Oliveira, L. Giestas, J. C. Lima, C. Lodeiro, Inorg. Chim. Acta. 8 (2008) 2183; (c) S. P. G. Costa, E. Oliveira, C. Lodeiro, M. M. M. Raposo. Sensors, 7 (2007) 2096; (d) B. Pedras, H. M. Santos, L. Fernandes, B. Covelo, A. Tamayo, E. Bértolo, T. Avilés, J. L. Capelo, C. Lodeiro, Inorg. Chem. Commun., 10 (2007), 929.; (e) A. Tamayo, L. Escriche, J. Casabó, B. Covelo, C. Lodeiro, Eur. J. Inorg. Chem., (2006) 2997.

[9] Precursor **1** was synthesized following the published method: (a) P. A. Tasker, Y. E. B. Fleisher, J. Am. Chem. Soc., 92 (1970) 7072; b) M. Vicente, C. Lodeiro, H. Adams, R. Bastida, A. de Blás, D. E. Fenton, A. Macías, Rodríguez, A.; T. Rodríguez-Blás, Eur. J. Inorg. Chem., (2000) 1015.

[10] Ligand **L** was prepared as follows. A solution of 1,7-bis(2'-formylphenyl)-1,4,7-trioxaheptane (1 mmol) in absolute ethanol (40 mL) was added dropwise to a solution of and 2-hydroxy-1-naphthaldehyde (2 mmol) in the same solvent (30 mL). The resulting solution was gently refluxed with magnetic stirring for ca. 2 h. The initial yellow colour of the solution changed quickly to orange. The solution,

kept under Argon atmosphere, was stirred for 4h. A yellow powder precipitate formed, which was then filtered off, washed with cold absolute ethanol and cold diethyl ether, and dried under vacuum. **L**: Colour: Yellow. Yield 0.44 g (70%). Anal. Calcd for $C_{38}H_{22}N_2O_5.0.5H_2O$: C, 75.35; H, 5.50; N, 4.63; Found: C, 75.55; H, 5.26; N, 4.54; IR (cm^{-1}): $\nu(C=N)_{imine}$ 1620 cm^{-1}, $\nu(C=C)$ 1456 cm^{-1}, $\nu(C-O-C)$ 1158 cm^{-1}; H^1-NMR (DMSO-d^6), δ (ppm): 9.83 (d, 2H, Ar-OH); 9.68 (d, 2H, CH_{imine}); 6.68-8.07 (m, 20H, Ar-H); 4.11 (d, 4H, Ar-O-CH_2); 3.79 (d, 4H, CH_2-O-R); MALDI-TOF MS (*m/z*): 597.2 $[\mathbf{L}H]^+$.

[11] Geometry optimizations of the free ligand (L) and its Cu2+ F- and CN- complexes have been carried out at the B3LYP/6-31G(d) level, using the LANL2DZ electron core potential and its associated basis set for copper. Harmonic analysis was used to confirm that all optimized structures correspond to minima, and wave functions have been shown to be stable for all structures considered. Single point calculations have been performed on the optimized geometries to take into account the effect of solvent, using a continuum model (PCM) with the dielectric constant of dimethyl sulfoxide. All calculations have been performed with Gaussian03. (M. J. Frisch, G. W. Trucks, H. B. Schlegel, G. E. Scuseria, M. A. Robb, J. R. Cheeseman, J. A. Montgomery, Jr., T. Vreven, K. N. Kudin, J. C. Burant, J. M. Millam, S. S. Iyengar, J. Tomasi, V. Barone, B. Mennucci, M. Cossi, G. Scalmani, N. Rega, G. A. Petersson, H. Nakatsuji, M. Hada, M. Ehara, K. Toyota, R. Fukuda, J. Hasegawa, M. Ishida, T. Nakajima, Y. Honda, O. Kitao, H. Nakai, M. Klene, X. Li, J. E. Knox, H. P. Hratchian, J. B. Cross, V. Bakken, C. Adamo, J. Jaramillo, R. Gomperts, R. E. Stratmann, O. Yazyev, A. J. Austin, R. Cammi, C. Pomelli, J. W. Ochterski, P. Y. Ayala, K. Morokuma, G. A. Voth, P. Salvador, J. J. Dannenberg, V. G. Zakrzewski, S. Dapprich, A. D. Daniels, M. C. Strain, O. Farkas, D. K. Malick, A. D. Rabuck, K. Raghavachari, J. B. Foresman, J. V. Ortiz, Q. Cui, A. G. Baboul, S. Clifford, J. Cioslowski, B. B. Stefanov, G. Liu, A. Liashenko, P. Piskorz, I. Komaromi, R. L. Martin, D. J. Fox, T. Keith, M. A. Al-Laham, C. Y. Peng, A. Nanayakkara, M. Challacombe, P. M. W. Gill, B. Johnson, W. Chen, M. W. Wong, C. Gonzalez, and J. A. Pople, Gaussian 03, Revision C.02, Gaussian, Inc., Wallingford CT (2004)

[12] Fernández-G., J. M.; Lembrino-Canales, J. J.; Villena-I. R. Monatshefte für hemie, 125, (1994), 275.

[13] **Metal complexes**. *General Procedure*. Work was performed under argon atmosphere using vacuum line techniques, as well as dried solvents. A solution of the corresponding metal salt (0.15 mmol) dissolved in absolute ethanol (10 mL) was added to a refluxing solution of **L** (0.15 mmol) in DMSO/acetone (90/10 v/v, 20 mL). The resulting mixture was stirred overnight at room temperature. A precipitate was formed, which was then filtered off, washed with cold diethyl ether and dried under vacuum. **LCu.4H$_2$O:** Color: dark orange. Yield 0.105 g (73%). Anal. Calcd for $C_{38}H_{38}CuN_2O_9$: C, 62.50; H, 5.24; Cu, 8.70; N, 3.84; Found: C, 62.32; H, 5.31; Cu, 8.92; N, 3.66; IR (cm^{-1}): ν(C=N)$_{imine}$, 1615; ν(C=C) 1460 cm^{-1}; MALDI-TOF MS (*m/z*): 597.2 [**L**H]$^+$; 657.3 [**L**Cu-2H]$^+$; 673.5 [**L**Cu(H$_2$O)]$^+$. The compound is soluble in chloroform, acetone, DMSO and insoluble in water and diethyl ether. **LZn(CF$_3$SO$_3$)$_2$.H$_2$O:** Color: yellow. Yield 0.038 g (26%). Anal. Calcd for $C_{41}H_{34}F_9N_2O_{15}S_3Zn$: C, 43.68; H, 3.04; N, 2.49; S, 8.53; Zn, 5.80 Found: C, 43.92; H, 3.31; N, 2.66; S, 8.93; Zn, 5.30. IR (cm^{-1}): ν(C=N)$_{imine}$, 1622; ν(C=C) 1458 cm^{-1}; MALDI-TOF MS (*m/z*): 597.7 [**L**H]$^+$; 661.3 [**L**Zn-H]$^+$. The compound is soluble in chloroform, acetone, DMSO and insoluble in water and diethyl ether. **LCd(ClO$_4$)$_2$.2H$_2$O:** Color: Yellow. Yield 0.031 g (22%). Anal. Calcd for $C_{38}H_{36}CdCl_2N_2O_{15}$: C, 48.35; H, 3.84; N, 2.97; Found: C, 47.95; H, 3.51; N, 2.66; IR (cm^{-1}): ν(C=N)$_{imine}$, 1640; ν(C=C) 1456 cm^{-1}; MALDI-TOF MS (*m/z*): 597.4 [**L**H]$^+$; 710.8 [**L**Cd]$^+$. The compound is soluble in chloroform, acetone, DMSO and insoluble in water and diethyl ether.

[14] C. Lodeiro, J. C. Lima, A. J. Parola, J. S. S. de Melo, J. L. Capelo, B. Covelo, A. Tamayo, B. Pedras, Sens. Act. B. Chem., 115 (2006) 276.

[15] Elemental analyses were carried out at the REQUIMTE DQ Service (Universidade Nova de Lisboa), on a Thermo Finnigan-CE Flash-EA 1112-CHNS instrument. Infrared spectra were recorded as KBr discs using Bio-Rad FTS 175-C spectrophotometer. Proton NMR spectra were recorded using a Bruker WM-400 spectrometer. MALDI-TOF MS analysis were performed in a MALDI-TOF MS model voyager DE-PRO biospectrometry workstation equipped with a nitrogen laser radiating at 337 nm from Applied Biosystems (Foster City, United States) at

the REQUIMTE DQ, Universidade Nova de Lisboa. The acceleration voltage was 2.0×10^4 kV with a delayed extraction (DE) time of 200 ns. The spectra represent accumulations of 5×100 laser shots. The reflectron mode was used. The ion source and flight tube pressures were less than 1.80×10^{-7} and 5.60×10^{-8} Torr, respectively. The MALDI mass spectra of the soluble samples (1 or 2 μg/μL) such as metal salts and anions were recorded using the conventional sample preparation method for MALDI-MS. 1μL was placed on the sample holder on which the chelating ligand had been previously spotted. The sample holder was inserted in the ion source. Chemical reaction between the ligand and the analyte occurred in the holder and complexed species were produced. Absorption spectra were recorded on a Perkin Elmer lambda 35 spectrophotometer, and fluorescence emission on a Perkin Elmer LS45. The linearity of the fluorescence emission *vs.* concentration was checked in the concentration range used (10^{-4}-10^{-6} M). Corrections for the absorbed light and dilutions were performed when necessary. All spectrofluorimetric titrations were performed as follows: a stock solution of the ligand (ca. 1.00×10^{-3} M) were prepared by dissolving an appropriate amount of the ligand in a 50 mL volumetric flask and diluting to the mark with DMSO UVA-sol. The titration solutions ([**L**] = 1.00×10^{-6} and 1.00×10^{-5} M) were prepared by appropriate dilution of the stock solution. Titrations were carried out by addition of microliter amounts of standard solutions of the ions dissolved in absolute ethanol or DMSO. Fluorescence spectra of solid samples were recorded on the Horiba-Jobin-Yvon SPEX Fluorolog 3.22 spectrofluorimeter using a fiber optic device exciting at appropriated λ (nm) the solid compounds. Cu^{2+} determinations were performed in a Varian model Zeeman spectrAA300 plus atomic absorption spectrometer in combination with an auto sampler; pyrolitic graphite-coated graphite tubes with platform were used. For the determination of copper concentration, 20 μL of solution were injected into the graphite furnace, where it was dried, ashed and atomized. The signal was measured in the peak area mode. Each completed determination was followed by a 2 s clean-up cycle of the graphite furnace at 2800 ºC. During the drying, ashing, and clean-up cycles, the internal argon gas was passed through the graphite furnace at 300 mL/min. The internal argon gas flow was interrupted during the atomization cycle, but was restored for the clean-up cycle. The relative standard deviation among replicate

was typically <5%. The FAAS measurements of Zn^{2+} were made using a Varian (Cambridge, UK) atomic absorption spectrometer model SpectrAA 20 plus equipped with a 10 cm burner head. A hollow-cathode lamp operated at 5 mA was used. The wavelength used was 213.9 nm, and the slit width 1.0 nm.

[16] M. Montalti, A. Credi L. Prodi, M. T. Gandolfi. "Handbook of Photochemistry", 3th Ed. CRC Press, Taylor & Francis Group, Boca Raton, New York (2006).

[17] SPECFIT/32 Global Analysis System, v. 3.0 Spectrum Software Associates, Malborough, MA, USA.

[18] (a) D. Saravanakumar, S. Devaraj, S. Iyyampillai, K. Mohandoss, M. Kkandaswamy, Tetrahedron Let., 49 (2008) 127; (b) D.E. Gomez, L. Fabbrizzi, M. Liccheli, J. Org. Chem., *70* (2005) 5717; (c) V. Amendola, E. Boicchi, B. Colasson, L. Fabbrizzi, Inorg. Chem., 45 (2006) 6138.

Chapter V

Synthesis, characterization and fluorescence behavior of four novel macrocyclic emissive ligands containing a flexible 8-hydroxy-quinoline unit

Published in:

Tetrahedron, 65 (2009) 6179-6188

Cristina Núñez, Rufina Bastida, Alejandro Macias, Emília Bértolo, Luz Fernandes, José Luis Capelo e Carlos Lodeiro.

(DOI: 10.1016/j.tet.2009.05.046)

V.1 Abstract

Four emissive macrocyclic ligands mono-substituted with an 8-hydroxyquinoline pendant-arm are presented. The new compounds have been used for metal ion detection, which results from the competition between PET (photo-induced electron transfer) and PPT (photo-induced proton transfer) mechanisms. Solid metal complexes with divalent Cu(II), Zn(II) and Cd(II), and trivalent metal ions Al(III) and Cr(III) have been also synthesized and characterized. The compounds have been isolated as mononuclear or dinuclear (Cu(II)) complexes, confirming the stoichiometry observed in solution.

Keywords: Chemosensor; Fluorescence; 8H-Quinoline; Aluminum(III); Chromium(III); Zinc(II).

My contribution to this work was the optimization of sample treatment preparation for MALDI-TOF MS analysis, data acquisition and characterization, MALDI titrations and interpretation.

V.2 Introduction

The development of compounds that selectively respond to specific metal ions and thus can be used as ion sensors is an area of growing interest [1]. Emphasis has been placed on the development of compounds that can detect the presence of specific metal ions through guest-modulated effects, e.g., changes in redox potentials [2], UV-vis absorption spectra [3], or fluorescence spectra [1] as a result of the interaction between the sensor and the target ion. Particular attention has been paid to fluorescence chemosensors, since fluorescence modulation allows the detection of the target ions at very low concentrations [1b]; moreover, fluorescent sensors offer several distinct advantages such as selectivity, time response and spatial resolution.

8-Hydroxyquinoline (8-HQ) and derived compounds are known to be the best chelating agents after EDTA and its derivatives, due to their guest-modulated chromogenic and fluorescent behaviour. Accordingly, they have been used in chromatography [4] for the detection of metal ions [5], in the preparation of organic light emitting diode devices [6], in electrochemiluminiscence [7], etc. 8-HQ forms stable five-membered chelate rings with metal centres, and very stable complexes of the type $M(HQ)^+$, $M(HQ)_2$ or $M(HQ)_3$ with divalent transition and post-transition metal ions [8]. Macrocycles containing quinoline side arms have been employed as analytical reagents in absorption spectrometry, fluorometry, solvent extraction, and chromatography. [9] The potential use of some of these compounds as pesticides has also been explored [10].

A number of azacrown ethers containing 8-hydroxyquinoline (**I** [11], **II** [5c], **III** [12]), 5-chloro-8-hydroxyquinoline (**IV** [5c]), and 8-hydroxy-5-N,N-dimethylaminosulfonylquinoline (**V** [12]) have been reported (see Figure V.1). Prodi [5a], and co-workers reported systems **VI.a** and **VI.b** for the recognition of Mg(II) and Hg(II) respectively. In these complexes, the pK_a values for the hydroxyl groups of the 8-HQ moieties were low enough to become fluorescent in slightly acidic solutions [5c], [10], [13]. Addition of Mg(II) to **VI.a** or Hg(II) to **VI.b** in neutral MeOH-H_2O (1:1) solutions results in the strong enhancement of the luminescence bands at 520 nm and 476 nm, respectively. All these ligands have been designed to detect transition and post-transition metal ions through guest associated modulation of the absorption and fluorescence spectra of the ligands [14]. Less attention has been paid to macrocycles containing a pyridine head. R. Delgado and co-workers have published a small tetraaza donor macrocyclic

system (**VII**) substituted with two 5-chloro-8-hydroxyquinoline units; its interaction with Cu(II), Zn(II), Cd(II) and Pb(II) was studied, but no fluorescence data were reported [15].

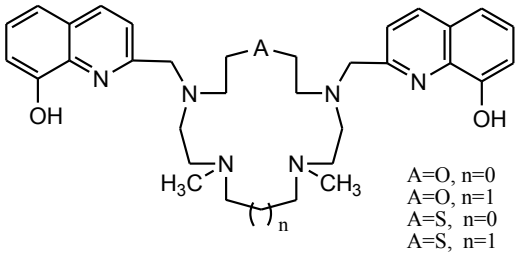

I

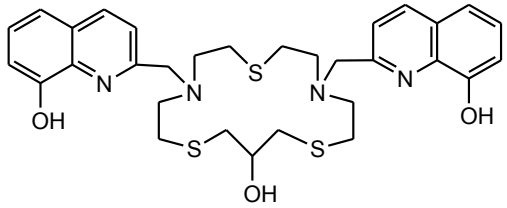

II

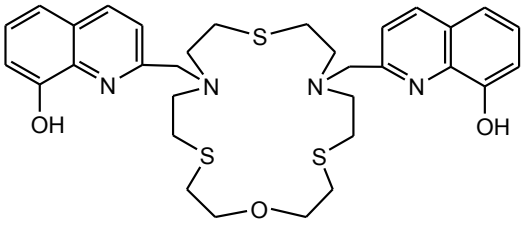

III

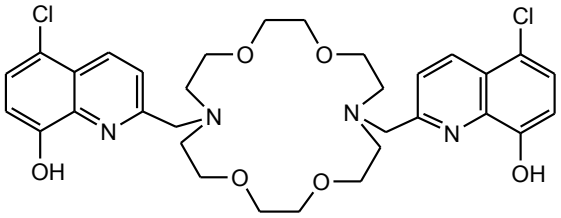

IV

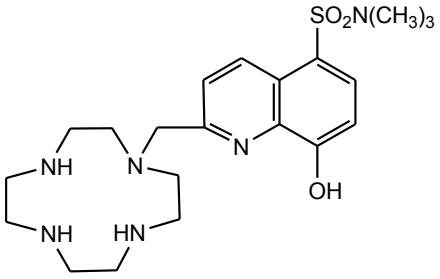

V

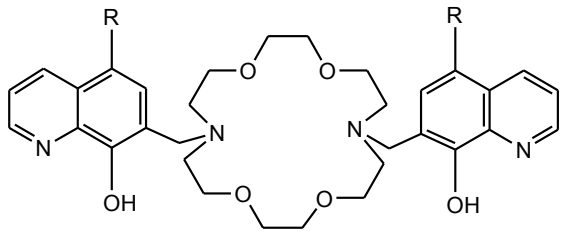

VI.a (R = Cl)
VI.b (R = NO_2)

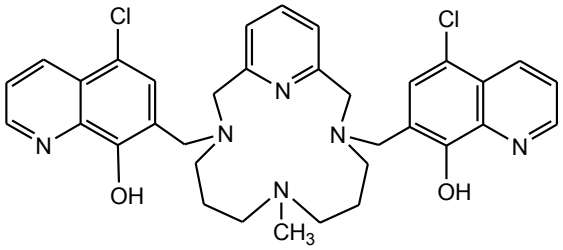

VII

Figure V.1 Macrocyclic ligands with quinoline pendeant arms reported for Pb^{2+} (I, II, II, VII), Co^{2+}(I), Ni^{2+}(I), Cu^{2+}(I, II), Zn^{2+}(I, II, III, V, VII), Cd^{2+}(I, II, III,VII), Hg^{2+}(VI), K^{+}(IV.b), Mg^{2+}(VI.a), and Ba^{2+}(IV).

The biological and biomedical significance of Cu(II), Zn(II), Cd(II), Al(III) or Cr(III) makes the detection these metal ions crucial [16]. The design and synthesis of

fluorescence chemosensors for Cu(II) has become a very active research area, due to the adverse effects of this metal ion when present in large concentration [17]-[19]. Elements from group 12 (Zn(II), Cd(II) and Hg(II)) are also attracting considerable attention, due to the biological importance of Zn(II) and the toxicological effects of Cd(II) and Hg(II) [20]. Zn(II) acts as a catalytic or co-catalytic factor in the active sites of more than 300 enzymes and, due to their chemical similarities, Zn(II) can be easily substituted by Cd(II). Their d [10] electron configurations make Zn(II) Cd(II) and Hg(II) spectroscopically silent; thus, research is now focused on the design of fluorescence chemosensors capable of determining their concentration in solution, especially in living cells [21].

Al(III) is widely used in water treatment, as food additive and in medicine; Cr(III) is used in harden and stainless steel, in alloys to prevent corrosion, and as inorganic catalyst. Many analytical (sample destructive) methods are used for the analysis of both metal ions; however, fewer examples of the use of fluorescence chemosensors (a non-destructive technique) have been reported. Most of the research has focused on chemosensors for aluminium [22], but less attention has been paid to the detection of chromium [23].

As an extension of our work on the synthesis of macrocyclic receptors possessing pyridine units [24] for metal-ion chelation, herein we report the synthesis and characterization of four new emissive macrocycles, L^1-L^4 (see Figure V.2). The starting material for L^1 and L^2 was the N_5O_2-donor ligand L, containing a free amine pendant-arm [25]. The precursor to L^3 and L^4 (L') was obtained via Schiff-base condensation of 2,2-(1,3-phenylenebis(methyleneoxy))dibenzaldehyde, and tris(2-aminoethyl)amine (tren-amine), followed by an in situ reductive demetallation reaction with NaBH4. Condensation of an 8-hydroxyquinoline unit with the free amine pendant-arm yielded the macrocycles L^1-L^4. The new ligands have been fully characterized by the usual techniques.

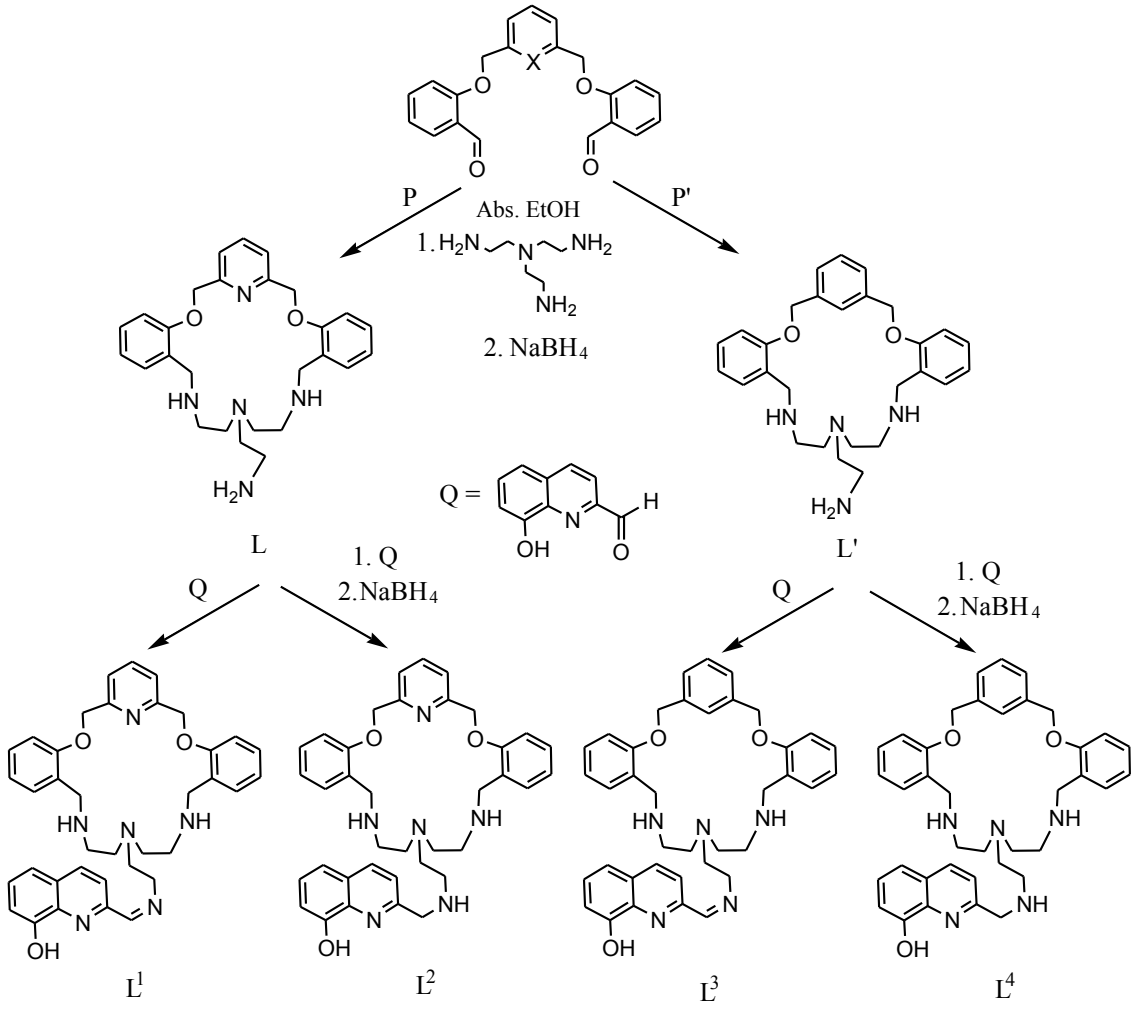

Figure V.2 Schematic synthetic route for ligands L^1-L^4 in absolute ethanol.

The protonation behaviour and sensing capability towards divalent Cu(II), Zn(II), Cd(II), and trivalent Al(III) and Cr(III) metal ions have been studied by UV-vis and fluorescent emission spectroscopy, and by MALDI-TOF-MS spectrometry. In order to compare with the results obtained in solution, some solid metal complexes with the same metal-ions were synthesized and characterized; these results are also discussed.

V.3 Results and discussion

V.3.1 Synthesis and characterization of the free ligands L^1-L^4 and metal complexes

V.3.1.1 Schiff-base macrocycles L^1 and L^3

We have previously reported the synthesis of the macrocycle L [25] obtained by a template cyclocondensation of tren-amine with 2,6-bis(2-formylphenoxymethyl)pyridine (P) [26]. Macrocyclic ligand L' was synthesized by the same template method, *via* cyclocondensation of tren-amine with 2,2-(1,3-phenylenebis(methyleneoxy)) dibenzaldehyde (P') in the presence of $Ba(ClO_4)_2.2H_2O$, followed by an in situ demetallation reaction with $NaBH_4$.

Subsequent condensation of L and L' with 8-hydroxyquinoline-2-carbaldehyde using a one step procedure, yielded L^1 and L^3; both ligands were isolated as air-stable orange solids, *ca.* 73.3% and 62.3% yield, respectively. The infrared spectra (KBr discs) show bands at 1642 (L^1) and 1641 (L^3) cm^{-1}, corresponding to the imine bond, and no peaks attributable to unreacted amine or carbonyl groups were present. The absorption bands corresponding to the ν(C=C) and ν(C=N) vibrations of the pyridine groups appear in the expected positions, 1597, 1453 cm^{-1}, and 1600, 1453 cm^{-1} respectively. The MALDI-TOF MS spectrum of L^1, shows a parent peak at 617 *m/z*, corresponding to the protonated form of the ligand $[L^1H]^+$. For L^3, the base peak in the FAB mass spectrum and in the MALDI-TOF MS was at 616 *m/z*, attributable to the protonated form $[L^3H]^+$. Elemental analysis data confirms that both Schiff-base ligands have been isolated. L^1 and L^3 were studied by ^1H NMR in $CDCl_3$; the spectra confirm the integrity of the ligands in solution (Table V.1). Both ^1H NMR spectra show a peak at ca. 8.2 ppm, corresponding to the imine protons, and no signals corresponding to the primary amine or aldehyde protons are present.

V.3.1.2 Synthesis and characterization of the amine macrocycles L^2 and L^4

Following a one step procedure involving the reduction of L^1 and L^3 with $NaBH_4$, macrocyclic ligands L^2 and L^4 were isolated as air-stable yellow solids, *ca.* 45.3 and 59.4 % yield respectively. The absence of a band at ca. 1640 cm^{-1} in the infrared spectra (KBr disc) confirms the reduction of the imine group. The absorption bands corresponding to ν(C=C) and ν(C=N) vibrations of the pyridine groups appear at 1597, 1451 cm^{-1}, and 1600, 1453 cm^{-1}, respectively.

Table V.1 ^{1}H NMR shifts (ppm) for L^1, L^2, L^3, and L^4 in CD_3Cl solutions (see Figure V.3 for labeling)

	L^1	L^2	L^3	L^4
$H_{1,2}$; H_{4-7}; H_{16-20}	7.9-6.7 (m),16H	7.8-6.8 (m), 16H	8.1-6.7 (m), 17H	8.0-6.5 (m), 17H
H_3	4.9 (s), 4H	5.3 (s), 4H	5.1 (s), 4H	5.0 (s), 4H
H_8	3.7 (m), 4H	3.7-3.6 (m), 4H	3.8 (s), 4H	3.7 (s), 4H
$H_{10,13}$	3.4 (m), 6H	3.6-3.5 (m), 6H	2.9-2.1 (m), 6H	2.6-2.1 (m), 6H
$H_{11,12}$	2.5 (m), 6H	2.8-2.3 (m), 6H	2.9-2.1 (m), 6H	2.6-2.1 (m), 6H
H_{15}	8.2 (s), 1H	4.0 (s), 2H	8.4 (s), 1H	3.4 (s), 2H
H_{21}	5.6 (s), 1H	5.9 (s), 1H	4.5 (s), 1H	4.0 (s), 1H

The ESI mass spectrum of L^2 shows a peak at 619 amu attributable to $[L^2H]^+$. For L^4, the highest peak in the FAB mass spectrum is at 618 amu, attributable to $[L^4H]^+$. Both peaks were observed also in the MALDI-TOF-MS spectra. Ligands L^2 and L^4 were studied by ^{1}H NMR in $CDCl_3$; the NMR spectra confirm the integrity of the ligands in solution. The absence of a peak at *ca*. 8.2 ppm in the ^{1}H NMR spectra confirms the reduction of the imine protons (see Table V.1).

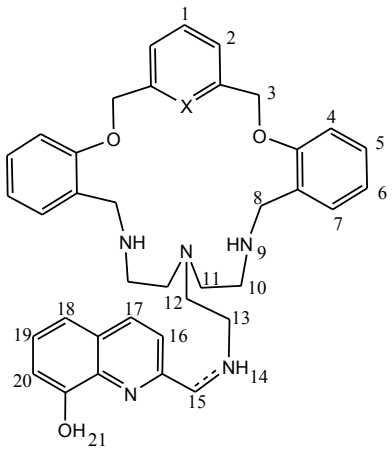

Figure V.3 Ligands L^1-L^4 with numbered atoms.

V.3.1.3 Synthesis and characterization of the metal complexes

The coordination ability of ligands L^1 to L^4 towards hydrated transition and post transition metal salts were studied in solution and in solid state. Reaction of L^1 and L^3 with Al(III) chloride in a 1:1 metal-ligand ratio in ethanol led to two compounds of formula $[AlL^1](Cl)_3.5H_2O$ and $[AlL^3](Cl)_3.6H_2O$ in good yields, 55.3 and 59.2% respectively. The complexes were characterized by elemental analysis, IR, and ESI-MS or FAB-MS spectra. The reaction was attempted also with the Zn(II) and Cr(III) salts, but only the aluminium products gave satisfactory microanalytical results. The ESI mass spectrum of $[AlL^1](Cl)_3.5H_2O$ displays peaks corresponding to the $[M_2L^1]^+$, $[M_2L^1Xz]^+$ (z= 3 and 5) fragments, and the FAB mass spectrum of $[AlL^3](Cl)_3.6H_2O$ displays a peak corresponding to the fragment $[M_3L^3X_2]^+$, confirming the formation of both complexes; the higher nuclearity suggests some complex formation in the gas phase. The IR spectra of the complexes were recorded as KBr discs. In both cases, the band due to the imine bond is shifted to lower wave numbers when compared to its position in the spectrum of the free ligand, and the ν(C=C) and ν(C=N) stretching modes of the pyridine rings appear .at higher wave numbers than those on the spectrum of the free ligand. Both effects suggest that the N_{py} atom of the quinoline pendant group could be involved in the coordination to the metal ion [27]. The broad absorption band in the region 3450-3380 cm^{-1} present is probably due to the existence of lattice and/or co-ordinated water in the molecule, and make it difficult to see the bands due to the ν(O-H) and ν(N-H) stretching vibrations which would appear in this region.

Ligands L^2 and L^4 reacted easily with transition and post-transition ions producing air-stable solid complexes, which were characterized by elemental analysis, IR, ESI MS (L^2 complexes), and FAB MS (L^4 complexes). The elemental analysis data indicate the formation of mononuclear complexes with empirical formulas $CdL^2(ClO_4)_2 \cdot xC2H6O$, $ZnL^2(NO_3)_2 \cdot xH_2O$, $CrL_2(NO_3)_3 \cdot xH_2O$, $ML^4(NO_3)_2 \cdot xH_2O$ (M=Zn, Cd), $CrL^4(NO_3)_3 \cdot xH_2O$, $AlL^2(Cl)_3 \cdot xH_2O$, $AlL^4(Cl)_3 \cdot xH_2O$ and the dinuclear complexes $Cu_2L^2(NO_3)_4 \cdot xC_2H_6O$ and $Cu_2L^4(NO_3)_4 \cdot xH_2O$. The ESI mass spectra for L^2 complexes display peaks corresponding to the $[ML^2]^+$, $[ML^2X]^+$, $[ML^2X_2]^+$, $[M_2L^2X]^+$, $[M_2L^2X_2]^+$ fragments, and the FAB mass spectra for L^4 complexes display a peak attributable to the $[ML^4]^+$ fragment, confirming the formation of the complexes in both cases. The IR spectra of all the complexes were recorded as KBr discs and all show similar features. As in the free ligands there are split bands associated with ν(C=C) and ν(C=N) vibrations of the pyridine rings, which have undergone a shift towards higher wave numbers on complexation [27]. As in the complexes with L^1 and L^3, the presence of an intense broad band at ca. 3400 cm-1 make it difficult to see the bands corresponding to the ν(O-H) and ν(N-H) which would appear in this region. The spectra of the nitrate complexes show a band at 1384 cm^{-1} associated with the presence of ionic nitrate. For $CdL^2(ClO_4)_2.2C_2H_6O$, bands attributable to the asymmetric Cl-O stretching mode at ca. 1088 cm^{-1} (ν_3) and the asymmetric Cl-O bending mode (ν_4) at ca. 627 cm^{-1} can be observed. The highest energy band shows considerable splitting, with three maxima at ca. 1050, 1088 and 1121 cm^{-1}, suggesting some interaction of at least one of the ClO_4^- anions with the metal [28].

V.3.2 Spectrophotometric and spectrometric studies

V.3.2.1 Spectrophotometric studies: UV-vis and Fluorescence emission spectroscopy

Ligands L^1-L^4 have a low solubility in water. In addition in water-absolute ethanol solution (50:50, v/v) those ligands precipitated. For the aforementioned reasons all the spectroscopic studies have been done in absolute ethanol.

The absorption spectra of ligands L^1, L^2, L^3 and L^4 in absolute ethanol solution show one band centered at 248-250 nm, attributable to the π-π* transitions in the ligand. The band presents a long tail, up to 400 nm. The spectrum is independent on the acidic conditions, and addition of up to five equivalents of HBF_4 does not affect the absorption

band; this result is in agreement with other polyamine macrocyclic ligands containing aromatic units. The spectra for L^1 and L^2 show an emission band centered at 524 nm. The intensity of this band increases with the addition of protons, achieving a plateau when four equivalents of HBF_4 are added. The spectra for L^3 and L^4 (without the pyridine head) show the emission band centered at 514 nm; addition of acid results in an increase of this band, also achieving a plateau with the addition of four equivalents. These results suggest that the pyridine ring present in the macrocyclic skeleton of L^1 and L^2 may not be protonated on these conditions. Addition of a tetrabuthylamonium hydroxide solution to an ethanolic solution of ligands L^1 and L^3 reduced the intensity of the emission in ca. 50%. 2 equivalents of base are enough to achieve a plateau. A generic spectrophotometric characterization is shown in Figure V.4.

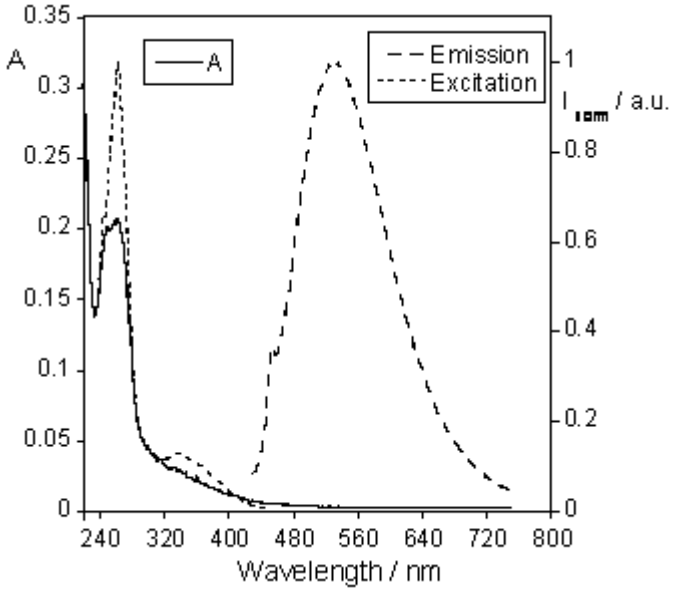

Figure V.4 Absorption, emission, and excitation spectra of ligand L^2 in absolute ethanol solution ($[L^2]=1.0\times10^{-5}$ M, λ_{exc}=400nm, λ_{em}=530nm).

The photophysical properties of compounds including 8-HQ as chromophore have been studied in detail [29]. In their fluorescence spectra, a non-structured band centered between 360 and 460 nm, strongly dependent on the solvent, was observed [29]. In our case, the emission band is red-shifted in at least 60 nm, which could facilitate their potential applications in biological systems. The emissive compounds could be irradiated in the presence of bio-molecules without any damage to the chromophores present in aminoacids, peptides, proteins, DNA, etc.

The relative fluorescence quantum yields of ligands L^1 to L^4 were determined using a 0.1 M solution of quinine sulphate in H_2SO_4 0.5M as standard (ϕ=0.546); the values obtained were always below 1×10^{-3} [30], [29c]. The fluorescence of chemosensors with 8-HQ units is weak due to the competition between the intermolecular photo-induced proton transfer (PPT) from the hydroxyl group of the molecule, and the photo-induced electron transfer (PET) from the amines [5a]. Moreover, in proton-donor solvents, a PPT process involving solvent molecules opens another way to further deactivate fluorescence. Consequently, both PPT and PET processes can quench the fluorescence emission in substituted quinolines. The quenching effect observed after the addition of tetrabuthylamonium hydroxide is consistent with this explanation; in this case, the PET mechanism is stronger than the PPT.

Table V.2 Optical data for the metal complexes of L^1, L^2, L^3 and L^4 in absolute solutions (λ_{exc}=400nm; 25ºC)

METAL COMPLEX	**λ_{max}(nm); log ε**	**λ_{em} (nm)**
$AlL^1(Cl)_3.5H_2O$	269;4.46	546
$AlL^2(Cl)_3.2H_2O$	261; 4.20	543
$AlL^3(Cl)_3.6H_2O$	260; 4.19	545
$AlL^4(Cl)_3.5H_2O$	262; 4.77	545
$CrL^2(NO_3)_3.6H_2O$	255; 4.61	535
$CrL^4(NO_3)_3.2H_2O$	251; 4.61	536
$Cu_2L^2(NO_3)_4.3C_2H_6O$	266; 4.80	-
$Cu_2L^4(NO_3)_4.3H_2O$	275; 4.35	-
$ZnL^2(NO_3)_2.6H_2O$	265; 4.41	573
$ZnL^4(NO_3)_2.3H_2O$	273; 4.21	565
$CdL^2(ClO_4)_2.2C_2H_6O$	260; 4.56	508
$CdL^4(NO_3)_2.3H_2O$	248; 4.17	505
	269; 4.18	
	300; 3.76	

The sensing behavior of the compound towards Zn(II), Cd(II), Cu(II), Al(III) and Cr(III) has been studied in solution, using absolute ethanol as the solvent. For comparison purposes, all the synthesized metal complexes have been also optically characterized and the data is given in table V.2.

Addition of increasing amounts of anhydrous zinc and cadmium triflates to a ethanolic solution of L^2 or L^4 ($1.00E^{-5}$ M), at 298 K, led to a decrease on the absorption band centered at 249 nm, and the appearance of a new band centered at *ca.* 270 nm. This spectrum has a long tail up to 400 nm. In this region, the absorption increases with the addition of metal ions, suggesting the involvement of the quinoline ring in the metal complexation. An isosbestic point at 260 nm was observed for all the metal titrations, confirming the presence of two species in solution, the free ligand and the metal complex. As an example, Figure V.5 depicts the absorption and emission metal titration of L^2 with Zn(II) and Cd(II).

Excitation at 400 nm (quinoline tail), gave emission spectra centered at 555 nm. The band is red-shifted upon complexation, as it can be seen on figures V.5B and V.5D for Zn(II) and Cd(II) respectively. The same behaviour was observed when the metal ion used was Al(III). A *Chelation Enhanced Fluorescence (CHEF)* effect was observed in all cases. This well known phenomenon is consistent with the involvement of the amines and the quinoline ring in complexation. The lone pairs of the nitrogen atom are bound to the metal ion preventing the PET processes, while the 8-HQ is coordinated to the metal preventing the PPT process; thus, complexation results in an enhancement of the fluorescence signal.

As it can be seen in Figure V.5A and V.5B, a plateau is reached after addition of one metal equivalent, suggesting that the macrocyclic unit is coordinated to one metal ion. This result confirms the stoichiometry observed for the solid metal complexes synthesized. Copper(II) ions are well know to quench excited states [31]. Addition of increasing amounts of all d^n metals studied leads to the formation of non emissive complexes. These results are in agreement with the fluorescence behaviour observed for the analytically pure complexes isolated (See experimental section).

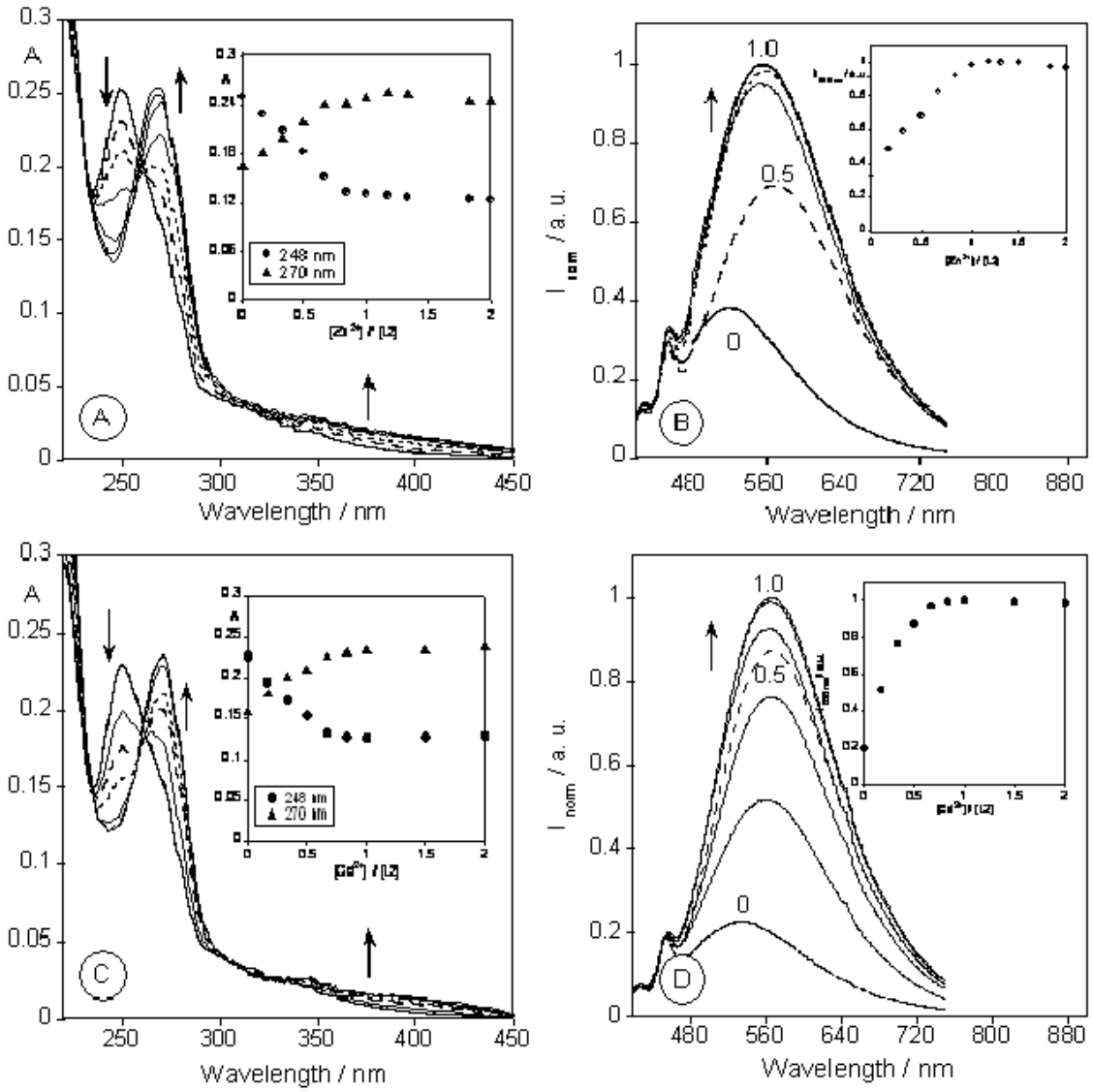

Figure V.5 Absorption (A and C) and fluorescence emission (B and D) titration of absolute ethanol solution of L^2 as a function of increasing amounts of Zn^{2+} (A and B) or Cd^{2+} (C and D) ions. The inset shows the absorption at 248 and 270 nm, and the normalized fluorescence intensity at 555 nm ($[L^2]=1.00\times10^{-5}$ M, λ_{exc}=400nm).

Figure V.6 shows the absorption and emission spectra of L^2 in the presence of increasing amounts of Cu(II); the inset shows the normalized fluorescence intensity at 555 nm. Upon addition of two equivalents of metal ion, the emission disappears, achieving a plateau; this suggests the formation of a dinuclear complex. A similar CHEQ effect was observed in the presence of Cr(III), but the plateau was achieved for one metal ion, suggesting the formation of a mononuclear complex. Both results agree with the stoichiometry found in the solid metal complexes synthesized.

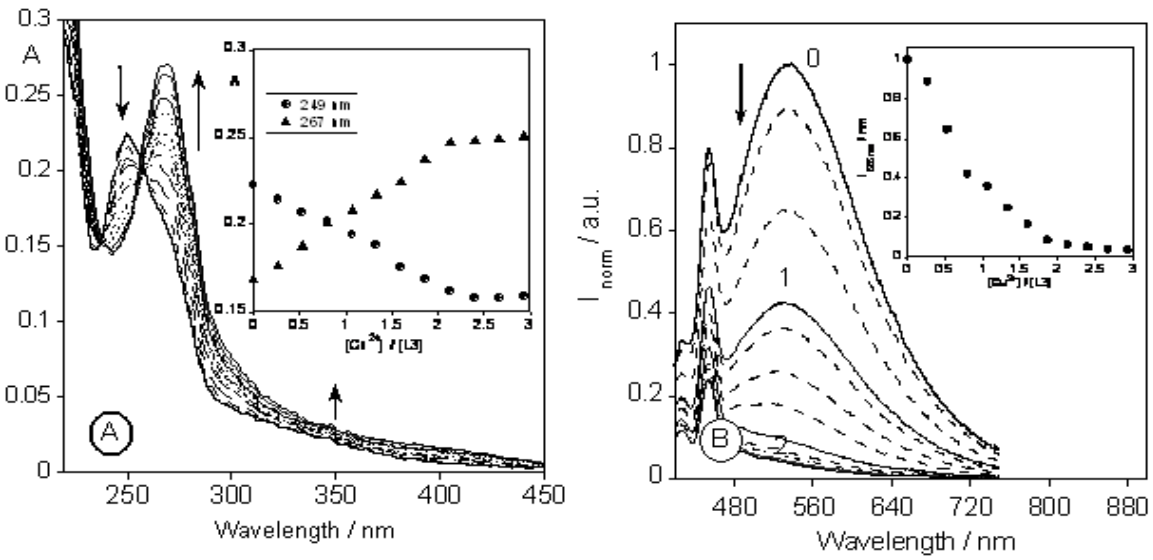

Figure V.6 Absorption (A) and fluorescence emission (B) titrations of absolute ethanol solution of L2 as a function of increasing amounts of Cu2+ ions. The inset shows the absorption at 249 and 257 nm, and the normalized fluorescence intensity at 555 nm. ([L2] = 1.00xE-5 M, λexc = 400 nm)

Protonation and/or complexation of a pyridine ring lead to a quenching effect for molecules that incorporate both a pyridine and an emissive chromophore unit in their structure [32]. The presence of the pyridine head in L^1 and L^2 creates another inverse PET mechanism for quenching the emission. The analogous ligands L^3 and L^4, without the pyridine unit, were synthesized for comparative purposes. Unfortunately, the results observed with L^3 and L^4 are similar to those ligands L^1 and L^2, due to the strong PPT and PET processes mentioned previously.

The fluorescence quantum yields for all the complexes have been calculated using a solution of quinine sulphate as pattern. In all cases, and in accordance with the results obtained for the free ligands, the values are very small, always below 10-3. This quenching can be attributed to the high number of donor atoms present in the ligands; some of them may not be coordinated to the metal centres, specially the nitrogens that activate the quenching through the PET phenomena. As it can be observed in table V.2, the maximum of the emission for each metal complex is slightly different, opening up the possibility of using these ligands to recognize these metals in solution.

V.3.2.2 Spectrometric studies by MALDI-TOF-MS spectrometry

Taking into account the biological importance of Zn(II) ions, and the environmental problems by Al(III) excess, these two metal ions were selected for the gas phase studies by MALDI-TOF MS using ligands L^2 and L^4 as molecular probe. To perform the metal titrations, both ligands were dissolved in chloroform and the metal salts in absolute ethanol. Two different strategies were explored. First, three solutions containing the ligand (1μL), the MALDI matrix (dithranol) and the metal salt (1μL) were mixed and then applied in the MALDI-TOF sample holder. The second method consisted of a layer by layer addition: a solution of L^2 or L^4 mixed with the matrix (dithranol) was spotted in the MALDI-TOF plate and then dried; subsequently, 1μL of the solution containing the metal salt was placed on the sample holder, which was then inserted in the ion source. For the second case, the chemical reaction between the ligand and the metal salts occurred in the holder, and the complex species were produced in gas phase.

The results were the same in both cases. Addition of one metal equivalent led to the formation of the mononuclear complex. Addition of increasing amounts of metal ion did not produce any peaks attributable to the formation of dinuclear complexes. The results with Al(III) and Zn(II) confirm both the stoichiometry observed in the synthesized solid metal complexes, and the data obtained in solution by absorption and fluorescence emission spectroscopy.

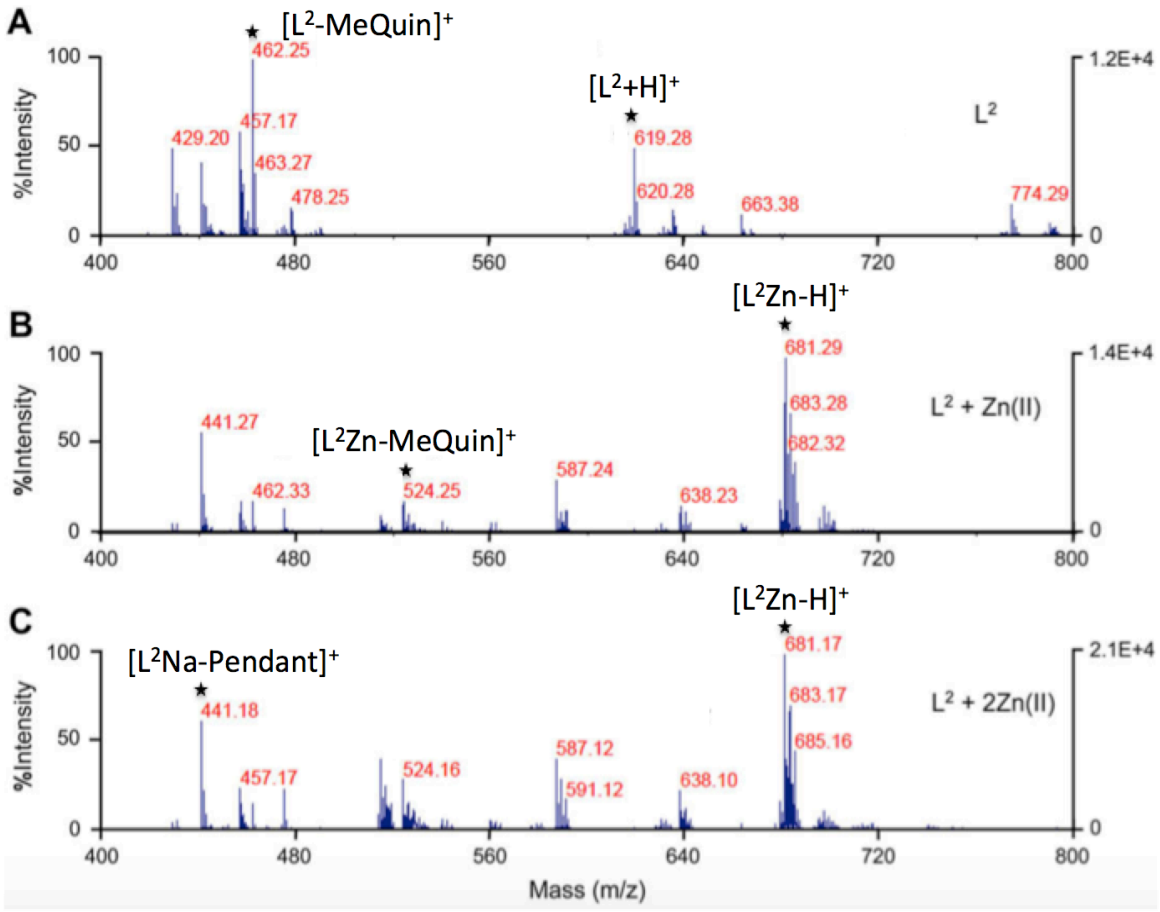

Figure V.7 (A) MALDI-TOF-MS spectra of L^2 using dithranol as MALDI matrix, (B) in the presence of 1 equiv of Zn(II), and (C) in the presence of 2 equiv. of Zn(II).

Figure V.7 summarizes the MALDI-TOF MS spectra for ligand L^2. In the presence of one and two equivalent of Zn(II), peaks at *m/z* 619.3, attributable to the protonated ligand $[L^2H]^+$, and *m/z* 462.2, attributed to the loss of the methyl-8-HQ group were observed. Small peaks at higher mass values, attributable to species with two, three and four pendant-arms, can be observed; these are indicative of the interaction of the quinoline group with the ligand in the gas phase (see Figure V.8). After addition of the metal salt, the peak corresponding to the protonated ligand disappears, and new peaks at *m/z* 681.3, 524.2 and 441.2, attributable to the $[L^2Zn\text{-}H]^+$, $[L^2Zn\text{-}MeQuinoline]^+$ and $[L^2Na\text{-}Pendant]^+$ species respectively, were observed.

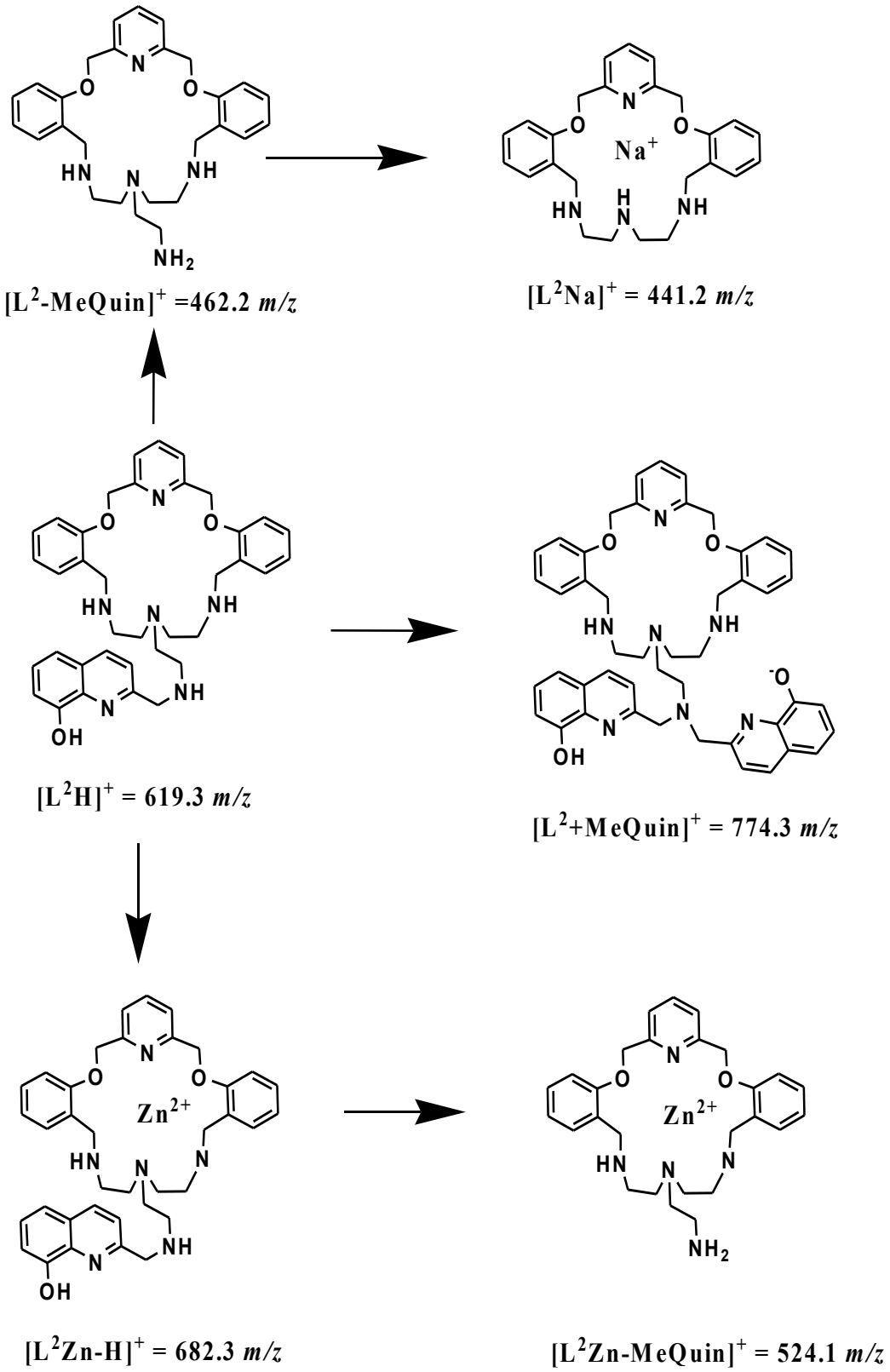

Figure V.8 MALDI-TOF-MS fragmentation peak observed for L^2 and L^2Zn(II) complex.

V.4 Conclusions

Four macrocyclic ligands containing a 8-HQ pendant arm have been synthesized and fully characterized. The protonation behaviour and sensing capability of these ligands towards divalent, Cu(II), Zn(II), Cd(II), and trivalent, Al(III) and Cr(III) metal ions have been studied by UV-vis and fluorescent emission spectroscopy. Several metal complexes have also been synthesized and characterized, confirming the stoichiometry and all the data obtained in solution.

The photophysical characterization of the ligands shows two quenching mechanisms active, PPT and PET. Coordination with Zn(II), Cd(II) and Al(III) partially prevents this quenching trough a CHEF effect. Cu(II) and Cr(III) gave non emissive complexes due to the quenching, *via* a CHEQ effect, of the low emission observed for the free macrocycles. Both phenomena could be used for sensing purposes, opening up the possibility of using these ligands in solution for metal ion recognition.

Titrations of L^2 and L^4 with Zn(II) and Al(III) solutions were followed by MALDI-TOF-MS spectrometry. In all cases, the formation of the complex peak was observed. These results confirm the formation of the metal complexes also in the gas phase.

V.5 Experimental

V.5.1 General

The chemical analysis of the dialdehyde precursor, 2,2-(1,3-phenylenebis(methyleneoxy))dibenzaldehyde, was carried out on a Carlo Erba 1106 CHN analyser. Elemental analyses of the ligands were performed on a Fisons Instruments EA1108 micro analyser by the Universidade de Santiago de Compostela. The IR spectra of the precursors were recorded on a Pye Umicam SP3-100 infrared spectrometer. Infra-red spectra of free ligands were recorded as KBr discs on a BIO-RAD FTS 175-C spectrometer. FAB mass spectra were recorded using a KRATOS MS50TC spectrometer with 3-nitrobenzyl alcohol as the matrix. The ^{1}H NMR spectrum of the dialdehyde precursor was recorded on a JEOL GSX 270 FT NMR spectrometer. The ^{1}H, ^{13}C NMR, COSY, DEPT and HMQC spectra were recorded on a Bruker 500 MHz spectrometer, using CD_3Cl as the solvent.

MALDI-TOF-MS spectra have been performed in a MALDI-TOF-MS model Voyager DE-PRO Biospectrometry Workstation equipped with a nitrogen laser radiating at 337 nm from Applied Biosystems (Foster City, United States) from the MALDI-TOF-MS Service of the REQUIMTE, Chemistry Department, Universidade Nova de Lisboa. The acceleration voltage was 2.0×10^{4} kV with a delayed extraction (DE) time of 200 ns. The spectra represent accumulations of 5×100 laser shots. The reflection mode was used. The ion source and flight tube pressures were less than 1.80×10^{-7} and 5.60×10^{-8} Torr, respectively. The MALDI mass spectra of the soluble samples (1 or 2 μg/μL) such as the ligand and metal complexes were recorded using the conventional sample preparation method for MALDI-MS. In the metal titrations by MALDI 1μL of the metal sample were put on the sample holder on which the chelating ligand had been previously spotted with the matrix (dithranol). The sample holder was inserted in the ion source. Chemical reaction between the ligand and metal salts occurred in the holder and complex species were produced.

Absorption spectra were recorded on a Shimadzu UV-2501PC or in a Perkin Elmer lambda 35 spectrophotometers. Fluorescence emission spectra were recorded on a Horiba-Jobin-Yvon SPEX Fluorolog 3.22 or a Perkin Elmer LS45 espectrofluorimeters.

The linearity of the fluorescence emission vs. concentration was checked in the concentration range used (10^{-4} to 10^{-6} M). A correction for the absorbed light was performed when necessary. All spectrofluorimetric titrations were performed as follows: the stock solutions of the ligand (ca. 1×10^{-3} M) were prepared by dissolving an appropriate amount of the ligand in a 50 mL volumetric flask and diluting to the mark with absolute ethanol UVA-sol. All measurements were performed at 298 K. The titration solutions (ca. [L]=1.0×10^{-5}M) were prepared by appropriate dilution of the stock solutions. Titrations of the ligand were carried out by addition of microliter amounts of standard solutions of the ions in absolute ethanol. HBF_4 and tetrabuthylamonium hydroxide were used to change the acidity conditions of the ethanolic solutions. Luminescence quantum yields were measured using a solution of quinine sulphate in H_2SO_4 (0.1M) as a standard [ϕ_F]=0.546] [30].

V.5.2 Chemicals and starting material

Salicylaldehyde, 1,3-bis(bromomethyl)benzene, tris(2-aminoethyl)amine, 8-hydroxyquinoline-2-carbaldehyde and hydrated chloride, nitrate and perchlorate salts were commercial products from Alfa and Aldrich. Solvents used were of reagent grade and purified by the usual methods. CD_3Cl (99.8%) was obtained from Aldrich. All triflates metallic salts were purchased from Strem, chemicals for research. The starting materials, 2,6-(bis(2-formylphenoxymethyl)pyridine [26] and the macrocyclic ligand L [25] were synthesized as previously published.

V.5.3 Synthesis

V.5.3.1 Synthesis of 2,2-(1,3-phenylenebis(methyleneoxy))-dibenzaldehyde

A solution of NaOH (1.512 g, 37.8 mmol) in 50 mL of distilled water was added dropwise to a solution of salicylaldehyde (4.710 g, 37.8 mmol) in 10 mL in absolute ethanol. After heating gently for approximately 10 minutes, 1,3-bis(bromomethyl)benzene (4.741 g, 18.9 mmol) was added dropwise. Absolute ethanol (80 mL) was slowly added, and the resulting solution refluxed gently for 4 h while maintaining magnetic stirring. The solution was then allowed to cool, and a white solid

appeared. The solid was filtered off and dried. The compound is air stable, soluble in chloroform and dichloromethane, moderately soluble in hexane, absolute ethanol, diethyl ether, and methanol and insoluble in distilled water.

$C_{22}H_{18}O_4.0.5H_2O$. Mp(ºC): 80-85 ºC; Anal. Calcd for $C_{22}H_{19}O_{4,5}$: C, 74.36; H, 5.07. Found: C, 74.30; H, 5.04 %. Yield: 78%. IR (NaCl windows, cm^{-1}): 1690 [ν(C=O)]; 1600 [ν(C=C)]. MS (FAB^+, *m/z*): 347 $[L'H]^+$.

^{1}H-NMR ($CDCl_3$), δ (ppm): 10.5 (s), 2H (CO*H*); 7.9-7.0 (m), 12H (aromatics); 5.2 (s), 4H (aromatic-CH_2-O).

V.5.3.2 Template synthesis of the macrocyclic ligand L`

A solution of tris(2-aminoethyl)amine (0.512 g, 1 mmol) in methanol (25 mL) was added dropwise to a refluxing solution of 2,2-(1,3-phenylenebis(methyleneoxy))dibenzaldehyde (0.346 g, 1 mmol) and barium perchlorate (0.336 g, 1 mmol) in methanol (75 mL). The resulting solution was gently refluxed with magnetic stirring for ca. 4h. The solution was allowed to cool and $NaBH_4$ (0.378 g, 10 mmol) was added; magnetic stirring was maintained for a further 2h period. The mixture was filtered off and evaporated to dryness. The residue was then extracted with water-chloroform. The organic layer was dried over anhydrous Na_2SO_4 and evaporated to yield a yellow oil that was dried under vacuum.

$C_{28}N_4O_2H_{36}.4H_2O$ (L'). Anal. Calcd for $C_{28}N_4O_6H_{44}$: C, 63.15; H, 8.30; N, 10.53. Found: C, 62.90; H, 8.63; N, 10.85 %. Yield: 70.3%. IR (KBr, cm^{-1}): 1601 [ν(C=C)]. MS (FAB, *m/z*): 461 $[L'H]^+$.

^{1}H-NMR of L' ($CDCl_3$), δ (ppm): 7.7-6.7 (m), 12H (Ph); 5.0 (s), 4H (Ph-CH_2-O); 3.6 (s), 4H (Ph-CH_2-NH); 2.6-2.0 (m), 12H (-CH_2CH_2); 1.7 (s) (-N*H*).

^{13}C-NMR ($CDCl_3$), δ (ppm): 156.9-111.9, 18C (aromatics); 70.2, 2C (aromatic-CH_2-O); 49.1, 2C (aromatic-*C*H_2-NH); 57.5-53.8, 6C (-*C*H_2CH_2).

V.5.3.3 Synthesis of the imine macrocyclic ligands L^1 and L^3: general method

A solution of 8-hydroxyquinoline-2-carbaldehyde (0.069 g, 0.4 mmol) for L^1 and (0.034 g, 0.2 mmol) for L^3 in absolute ethanol (10 mL) was added dropwise to a refluxing solution of L (0.184 g, 0.4 mmol) and L' (0.092 g, 0.2 mmol) in the same solvent (70 mL for L^1 and 35 mL for L^3). The resulting solution was gently refluxed with magnetic stirring for *ca*. 4h. The colour changed from yellow to orange in both cases. The solution was allowed to cool, filtered off to eliminate the solid precipitate, and then concentrated in the rotary evaporator. The resulting orange oil was stirred with acetonitrile (to eliminate possible excess of L or L') and then with cold diethyl ether. The orange powder precipitates, later characterized as L^1 or L^3, were separated by centrifugation and dried under vacuum.

$C_{37}N_6O_3H_{40}.2H_2O$ (L^1) **.** Mp(ºC): 170-175; Anal. Calcd for $C_{37}N_6O_5H_{44}$: C, 68.10; H, 6.74; N, 12.88. Found: C, 68.59; H, 6.10; N, 12.98 %. Yield: 73.3%. IR (KBr, cm^{-1}): 1642 [ν(C=N)$_{imine}$]; 1597, 1453 [ν(C=C) and ν(C=N)$_{py}$]. MS (ESI, *m/z*): 617 $[L^1H]^+$; MS (MALDI-TOF-MS, *m/z*): 616 $[L^1H]^+$.

^{1}H-NMR of L^1 ($CDCl_3$), δ (ppm): 8.2 (s), 1H, (*H*C=N)$_{imine}$; 7.9-6.7 (m), 16H (aromatics); 5.6 (s), 1H (O*H*); 4.9(s), 4H (Py-CH_2-O); 3.7 (m), 4H (Ph-CH_2-NH); 2.0 (s) (-N*H*); 3.4-2.5 (m), 12H (-CH_2CH_2).

$C_{38}N_5O_3H_{41}.3H_2O$ (L^3). Mp(ºC): 165-170; Anal. Calcd for $C_{38}N_5O_6H_{47}$: C, 68.15; H, 7.02; N, 10.45. Found: C, 68.20; H, 7.53; N, 10.08 %. Yield: 62.3%. IR (KBr, cm^{-1}): 1641 [ν(C=N)$_{imine}$]; 1600, 1453 [ν(C=C) and ν(C=N)$_{py}$]. MS (FAB^+, *m/z*): 616 $[L^3H]^+$. MS (MALDI-TOF-MS, *m/z*): 616 $[L^3H]^+$.

^{1}H-NMR of L^3 ($CDCl_3$), δ (ppm): 8.4 (s), 1H (C=N)$_{imine}$; 8.1-6.7 (m), 17H (aromatics); 4.5 (s), 1H (OH); 5.1 (s) 4H (Py-CH_2-O); 3.8 (s), 4H (Ph-CH_2-NH); 2.9-2.1 (m), 12H (-CH_2CH_2).

V.5.3.4 Synthesis of the amine macrocyclic ligands L^2 and L^4: general method

$NaBH_4$ was added in excess (20%) to a solution of L^1 (0.123 g, 0.2 mmol) and L^3 (0.062 g, 0.1 mmol) in methanol at room temperature. The resulting solutions were gently refluxed with magnetic stirring for 4h; within that time, the colour changed slowly from orange to pale yellow. The mixtures were filtered off and evaporated to dryness. The residues were then extracted with water-chloroform. The organic layer was dried over anhydrous Na_2SO_4 and evaporated to yield a yellow oil that was stirred with diethyl ether. The yellow powder formed was separated by centrifugation and dried under vacuum. These compounds were characterized as L^2 and L^4.

$C_{37}N_6O_3H_{42}.2H_2O$ (L^2). Mp(ºC): 175-180; Anal. Calcd for $C_{37}N_6O_5H_{46}$: C, 66.07; H, 7.14; N, 12.50. Found: C, 66.70; H, 6.90; N, 12.20 %. Yield: 45.3 %. IR (KBr, cm^{-1}): 1597, 1451 [ν(C=C) and $\nu(C=N)_{py}$]. MS (ESI, *m/z*): 619 $[L^2H]^+$. MS (MALDI-TOF-MS, *m/z*): 619 $[L^2H]^+$.

^{1}H-NMR of L^2($CDCl_3$), δ (ppm): 7.8-6.8 (m), 16H (aromatics); 5.9 (s), 1H (O*H*); 5.3 (s) 4H (Py-CH_2-O); 3.7-3.6 (m), 4H (Ph-CH_2-NH); 3.6-2.3 (m), 12H (-CH_2CH_2); 4.0 (s), 2H (8-HQ-CH_2NH).

$C_{38}N_5O_3H_{43}.8H_2O$ (L^4). Anal. Calcd for $C_{38}N_5O_{11}H_{59}$: C, 59.90; H. 7.75; N, 9.20. Found: C, 60.57; H, 7.45; N, 8.85 %. Yield: 59.4 %. IR (KBr, cm^{-1}): 1600, 1453 [ν(C=C) and $\nu(C=N)_{py}$]. MS (FAB^+, *m/z*): 618 $[L^4+H]^+$. MS (MALDI-TOF-MS, *m/z*): 618 $[L^4H]^+$.

^{1}H-NMR of L^4($CDCl_3$), δ (ppm): 8.0-6.5 (m), 17H (Ph); 4.0 (s) 1H, (OH); 5.0 (s) 4H (Py-CH_2-O); 3.7 (s), 4H (Ph-CH_2-NH); 2,6-2,1 (m), 12H (-CH_2CH_2); 3.4 (s), 2H (8-HQ-CH_2NH).

V.5.3.5 General procedure for metal complexes with ligands L^1 and L^3

Hydrate aluminum chloride (0.02 mmol) in ethanol (5 mL) was added drop wise to a stirred solution of L^1 or L^3 (0.02 mmol) in the same solvent (15 mL). The resulting mixture was gently heated and magnetically stirred for 4h. The solution was then concentrated in a rotary evaporator to *ca.* 5 mL. A small volume of diethyl ether (ca. 3 mL) was slowly infused into the solution producing powdery precipitates. The products were separated by centrifugation and dried under vacuum. The compounds are air stable, soluble en absolute ethanol, methanol and dimethyl sulfoxide and insoluble in acetonitrile, ether and water. Attempts to grow single crystals of the complexes were unsuccessful.

$AlL^1Cl_3.5H_2O$ ***(1).*** Colour: yellow; Anal. Calcd for $C_{37}N_6O_3H_{40}Cl_3Al.5H_2O$: C, 52.88; H, 5.95; N, 10.00. Found: C, 52.33; H, 6.31; N, 9.45 %. Yield: 55.3 %. IR (KBr, cm^{-1}): 1599, 1456 [ν(C=C) and $\nu(C=N)_{py}$]. MS (ESI, *m/z*): 619 $[L^1]^+$, 670 $[Al_2L^1]^+$, 775 $[Al_2L^1Cl_3]^+$, 847 $[Al_2L^1Cl_5]^+$.

$AlL^3Cl_3.6H_2O$ ***(2).*** Colour: yellow; Anal. Calcd for $C_{38}N_5O_9H_{53}Cl_3Al$: C, 53.24; H, 6.18; N, 8.17. Found: C, 53.51; H, 5.90; N, 8.24 %. Yield: 59.2 %. IR (KBr, cm^{-1}): 1629 [$\nu(C=N)_{imin}$]; 1602, 1457 [ν(C=C) and $\nu(C=N)_{py}$]. MS (FAB, *m/z*): 765 $[Al_3L^3Cl_2]^+$.

V.5.3.6 General procedure for complexes with the amine macrocycles L^2 and L^4

The appropriate metal salt (0.02 mmol) in absolute ethanol (5 mL) was added dropwise to a stirred solution of the ligand L^2 or L^4 (0.02 mmol) in the same solvent (15 mL). The resulting mixture was gently heated and magnetically stirred for 4h. The solution was then concentrated in a rotary evaporator to *ca.* 5 mL. A small volume of diethyl ether (ca. 3 mL) was slowly infused into the solution producing powdery precipitates. The products were separated by centrifugation and dried under vacuum. The compounds were air stable, soluble en ethanol, methanol and dimethyl sulfoxide and insoluble in acetonitrile, ether and water. Attempts to grow single crystals of the complexes were unsuccessful.

$AlL^2(Cl)_3.2H_2O$ ***(3).*** Colour: yellow; Anal. Calcd for $C_{37}N_6O_5H_{46}Cl_3Al$: C, 56,25; H, 5,84; N, 10,66. Found: C, 56,83; H, 4,96; N, 11,32 %. Yield: 62,3 %. IR (KBr, cm^{-1}): 1604, 1457 [ν(C=C) and $\nu(C=N)_{py}$]. MS (ESI, *m/z*): 713 $[AlL^2Cl_2]^+$.

$AlL^4(Cl)_3.5H_2O$ ***(4).*** Colour: yellow; Anal. Calcd for $C_{38}N_5O_8H_{53}AlCl_3$: C, 54,26; H, 6,30; N, 8,33. Found: C, 54,35; H, 5,74; N, 8,15 %. Yield: 52,8 %. IR (KBr, cm^{-1}): 1603, 1456 [ν(C=C) and $\nu(C=N)_{py}$]. MS (FAB, *m/z*): 618 $[L^4]^+$, 683 $[AlL^4Cl]^+$.

$CrL^2(NO_3)_3.6H_2O$ ***(5).*** Colour: yellow; Anal. Calcd for $C_{37}N_9O_{18}H_{54}Cr$: C, 46.05; H, 5.60; N, 13.07. Found: C, 46.28; H, 5.79; N, 13.45 %. Yield: 54.4 %. IR (KBr, cm^{-1}): 1601, 1457 [$\nu(C=N)_{py}$ and ν(C=C)]; 839, 1384 [$\nu(NO_3^-)$]. MS (ESI, *m/z*): 619 $[L^2]^+$, 696 $[CrL^2Na]^+$, 754 $[CrL^2Na(NO_3)]^+$, 790 $[CrL^2(NO_3)_2]^+$.

$CrL^4(NO_3)_3.2H_2O$ ***(6)***. Colour: yellow; Anal. Calcd for $C_{38}N_8O_{14}H_{47}Cr$: C, 51.17; H, 5.27; N, 12.57. Found: C, 51.23; H, 5.12; N, 12.87 %. Yield: 49.8 %. IR (KBr, cm^{-1}): 1601, 1459 [ν(C=C) and $\nu(C=N)_{py}$]; 840, 1383 [$\nu(NO_3^-)$].

$Cu_2L^2(NO_3)_4.3C_2H_6O$ ***(7).*** Colour: green; Anal. Calcd for $C_{43}N_{10}O_{18}H_{60}Cu_2$: C, 45.62; H, 5.30; N, 12.37. Found: C, 45.56; H, 5.28; N, 11.90 %. Yield: 63.8 %. IR (KBr, cm^{-1}): 1599, 1454 [ν(C=C) and $\nu(C=N)_{py}$]; 839, 1384 [$\nu(NO_3^-)$]. MS (ESI, *m/z*): 619 $[L^2]^+$, 680 $[CuL^2]^+$, 766 $[Cu_2L^2(H_2O)]^+$, 806 $[Cu\ L^2(NO_3)_2]^+$, 822 $[CuL^2(NO_3)_2(H_2O)]^+$, 867 $[Cu_2L^2(NO_3)_2]^+$.

$Cu_2L^4(NO_3)_4.3H_2O$ ***(8).*** Colour: green; Anal. Calcd for $C_{38}N_9O_{18}H_{49}Cu_2$: C, 43.60; H, 4.68; N, 12.04. Found: C, 43.25; H, 4.20; N, 12.04 %. Yield: 41.5 %. IR (KBr, cm^{-1}): 1602, 1458 [ν(C=C) and $\nu(C=N)_{py}$]; 840, 1383 [$\nu(NO_3^-)$]. MS (FAB, *m/z*): 679 $[CuL^4]^+$.

$ZnL^2(NO_3)_2.6H_2O$ **(9).** Colour: yellow; Anal. Calcd for $C_{37}N_8O_{15}H_{54}Zn$: C, 48.50; H, 5.89; N, 12.23. Found: C, 48.50; H, 4.86; N, 12.44 %. Yield: 59.0 %. IR (KBr, cm^{-1}): 1600, 1454 [ν(C=C) and $\nu(C=N)_{py}$]; 839, 1384 [$\nu(NO_3^-)$]. (ESI, *m/z*): 619 $[L^2]^+$, 681 $[ZnL^2]^+$.

$ZnL^4(NO_3)_2.3H_2O$ **(10).** Colour: yellow; Anal. Calcd for $C_{38}N_7O_{12}H_{49}Zn$: C, 53.00; H, 5.69; N, 11.39. Found: C, 53.51; H, 5.32; N, 11.15 %. Yield: 68.3 %. IR (KBr, cm^{-1}): 1606, 1458 [ν(C=C) and $\nu(C=N)_{py}$]; 838, 1383 [$\nu(NO_3^-)$]. MS (FAB, *m/z*): 639 $[L^4Na]^+$, 680 $[ZnL^4]^+$, 701 $[ZnL^4H_2O]^+$.

$CdL^2(ClO_4)_2.2C_2H_6O$ **(11).** Colour: brown; Anal. Calcd for $C_{41}N_6O_{13}H_{54}Cl_2Cd$: C, 48.16; H, 5.28; N, 8.22. Found: C, 48.11; H, 5.34; N, 8.51 %. Yield: 71.4 %. IR (KBr, cm^{-1}): 1599, 1454 [ν(C=C) and $\nu(C=N)_{py}$]; 624, 636, 1087, 1109, 1121 [$\nu(ClO_4^-)$]. MS (ESI, *m/z*): 619 $[L^2]^+$, 731 $[Cd\ L^2]^+$, 929 $[CdL^2\ (ClO_4)]^+$, 942 $[Cd_2L^2(ClO_4)]^+$.

$CdL^4(NO_3)_2.3H_2O$ **(12).** Colour: brown; Anal. Calcd for $C_{38}N_7O_{12}H_{49}Cd$: C, 50.25; H, 5.40; N, 10.80. Found: C, 50.70; H, 5.87; N, 10.07 %. Yield: 58.3 %. IR (KBr, cm^{-1}): 1600, 1454 [ν(C=C) and $\nu(C=N)_{py}$]; 838, 1384 [$\nu(NO_3^-)$]. MS (FAB, *m/z*): 728 $[CdL^4]^+$, 790 $[CdL^4(NO_3^-)]^+$.

V.6 Acknowledgments

We thanks to Fundação para a Ciência e a Tecnologia / FEDER (Portugal/EU) (Project PTDC/QUI/66250/2006 FCT-FEDER), Xunta de Galicia (Spain) (Project PGIDIT07PXIB209039PR) for financial support. C.N, A.M, R.B, J. L. and C. L would like to thank the program "Joint Portuguese-Spanish Project 2007" for the bilateral agreement number 63/07(Portugal) / HP2006-0119 (Spain). C.N. thanks Xunta de Galicia for her Maria Barbeito program pre-doctoral contract. EB is grateful to Canterbury Christ Church University for financial support. J. L.C. and C. L. thank Xunta de Galicia for the Isidro Parga Pondal Research program.

V.7 References and notes

[1] For example see: (a) Fluorescent Chemosensors for Ion and Molecular Recognition; Czarnik, A. W., Ed.; American Chemical Society: Washington, DC, 1992. (b) de Silva, A. P.; Gunaratne, H. Q. N.; Gunnlaugsson, T.; Huxley, A. J. M.; McCoy, C. P.; Rademacher, J. T.; Rice, T. E. *Chem. Rev*. **1997**, 97, 1515. (c) Bargossi, C.; Fiorini, M. C.; Montalti, M.; Prodi, L.; Zaccheroni, N. *Coord. Chem. Rev.* **2000**, 208, 17. (d) Xue, G.-P; Savage, P. B.; Bradshaw, J. S.; Zhang, X. X.; Izatt, R. M. Functionalyzed Macrocycles Ligands as Sensory Molecules for Metal Ions. In *Advances in Supramolecular Chemistry*; Gokel, G. W., Ed., JAI Press: New York, **2000**; Vol. 7, pp 99-137. (e) Prodi, L.; Bolleta, F.; Montalti, M.; Zaccheroni, N. *Coord. Chem. Rev.* **2000**, 208, 59.

[2] For example, see: (a) Marsella, M. J.; Newland, R. J.; Carroll, P. J.; Swager, T. M. J. Am. Chem. Soc. 1995, 117, 9842. (b) Reinhoudt, D. N. Recl. Trav. Chim. Pays-Bas 1996, 115, 109.

[3] (a) Bartsch, R. A.; Chapoteau, E.; Czech, B. P.; Krykawasaki, J.; Kumar, A.; Robison, T. W. *J. Org. Chem*. **1994**, 59, 616. (b) Zazula, W.; Chapoteau, E.; Czech, B. P.; Kumar, A. *J. Org. Chem.* **1992**, 57, 6720. (c) Fery-Forgues, S., Bourson, S.; Dallery, L.; Valeur B. New *J. Chem.* **1990**, 14, 617.

[4] For example see: (a) Saroka, K.; Vithanage, R. S.; Phillips, D. A.; Walker, B.; Dasgupta P. K. *Anal. Chem.* **1987**, 59, 629; (b) Marshall, M. A.; Mottola, H. A. *Anal. Chem.* **1985**, 57, 375; (c) Lucy, C. A.; Liwen, Y. *J. Chromatogr., A* **1994**, 671, 121; (d) De Armas, G.; Miro, M.; Cladera, A.; Estela, J. M.; Cerda, V. *Anal. Chim. Acta* **2002**, 455, 149.

[5] For example see: (a) Bronson, R. T.; Montalti, M.; Prodi, L.; Zaccheroni, N.; Lamb, R. D.; Dalley, N. K.; Izatt, R. M.; Bradshaw, J. S.; Savage, P. B. *Tetrahedron* **2004**, 60, 11139; (b) Youk, J.-S; Kim, Y. H.; Kim, E.-J.; Youn, N. J.; Chang, S.-K. *Bull. Korean Chem. Soc.* **2004**, 25, 869; (c) Bronson, R. T.; Bradshaw, J. S.; Savage, P. B.; Fuangswasdi, S.; Lee, S. C.; Krakowiak, K. E.; Izatt, R. M. *J. Org. Chem.* **2001**, 66, 4752; (d) Kawakami, J.; Bronson, R. T.; Xue, G.; Bradshaw, J. S.; Izatt, R. M.; Savage, P. B. *Supramol. Chem.* **2001**, 1, 221; (e) Xue, G.; Bradshaw, J. S.; Dalley, N. K.; Savage, P. B.; Krakowiat, K. E.; Izatt, R. M.; Prodi, L.; Montalti, M.; Zaccheroni, N. *Tetrahedron* **2001**, 57, 7623; (f) Xue,

G.; Bradshaw, J. S.; Song, H.; Bronson, R. T.; Savage, P. B.; Krakowiat, K. E.; Izatt, R. M.; Prodi, L.; Montalti, M.; Zaccheroni, N. *Tetrahedron* **2001**, 57, 87; (g) Bordunov, A. V.; Bradshaw, J. S.; Zhang, X. X.; Dalley, N. K.; Kou, X.; Izatt, R. M. Inor. Chem. 1996, 35, 7229; (h) Zhang, X. X.; Bordunov, A. V.; Bradshaw, J. S.; Dalley, N. K.; Kou, X.; Izatt, R. M. *J. Am. Chem. Soc.* **1995**, 117, 11507.

[6] (a) Wang, S. *Coord. Chem. Rev.* **2001**, 215, 79; (b) Chen, C. H.; Shi, *J. Coord. Chem. Rev.* **1998**, 171, 161.

[7] For example see: (a) Gross, E. M.; Anderson, J. D.; Slaterbeck, A, F.; Thayumanavan, S; Barlow, S.; Zhang, Y.; Marder, S. R.; Hall, H. K.; Flore, N. M.; Wang, J.-F; Mash, E. A.; Armstrong, N. R.; Wightman, R. M. *J. Am. Chem. Soc.* **2000**, 122, 4972; (b) Muegge, B. D.; Brooks, S.; Richter, M. M. *Anal. Chem.* **2003**, 75, 1102.

[8] (a) Smith, R. M.; Martell, A. E.; Motekaitis, R. J.; *Nist Critical Stability Constants of Metal Complexes Database*, US Departament of Commerce, Gaithersburg, **1993**; (b) Pettit, L. D.; Powell, H. K. J.; *IUPAC Stability Constants Database*, Academic Software, Timble, **1993**.

[9] Bradshaw, J. S.; Izatt, R. M. *Acc. Chem. Res*. **1997**, 30, 338.

[10] Lee, S. C.; Izatt, R. M., Zhang, X. X.; Nelson, E. G.; Lamb, J. D.; Savage, P. B.; Bradshaw, J. S.; *Inorg. Chim. Acta* **2001**, 317, 174.

[11] Yang, Z.; Bradshaw, J. S.; Zhang, X.X.; Savage, P. B.; Krakoviat, K. E.; Dalley, N. K.; Su, N.; Bronson, R. T.; Izatt, R. M. *J. Org. Chem.* **1999**, 64, 3162.

[12] Aoki, S.; Sakurama, K.; Matsuo, N.; Yamada, Y.; Takasawa, R.; Tanuma, S.; Shiro, M.; Takeda, K.; Kimura, E. *Chem.-Eur. J*. **2006**, 12, 9066.

[13] (a) Prodi, L; Montalti, M.; Zaccheroni, N.; Bradshaw, J. S.; Izzat, R. M.; Savage, P. B. *Tetrahedron Lett.* **2001**, 42, 2941. (b) Prodi, L; Bargossi, C.; Montalti, M.; Zaccheroni, N.; Su, N.; Bradshaw, J. S.; Izzat, R. M.; Savage, P. B. *J. Am. Chem. Soc.* **2000**, 122, 6769.

[14] For example see: (a) Izatt, R. M.; Bradshaw, J. S.; Nielsen S. A.; Lamb, J. D.; Christensen, J. J.; Sen, D. *Chem. Rev.* **1985**, 85, 271. (b) Izatt, R. M.; Pawlak, K., Bradshaw, J. S.; Bruening, R. L. *Chem. Rev.* **1991**, 91, 1721. (c) Izatt, R. M.; Pawlak, K., Bradshaw, J. S.; Bruening, R. L. *Chem. Rev.* **1995**, 95, 1231.

[15] Cui, X.; Cabral, M. F.; Costa, J.; Delgado, R. *Inorg. Chim. Acta* **2003**, *356*, 133-141.

[16] Chemistry. An Introduction for Medical and Health Sciences, Jones, A. John Wiley & Sons, Chichester, **2005**.

[17] (a) Ghosh, P.; Bharadwaj, P. K.; Mandal, S.; Ghosh, S. *J. Am. Chem. Soc.* **1996**, *118*, 1553; (b) Inoue, M. B.; Medrano, F.; Inoue, M.; Raitsimring, A.; Fernando, Q. *Inorg. Chem.* **1997**, *36*, 2335; (c) Rurack, K.; Kollmannsberger, M.; Resch-Genger, U.; Daub, J. *J. Am. Chem. Soc.* **2000**, *122*, 968; (d) Xu, Z.; Xiao, Y.; Qian, X.; Cui, J.; Cui, D. *Org. Lett.* **2005**, *7*, 899; (e) Royzen, M.; Dai, Z.; Canary, J. W. *J. Am. Chem. Soc.* **2005**, *127*, 1612.

[18] For example see: (a) Park, S. M.; Kim, M. H.; Choe, J.-I; No, K. T.; Chang, S.-K. *J. Org. Chem.* **2007**, **72**, 3550; (b) Sasaki, D. Y.; Shnek, D. R.; Pack, D. W.; Arnold, F. H. *Angew. Chem., Int. Ed. Engl.* **1995**, *34*, 905; (c) Torrado, A.; Walkup, G. K.; Imperoali, B. *J. Am. Chem. Soc.* **1998**, *120*, 609.

[19] (a) Varnes, A. V.; Dodson, R. B.; Whery, E. L. *J. Am. Chem. Soc.* **1972**, *94*. 946; (b) Kelmo, J. A.; Shepherd, T. M. *Chem. Phys. Let.* **1977**, *47*, 158; (c) Rurack, K.; Resch, U.; Senoner, M.; Dahene, S. *J. Fluoresc.* **1993**, *3*, 141.

[20] (a) Fraústo da Silva, J. J. R.; Williams, R. J. P. *The Biological Chemistry of the Elements*, Clarendon, Oxford, **1991**; (b) Williams, R. J. P.; Fraústo da Silva, J. J. R. *Coord. Chem. Rev.* **2000**, *200-202*, 247-348.

[21] For example see: (a) Gunnlaugsson, T.; Lee, T. C. ; Parkesh, R.; *Org. Lett*. **2003**, 5, 4065; (b) Charles, S.; Dubois, F.; Yunus, S.; Vander Donckt, E. *J. Fluorescence* **2000**, 10, 99; (c) Blake, A. J.; Bencini, A.; Caltagirone, C.; De Filippo, G.; Dolci, L. S.; Garau, A.; Isaia, F.; Lippolis, V.; Mariani, P.; Prodi, L.; Montalti, L.; Zaccheroni, N.; Wilson, C. *Dalton Trans*., **2004**, 2771.; (d) Meng, X. M.; Zhu, M. Z.; Liu, L:; Guo, Q. X. *Tetrahedron Lett*., **2006**, 47, 1559; (e) Aragoni, M. C.; Arca, M.; Bencini, A.; Blake, A. J.; Caltagirone, C.; Decortes, A.; Demartin, F.;

Devillanova, F. A.; Faggi, E.; Dolci, L. S.; Garau, A.; Isaia, F.; Lippolis, V.; Prodi, L.; Wilson, C.; Valtancoli, B.; Zaccheroni, N. *Dalton Trans*, **2005**, 2994.

[22] For example see: (a) Zhao, Y. G.; Li, Z. H.; Liao, H.P.; Duan, C. Y.; Meng, Q. J. *Inorg. Chem. Commun*., **2006**, *9*, 699. (b) Oliveira, E.; Vicente,M.; Valencia, L.; Macias, A.; Bértolo, E.; Bastida, R.; Lodeiro, C. *Inorg. Chim. Acta*, **2007**, 360,

2734.; (c) Ben Othman, A.; Lee, J. W.; Huh, Y. D.; Abidi, R.; Kim, J.S.; Vicens, J. *Tetrahedron*, **2007**, 63, 10793. (d) Wang, J. Q.; Huang, L.; Gao, L.; Zhu,J. H.; Wang, Y.; Fan, X. X.; Zou, Z. G.; *Inorg. Chem. Commun*., **2008**, *11*, 203. (e) Arduini, M.; Felluga, F.; Mancin, F.; Rossi, P.; Tecilla, P.; Tonellato, U.; Valentinuzzi, N. *Chem. Commun.* **2003**, 1606; (f) Launay, F.; Alain, V.; Destandau, E.; Ramos, K. N.; Bardez, E., Baret, P.; Pierre, J.-L. *New J. Chem.* **2001**, *25*, 1269.

[23] For example see: (a) Kimura, M., Tsunenaga, M.; Takami, S.; Ohbayashi, Y. *Bull.Chem. Soc. Jpn.* **2005**, *78*, 929; (b) de Rosa, F.; Bu, X.; Pohaku, K.; Ford, P. C. *Inorg. Chem.* **2005**, *44*, 4166; (c) de Rosa, F.; Bu, X.; Ford, P. C. *Inorg. Chem.* **2005**, *44*, 4157. (d) Resendiz,M. J. E.; Noveron, J. C.; Disteldorf, H.; Fisher, S.; Stang, P. J., *Org. Lett*., **2004**, *6*, 651: (f) Sarkar, M.; Banthia, S.; Samanta, A.; *Tet. Lett*., **2006**, *47*, 7575; (g) Huang, K. W.; Yang, H.; Zhou, Z. G.; Yu, M. X.; Li, F. Y.; Gao, X.; Yi, T.; Huang, C. H.; *Org. Lett*., **2008**, 12, 2557.

[24] For example see: (a) Lodeiro, C.; Capelo, J.L.; Bértolo, E.; Bastida, R.; *Z. Anorg. Allg. Chem*. **2004**, 630, 1110 (b) Lodeiro, C.; Bastida, R.; Bértolo, E.; Macías, A.; Rodríguez, A. *Trans. Metal Chem*., **2003**, *28*, 388; (c) Lodeiro, C.; Bastida, R.; Bértolo, E.; Macías, A.; Rodríguez, A. *Polyhedron*, **2003**, *22*, 1701; (d) Tamayo, A.; Lodeiro, C.; Escriche, L.; Casabó, J.; Covelo, B.; González, P. *Inorg. Chem*., **2005**, *44*, 8105; (e) Freiría, A.; Bastida, R.; Valencia, L.; Macías, A.; Lodeiro, C.; Adans, H. *Inorg. Chim. Acta*., **2006**, *359*, 2383.; (f) Tamayo, A.; Pedras, B.; Lodeiro, C.; Escriche, L.; Casabó, C.; Capelo, J. L.; Covelo, B.; Sillanpaä, R.; Kivekäs, R., *Inorg. Chem*., **2007**, *46*, 7818; (g) Nuñez, C.; Valencia, L.; Macías, A.; Bastida, R.; Oliveira, E.; Giestas, L.; Lima, J. C.; Lodeiro, C., *Inorg. Chim. Acta*., **2008**, *8*, 2183.

[25] Lodeiro, C.; Bastida, R.; Bértolo, E.; Rodriguez, A. *Can. J. Chem*. **2004**, *82(3)*, 437-447.

[26] Bailey, N. A.; Fenton, D. E.; Kitchen, S. J.; Lilley, T. H.; Williams, M. G.; Tasjer, P. A.; Leong, A. J.; Lindoy, L. F. *J. Chem. Soc., Dalton Ttrans*., **1991**, 627.

[27] (a) Grill, N. S.; Nuttall, R. H.; Scaife, D. E.; Sharp, D. W. J. *Inorg. Nucl. Chem*. **1961**, *18*, 79; (b) Aime, S.; Botta, M.; Casellato, U.; Tamburini, S.; Vigato, P. A. *Inorg. Chem*. **1995**, *34*, 5825-5831.

[28] (a) Bértolo, E.; Bastida, R.; de Blas, A.; Fenton, D. E., Lodeiro, C.; Macías, A.; Rodríguez, A; Rodríguez-Blas, T. *J. Incl. Phenom. Macro. Chem.* **1999**, 191. (b) Vicente, M.; Lodeiro, C.; Adams, H.; Bastida, R.; de Blas, A.; Fenton, D. E.; Macías, A.; Rodríguez, A; Rodríguez-Blas, T. Eur. J. Inorg. Chem. **2000**, 1015.

[29] (a) Goldman, M.; Wehry, E.L. *Anal. Chem*., **1970**, *42*, 1178; (b) Bardez, E.; Devol, I.; Larrey, B.; Valeur, B.; *J. Phys. Chem*., **1997**, *101*, 7786; (c) Meech, S. R.; Philips, D. J.; *Photochem*. **1983**, 23, 193.

[30] Handbook of Photochemisty, 3th Ed. Montalti, M.; Credi, A.; Prodi,L.; Gandolfi, M.T., CRC Press, Taylor & Francis Group, Boca Raton, New York, **2006**.

[31] (a) Fabbrizzi, L.; Licchelli, M. ; Pallavicini, P.; Perotti, A.; Sacchi, D.; *Ang. Chem. Int. Ed. Engl*. **1994**, *33*, 1975; (b) Rurack, K.; *Spect. Acta. A,* **2001**, *57*, 2161.

[32] For examples see: (a) de Silva, A. P.; Gunaratne, H. Q. N.; Lynch, P. L. M. *J. Chem. Soc*. *Perkin Trans 2*, **1995**, 685; (b) deSilva, S. A.; Zavaleta, A.; Baron, D.E.; Allam, O.; Isidor, E.V.; Kashimura, N.; Percarpio, J.M.; *Tetrahedron Lett*. **1997**, *38*, 2237. (c) Fabbrizzi, L.; Gatti, F.; Pallavicini, P.; Parodi, L.; *New. J. Chem.* **1998**, 1403; (d) Aucejo, R.; Alarcón, J.; García-España, E.; Llinares, J.M.; Marchin, K. L.; Soriano, C.; Lodeiro, C.; Bernardo, A. M.; Pina, F.; Pina, J.; Seixas de Melo, J.; *Eur. J. Inorg. Chem*., **2005**, 4301.

Chapter VI

Ultrasonic Enhanced Applications in Proteomics Workflows: single probe versus multiprobe

Published in:

Journal of Integrated Omics, 1 (2011) 144–150

Luz Fernandes, Hugo. M. Santos, J. D. Nunes Miranda, Carlos Lodeiro and José. L. Capelo.

(DOI: 10.5584/jiomics.vlil.55)

VI.1 Abstract

A 96-well plate-based platform in conjunction with an ultrasonic multiprobe of four tips was assessed to develop various fast proteomics workflows for gel-based proteomics. The use of such protocols reduce sample time and handling, allowing rapid processing whilst reducing the risk of contamination. The procedure reduces the time to indentify proteins separated by gel electrophoresis to just 8 min/each. In addition, the ultrasonic multiprobe was compared with the single probe as a tool to obtain high sample throughput in proteomics workflows entailing identification and/or quantification of proteins using mass-spectrometry based approaches. The 18-O labeling-based method was used to study the type of peptides extracted from the gels when the extraction was done with the aid of ultrasonic energy. The assessment was done in ten standard proteins separated by gel elecrophoresis. Two proteins obtained from *D. desulfuricans,* and from *Cyprinus carpio*, Split-Soret cytochrome c, and Vitellogenin respectively, were also indentified as a further proof-of-the concept.

Keywords: ultrasonic, MALDI, vitellogenin, ^{18}O, inverse labeling.

My contribution to this work was the optimization of all experimental variables, MALDI-TOF MS analysis and interpretation.

VI.2 Introduction

Ultrasonication has been recently appointed as a powerful tool in mass spectrometry-based proteomics workflows for protein identification [1]-[7]. Ultrasonic energy can be used to enhance from hours to minutes protein denaturation, protein reduction, protein alkylation and protein digestion, the four mais steps of any common procedure nowadays used for protein identification relaying on mass spectrometry. Furthermore, ultrasonic energy can also be used to speed protocols relaying on ^{18}O isotopic labeling, which is a widely used method to tracking changes in protein level expression as well as in sequencing of peptides by mass spectrometry-based techniques [6],[7]. As a matter of fact ultrasonic energy has been recently integrated in rapid sample processing for ^{18}O-LC-MS-based quantitative proteomics [8].

Ultrasonic-based high throughput sample treatment for proteomics was recently reported for the treatment of liquid samples by joining a 96-well plate and an ultrasonic multiprobe. The present work shows a step forward of this protocol by applying it to proteins separated by gel-based approaches and also using it to study in an ^{18}O labeling-based method the type of peptides extracted from the gels when the extraction is done with the aid of ultrasonic energy. The study was done through the identification of 10 standard proteins and two proteins obtained from *D. desulfuricans,* and from Cyprinus carpio, Split-Soret cytochrome c, and Vitellogenin respectively.

VI.3 Material and methods

VI.3.1 Apparatus

Protein digestion was done in a 96-well plate (Digilab-Genomic Solutions, USA). A vacuum concentrator centrifuge from UniEquip (Martinsried, Germany) model UNIVAPO 100H with a refrigerated aspirator vacuum pump model Unijet II was used for (i) sample drying and (ii) sample pre-concentration. A minicentrifuge, model Spectrafuge-mini, from Labnet (Madrid, Spain), and a minicentrifuge-vortex, model Sky Line, from ELMI (Riga, Latvia) were used throughout the sample treatment, when necessary. A Simplicity^{TM} 185 from Millipore (Milan, Italy) was used to obtain Milli-Q water throughout the experiments.

VI.3.2 Ultrasonic devices

(i) Ultrasonic probe, model UP 100H (dr. Hielscher, Teltow, Switzerland, 200 W, 30 kHz ultrasonic frequency, 0.5 mm of diameter probe).

(ii) Ultrasonic multi-probe from Branson Ultrasonics Corporation (USA), model SLPe (150 W, 40 kHz ultrasonic frequency, 1 mm diameter probe). The ultrasonic generator SLPe is equipped with a multi-probe detachable horn (model 4c15), with four tips for simultaneous ultrasonication of four samples and it was used in conjunction with a 96-well plate.

VI.3.3 Standards and reagents

The following protein standards were used: α-lactalbumin from bovine milk (≥85%), BSA (>97%) and carbonic anhydrase (>93%) from Sigma (Steinheim, Germany), albumin from hen white (>95%) from Fluka (Buchs, Switzerland). Chymotrypsinogen A, catalase bovine and aldolase from rabbit were standards for gel filtration calibration kit high molecular weight from Amersham Biosciences (Piscataway, USA).

Low molecular weight standard protein mixture of glycogen phosphorylase b, bovine serum albumin, BSA, ovalbumin, carbonic anhydrase, trypsin inhibitor and α-lactalbumin were purchased from Amersham Biosciences (Piscataway, USA). Thyroglobulin and Lactate dehydrogenase were purchased from Amersham Biosciences (Piscataway, USA)

Carp vitellogenin standard was purchased from Biosense Laboratories (Bergen, Norway).

Trypsin enzyme, sequencing grade was purchased from Sigma. All materials were used without further purification. α-cyano-4-hydroxycinnamic acid (α-CHCA) puriss for MALDI–MS from Fluka was used as MALDI matrix. ProteoMass™ Peptide MALDI-MS Calibration Kit (MSCAL2) from Sigma was used as mass calibration standard for MALDI-TOF MS.

The following reagents were used for protein depletion: sodium chloride puriss. p.a. and magnesium chloride hexahydrate puriss. p.a. were purchased from Fluka;

ethylenediaminetetraacetic acid disodium salt dehydrate puriss. p.a. was from Riedle-de Haën (Seelze, Germany).

The following reagents were used for protein digestion: acetonitrile, iodoacetamide (IAA) and DL-dithiothreitol (DTT) (99%) were purchased from Sigma; formic acid and ammonium bicarbonate (>99.5%) were from Fluka; trifluoroacetic acid (TFA, 99%) were from Riedel-de-Haën (Seelze, Germany); and urea (99%) was from Panreac (Barcelona, Spain).

VI.3.4 Sample treatment

VI.3.4.1 Protein separation by 1D-SDS-PAGE

Amounts of protein ranging from 0.5 to 3.7 µg were dissolved in 5 µL of water plus 5 µL of sample buffer (5 mL of 0.5 M Tris-Base + 8 mL of 10 % SDS + 1 mL of β-mercaptoethanol + 2 mL of glycerol + 4 mg of bromophenol blue in a final volume of 20 mL in water) for analysis by sodium dodecyl sulphate polyacrilamide gel electrophoresis (SDS-PAGE) (10% 0.5 mm thickness). After gel electrophoresis (65 min, 120 V, 400 mA), the gel was stained with Coomassie blue R-250 and destained in order to visualize the proteins bands.

VI.3.4.2 In-gel sample treatments

(i) Overnight method. For in-gel digestion optimization, 2.1 µg of BSA and 2.9 µg of α-lactalbumin were loaded onto 10% SDS-PAGE gels. Coomassie Blue-stained protein bands were excised from the gels, cut into pieces and subjected to digestion. Excised gel bands were then washed with water (3 times with agitation/centrifugation, 10min each), and dehydrated with acetonitrile (2 times, 3 min each + 1 time, 20 min with agitation/centrifugation) and dried in a vacuum centrifuge. Gel pieces were further rehydrated with 10 mM of DTT in 25 mM ammonium bicarbonate buffer and incubated 10 min at 60 ºC for protein reduction. Then DTT solution was replaced by IAA 55 mM in 25 mM ammonium bicarbonate buffer and incubated in the dark and room temperature by 35 min. After protein reduction and alkylation gel pieces were dried and rehydrated in ice

bath in a 0.025 μg/μL solution of trypsin in 12.5 mM ammonium bicarbonate buffer, to a final volume of 25 μL, during 1 h.

After the rehydration step, samples were digested overnight at 37 °C. Next, trypsin activity was stopped by the addition of 20 μL of 5% formic acid. The supernatant was withdrawn and retained, and the peptides were extracted from the gel pieces by adding 50-100 μL of a mixture of acetonitrile/TFA (500 μL H_2O+500 μL AC+1 μL TFA) and incubating them for 15 min at 37 ºC in a shaker. This extraction was done twice. Then, all supernatants were combined and evaporated to dryness in a vacuum concentrator centrifuge and finally the dried peptides obtained were reconstituted with 10 μL of 0.3% v/v formic acid.

(ii) Accelerated method. this method, the protocol described above and referred as "overnight method" was followed but (i) washing steps (ii) alkylation, (iii) reduction, (iv) digestion of gel bands and (v) extraction peptides were done in 8 min (2 min each washing step, 30% ultrasonic amplitude, total of 3), 5 min (30% ultrasonic amplitude), 5 min (30% ultrasonic amplitude), 4 min (25% ultrasonic amplitude) and 8 min (two extraction steps, 2 min each) respectively, using ultrasonication at 30 kHz, with a single probe or 40 kHz with the four tip multiprobe.

VI.3.5 Case studies

VI.3.5.1. Desulfovibrio desulfuricans ATCC27774

Desulfovibrio desulfuricans ATCC27774 cells were cultured in sulfate-lactate medium. Cells were collected by centrifugation (8000 × g during 15 min at 4 ºC), resuspended in 10 mM Tris-HCl buffer and ruptured in a French press at 9000 psi. After centrifugation (10000 × g, 45 min) and ultracentrifugation (180000 × g, 60 min) the supernatant was dialyzed against 10 mM Tris-HCl buffer. Both proteins were isolated from the soluble extract using chromatographic columns (anionic exchange, Hydroxyapatite column and molecular exclusion chromatography). The purity of the proteins was evaluated by SDS-PAGE and UV-visible spectroscopy. All purification procedures were performed under aerobic conditions at 4 ºC and pH 7.6. Split-soret cytochrome c from *Desulfovibrio desulfuricans* ATCC27774 was in gel digested

according to the accelerated method described in VI.3.4.2. Protein identification was done using the PMF procedure by MALDI-TOF MS.

VI.3.5.2. Plasmatic vitellogenin from Cyprinus carpio

80 µL of plasma from *Cyprinus carpio* was diluted to 100 µL with cold PBS (Phosphate Buffer Solution). 300 µL of -20 ºC cold acetone were added into the diluted plasma solution and kept overnight on ice. The sample was centrifuged at 10000 g, 4 ºC for 30 min. The supernatant was removed and the pellet was suspended in 100 µL of buffer (10 mM Tris-HCl pH 7.4; 2% of SDS; 1% of β-mercaptoethanol). Amounts of delipidated plasma (5 µL) were mixed with 5 µL of sample buffer (5 mL of 0.5 M Tris-Base + 8 mL of 10 % SDS + 1 mL of β-mercaptoethanol + 2 mL of glycerol + 4 mg of bromophenol blue in a final volume of 20 mL in water) for analysis by sodium dodecyl sulphate polyacrylamide gel electrophoresis (SDS-PAGE) (7.5% 0.5 mm thickness). After gel electrophoresis (65 min, 120 V, 400 mA), the gel was stained with Coomassie blue R-250 and destained in order to visualize the proteins bands. Vitellogenin was in gel digested according to the accelerated method described in VI.3.4.2. Protein identification was done using the PMF procedure by MALDI-TOF MS.

VI.3.6 Inverse ^{18}O labeling of peptides

Protein BSA was used to study the effect of ultrasonication in the release of peptides from gels. BSA was separated by 1D-PAGE, and then submitted to the protocol described in section VI.3.4.2 (ii). Once the protein was digested, gel pieces were removed and the solutions containing the peptides were dried in a speed vacuum. Then, peptides obtained were recomposed in (i) normal water or (ii) ^{18}O water and then both methods were compared following the inverse ^{18}O labeling protocol as described by Wang et al [10].

VI.3.7 MALDI-TOF MS analysis

A MALDI-TOF MS model Voyager DE-PRO Biospectrometry Workstation equipped with a nitrogen laser radiating at 337 nm from Applied Biosystems (Foster City, USA), was used to obtain the PMF. MALDI mass spectra were acquired as recommended by the manufacturer and treated with the Data Explorer™ software version 4 series. Prior to MALDI-TOF MS analysis, the sample was mixed with the matrix solution. α-CHCA matrix was used throughout this work and was prepared as follows: 10 mg of α-CHCA was dissolved in 1 mL of Milli-Q water/acetonitrile/TFA (1mL+1mL+2μL). Then, 2 μL of the aforementioned matrix solution was mixed with 2 μL of sample and the mixture was shaken in a vortex for 30 s. Finally, 1 μl of the sample/matrix mixture was spotted on a well of a MALDI-TOF MS sample plate and was allowed to dry.

Measurements were done in the reflector positive ion mode, with a 20 kV accelerating voltage, 75.1 % grid voltage, 0.002 % guide wire and a delay time of 100 ns. Two close external calibrations were performed with the monoisotopic peaks of the Bradykinin, Angiotensin II, P14R and ACTH peptide fragments (m/z: 757.3997, 1046.5423, 1533.8582 and 2465.1989, respectively). Monoisotopic peaks were manually selected from each of the spectra obtained. Mass spectral analysis for each sample was based on the average of 500 laser shots. Peptide mass fingerprints were searched with the MASCOT [http://www.matrixscience.com/search_form_select.htmL] search engine with the following parameters: (i) SwissProt. 2006 Database; (ii) molecular weight (MW) of protein: all; (iii) one missed cleavage; (iv) fixed modifications: carbamidomethylation (C); (v) variable modifications: oxidation (M); (vi) peptide tolerance up to 150 ppm. A match was considered successful when the protein identification score is located out of the random region and the protein analysed scores first.

VI.4 Results and discussion

VI.4.1 96 well plate method for proteins separated by gel electrophoresis

The protein concentration loaded onto the gel was 2.1 μg/μL for BSA and 2.9 μg/μL for α-lactalbumin. Results, including the values setting for each variable, are presented in Fig. VI.1. As may be seen, ultrasonic amplitude was found a critical parameter. For BSA protein, when the lower amplitude was used in the digestion step (10%), longer treatment times were required to obtain good results, whilst the highest amplitude used (50%) degrades the gel in such a way that protein identification by MALDI was not possible. In the case of the α-lactalbumin this problem was even worst since using the lower amplitude in the digestion step no identification was possible at all in the range time assessed (60s-240s), whilst for the highest amplitude the identification was only possible in times comprised between 120 and 240 s. These results could be explained on the basis of recent research in ultrasonic applications in medicine and drug delivery that has estimated the pressure at the tip of the jet generated by bubble collapse (cavitation phenomena) around 60 MPa [11]. This is high enough to penetrate small pores, such as the ones present in the gels in which proteins are separated. Hence, liquid jets may act as microsyringes, delivering the enzyme to a region of interest. However, the ultrasonic energy needed to do such delivering must be reached, and we hypothesized that this is the reason why the lower amplitude studied did not perform well, because it is not powerful enough to deliver the enzyme inside the gel, as it was the case for α-lactalbumin. As the amplitude and time is increased, the enzymatic cleavage performs better for both proteins, until a maximum is reached. Then, the gel is degraded and the protein identification becomes difficult or impossible, as it was the case for both proteins for the highest amplitude and time studied. Gel degradation can be explained on basis on the fact that when a cavitation bubble collapses near the surface of a solid sample particle, micro-jets of solvent propagate toward the surface at velocities greater than 100 m s^{-1}, causing pitting and mechanical erosion of the solid surface, thus leading to particle rupture (i.e., disruption) [12]. Although this process could be favorably used to enhance peptide release from the gel, at some point it becomes a problem interfering the subsequent analysis by mass spectrometry or even blocking HPLC columns. However, it is noteworthy that the multi-probe and the 96-well plate performed well for gel-based protein separations, once the process has been optimized. In addition, it was not found

differences between the two frequencies studied. Furthermore, the best results obtained with the multi-probe were not different from the ones obtained using the overnight protocol.

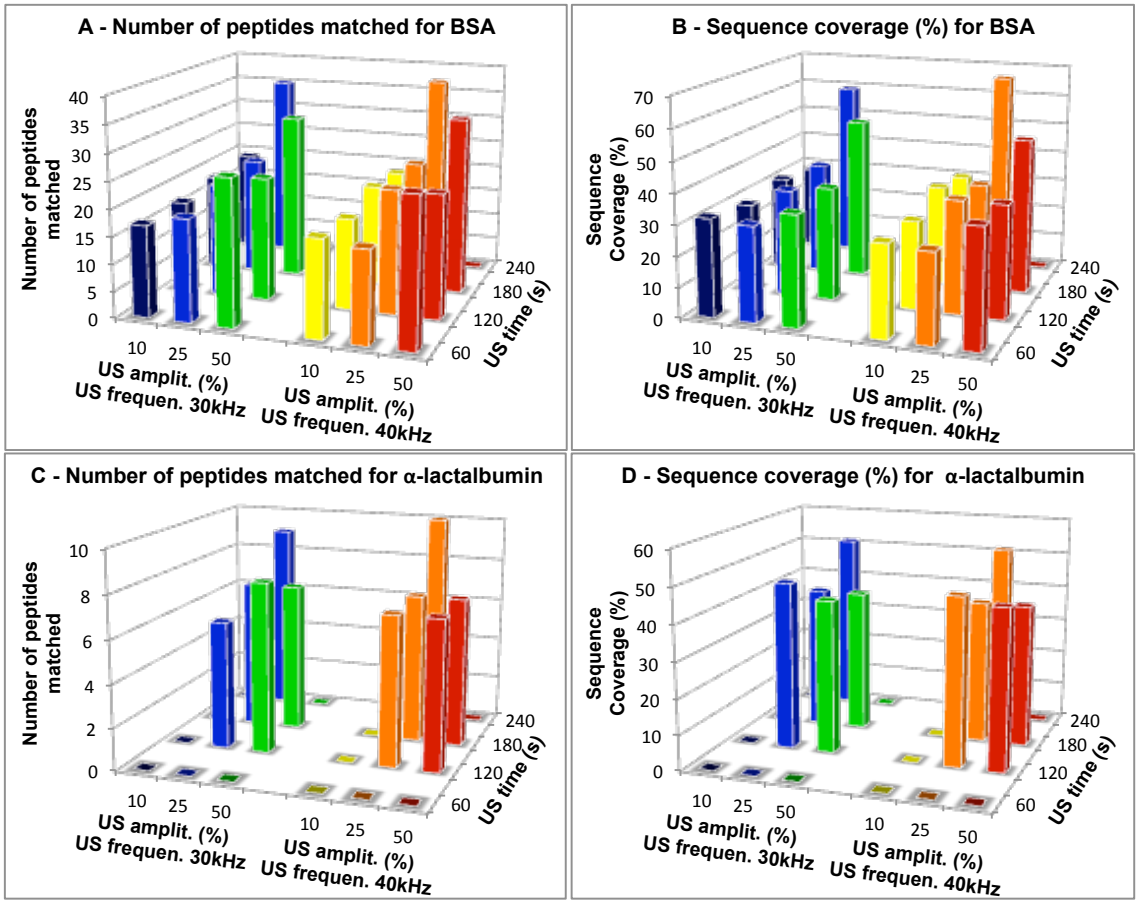

Figure VI.1 Number of peptides matched and sequence coverage for BSA and α-lactalbumin as a function of time, amplitude and frequency of sonication. Proteins were separated by Gel electrophoresis. Peptides matched and sequence coverage for the overnight method was 42±6 and 70±4 respectively for BSA and 11±2 and 51±1 for α-lactalbumin.

To complete the study a set of 8 further proteins was mixed and separated using gel electrophoresis to proceed to protein identification through the ultrasonic method. Results showed in Table VI.1 demonstrate the successful accomplishment between the 96-well plate and the multi-probe since all proteins were identified with similar protein coverage and number of peptides matched than using the overnight protocol.

Table VI.1 Number of peptides matched and protein sequence coverage for in gel-protein digestion by the overnight method and accelerated method.

Protein	theor. M_r (kDa)	overnight method (n = 2)			accelerated method (n = 2)					
		mascot score	sequence coverage (%)	no. of peptides matched	mascot score		sequence coverage (%)		no. of peptides matched	
					30 kHz	40 kHz	30 kHz	40 kHz	30 kHz	40 kHz
α-Lactalbumin	16.7	130±5	51±1	11±2	110±2	104±5	50±2	51±0	9±1	10±0
Trypsin inhibitor	24.3	87±3	51±1	18±0	69±3	64±5	28±2	27±1	7±1	7±0
Carbonic anhydrase	29.1	115±3	69±0	20±0	240±2	238±3	71±2	64±0	19±0	18±1
Ovalbumin	43.2	100±2	49±6	20±1	82±2	84±5	50±2	44±4	16±2	15±0
BSA	71.2	152±4	70±4	42±6	220±1	222±3	64±2	66±5	40±3	37±1
Aldolase rabit	39.8	152±6	72±6	21±2	109±3	103±4	68±1	68±0	20±1	19±0
Catalase bovine	60.1	98±4	43±2	26±2	218±2	220±0	37±4	43±0	22±1	24±0
Phosphorylase b	97.7	92±5	66±1	64±1	298±1	305±3	48±3	52±2	40±2	38±1
Thyroglobulin subunit*	310.0	194±8	28±1	76±6	188±2	194±6	28±1	25±7	80±2	81±1
Lactate dehydrogenase subunit*	36.9	79±2	46±4	21±1	83±1	182±4	46±2	49±0	20±1	21±0
Split-Soret cytochrome c *D. desulfuricans*	27.8	128±4	51±4	11±1	100±4	96±6	40±5	37±0	10±2	10±1
Vitellogenin *Cyprinus carpio*	148.8	176±6	42±4	49±1	150±3	141±6	42±1	41±1	50±2	51±1

* HMW-Native standard under denaturant conditions.

A comparison of the total time and number of steps involved in the handling of the five sample treatments reported in this manuscript is presented in Table VI.2. As may be seen, the ultrasonic method with multiprobe allows for the treatment of 4 samples in 30 minutes. This number can be exponentially increased using the new generation of multiprobes that allow treating 96 samples at once [11]. Hence, this method has a great potential for clinical purposes, where a high number of samples are generally handled daily.

Table VI.2 Comparison of handling and time consumed for the five methods studied with the 96 well plate ultrasonic method.

		Denaturation	**Reduction**	**Alkylation**	**Digestion**	**Desalting**	**Total steps**	**Total time**
Proteins in gel	Overnight	5 min heating before electrophoresis	10 min	35 min	12 hours	no	25*	24 h
	Ultrasonic	5 min heating before electrophoresis	5 min	5 min	4 min	no	20**	30 min

* Including: electrophoresis, band excision, 12 steps for gel washing, 10×3 min each and 2×20 min each, trypsin incubation on ice before digestion, peptides extraction (2 extractions) and evaporated to dryness (3 times).
** Including: electrophoresis, band excision, 8 steps for gel washing, 2×2 min each, digestion and peptides extraction and evaporated to dryness (3 times). With the in gel ultrasonic digestion no incubation of trypsin on ice is needed.

VI.4.2 Effect of ultrasonication in the release of peptides from gels

To investigate the role of ultrasonication in the release of peptides from gels, a set of experiments using the ^{18}O isotopic labeling of the protein BSA was done to compare, the type of peptides released using the overnight, ON, or the ultrasonic, US, treatments [6],[7]. The same amount of BSA was loaded onto a gel, and the protein was in-gel digested, using the overnight or the ultrasonic protocol. The supernatants were withdrawn from the tubes and dried down in a vacuum centrifuge. Then samples were recomposed in ^{16}O or in ^{18}O water. Since under conventional conditions, the yield of peptides extracted from a gel is protein-dependant and it varies for different peptides that originate from the same protein, we decide to use the inverse labeling as described by Wang et al [10] to ensure a correct identification of peptides extracted and unambiguous assessment of differential peptide extraction. To avoid any biased yields own to the sample treatment, all steps were exactly the same for the overnight or ultrasonic protocols, with the exception of the protein digestion step.

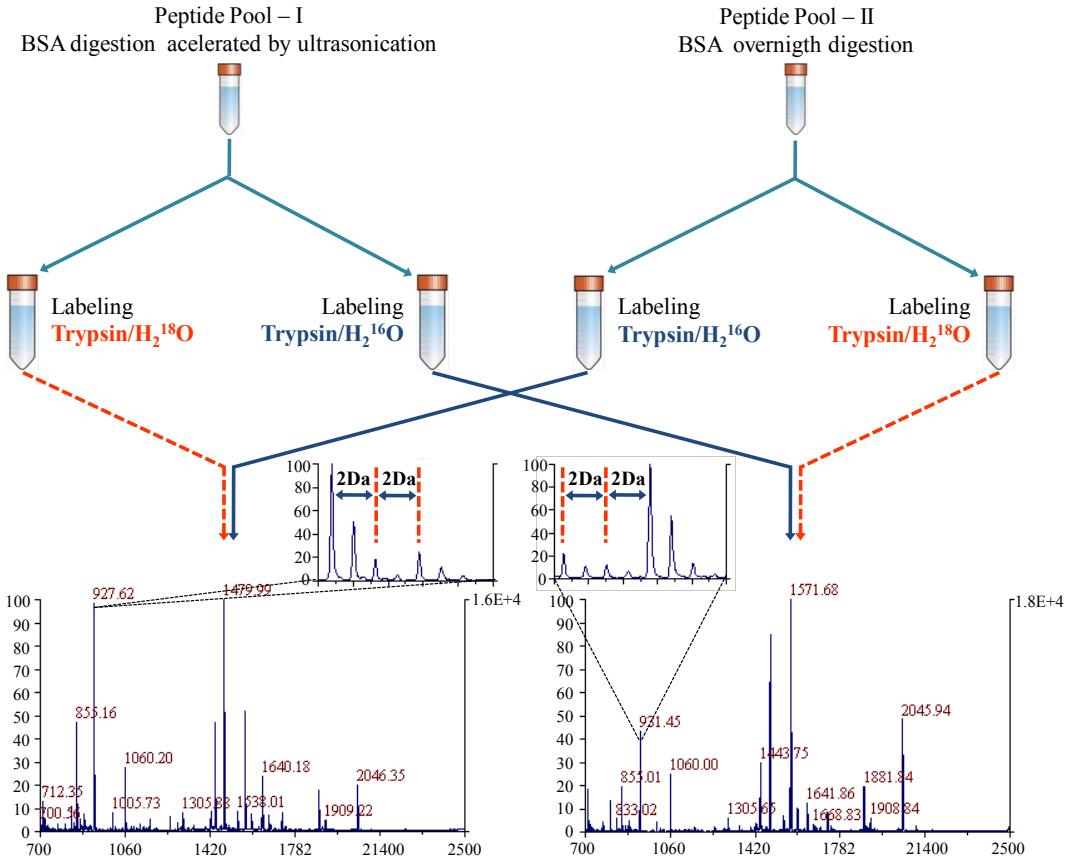

Figure VI.2 The inverse labeling method for the unambiguous identification of peptides released from gels using the overnight or the ultrasonic digestion protocol.

Figure VI.2 shows the inverse labeling method for the unambiguous identification of peptides used. The result of this set of experiments are shown in Table VI.3, where may be seen that a total of 40 peptides were identified as BSA peptides. Interestingly, from those 40 peptides, 15 peptides were labeled either in the direct or in the reverse process, whilst 21 peptides from the total, were also identified but they were not labeled. This put forwards that after sample recomposition not all peptides are labeled. This result is in agreement with data published by other authors [13]. From this 21 non labeled peptides, 6 were observed in the direct and reverse method, suggesting that they are produced regardless of the digestion method used; 9 were found in the mixture $US^{16}O$ / $ON^{18}O$ and six were found in the mixture $US^{18}O$ / $ON^{16}O$.

Table VI.3. Results from the BSA ^{18}O-inverse labeling experiments. All peptides were manually verified. (n=2)

	No. of peptides	Peptide fragment
Direct & reverse Labeled peptides $US^{16}O$ / $ON^{18}O$ and $US^{18}O$ / $ON^{16}O$	15±2	(SEIAHR)H^+; (YLYEIAR)H^+; (LVNELTEFAK)H^+; (HPEYAVSVLLR)H^+; (SLHTLFGDELCK)H^+; (RHPEYAVSVLLR)H^+; (YICDNQDTISSK)H^+; (TCVADESHAGCEK)H^+; (LGEYGFQNALIVR) H^+; (HPEYAVSVLLRLAK)H^+; (KVPQVSTPTLVEVSR) H^+; (MPCTEDYLSLILNR)H^+; (RPCFSALTPDETYVPK) H^+; (LFTFHADICTLPDTEK)H^+; (RHPYFYAPELLYYANK)H^+
Direct & reverse non-labeled peptides $US^{16}O$ / $ON^{18}O$ and $US^{18}O$ / $ON^{16}O$	6±1	(CASIQK)H^+; (TPVSEKVTK)H^+; (CCTESLVNR)H^+; (DTHKSEIAHR)H^+; (FKDLGEEHFK)H^+; (TVMENFVAFVDK)H^+
Labeled peptides from mixture $US^{16}O$ / $ON^{18}O$	3±1	(GACLLPK)H^+; (LCVLHEKTPVSEK)H^+; (MPCTEDYLSLILNR)H^+ Oxidation (M)
Non-labeled peptides from mixture $US^{16}O$ / $ON^{18}O$	9±1	(ALKAWSVAR)H^+; (HLVDEPQNLIK)H^+; (TVMENFVAFVDK)H^+ Oxidation (M); (VTKCCTESLVNR)H^+; (ETYGDMADCCEK)H^+; (LKHLVDEPQNLIK)H^+; (DDPHACYSTVFDK)H^+; (AEFVEVTKLVTDLTK)H^+; (YNGVFQECCQAEDK)H^+; (HPYFYAPELLYYANK)H^+;
Labeled peptides from mixture $US^{18}O$ / $ON^{16}O$	3±0	(VLASSAR)H^+; (ALKAWSVAR)H^+ ; (HLVDEPQNLIK)H^+
Non-labeled peptides from mixture $US^{18}O$ / $ON^{16}O$	6±1	(LVTDLTK)H^+; (LSQKFPK)H^+; (IETMREK)H^+; (SEIAHRFK)H^+; (NECFLSHK)H^+; (CCTKPESER)H^+; (LKECCDKPLLEK)H^+

Therefore it can be concluded that some peptides are preferentially formed as a function of the digestion method. Thus, peptides $(GACLLPK)H^+$; $(LCVLHEKTPVSEK)H^+$; $(MPCTEDYLSLILNR)H^+$ are formed in the overnight digestion, whilst peptides $(VLASSAR)H^+$; $(ALKAWSVAR)H^+$; $(HLVDEPQNLIK)H^+$ are formed in the ultrasonic method. On the overall, both methods produced the same number of total peptides, c.a. 40, confirming that both methodologies work well for protein digestion. Another interesting finding is that protein modifications as consequence of the heating/cavitation caused by the ultrasonic energy were not found. For instance, no extra oxidations or carbamydomethylations were detected.

These results confirm the utility of ^{18}O labeling in relative proteomics discovering and confirms the usefulness of the combination of ultrasonication and a 96-well plate for proteomics applications.

VI.5 Future prospects

The speed, simplicity, high throughput and number of potential proteomics applications that can be developed jointing 96-well plate and ultrasonic multiprobes, it makes of this combination an ideal tool for robotic platforms. As an example, if a multiprobe of 96 tips was acomplisehd with a 96 well plate, the time need to identified a protein separated by gel electrophoresis could be reduced to just 20 s. Therefore developments in this area of research are anticipated.

VI.6 Conclusions and perspectives

It has been proven that the combination of a 96-well plate and an ultrasonic multi-probe is a powerful tool in sample treatment for proteomics, allowing high sample throughput and a potentially enormous number of different proteomics applications. The huge variety of protocols that can be used with this accomplishment has it been demonstrated through different proteomics sample treatments for protein identification and 18-O based labelling. Sample preparation steps including destaining, washing, reduction & alkylation, digestion, spotting on MALDI targets or transfer to LC/MS input plates can be combined on a single automated platform making use of ultrasonication.

This allows for rapid processing, minimizes the risk of contamination and therefore reduces the chance of application errors and improves the quality of data. The results showed that for protein digestion low or high ultrasonic amplitudes must be avoided when using a 96 well plate and an ultrasonic multiprobe. We have not found differences in performance for protein identification when using ultrasonic amplitudes of 30 (single probe) or 40 kHz (multiprobe).

We have demonstrated that using the direct and reverse ^{18}O labeling the effectiveness of different procedures for in-gel protein digestion can be compared in terms of number and type of peptides produced. In fact our findings showed a similar number of peptides obtained by either the overnight or the ultrasonic method. However, some peptides were preferentially formed for each digestion protocol.

VI.7 Acknowledgments

H. M. Santos and R. Carreira acknowledge the doctoral grants SRFH/BD/38509/2007 and SFRH/BD/28563/2006, respectively, from FCT (Science and Technological Foundation) from Portugal. The research findings here reported are protected by international laws under patent pendings PCT/IB2006/052314 and PT 103 303. FCT is acknowledged for financial support under the project POCI/ QUI/55519/2004 FCT-FEDER and PTDC/QUI-QUI/099907/2008. J. L. Capelo and C. Lodeiro acknowledge the Isidro Parga Pondal Program from Xunta de Galicia, Spain. Digilab-Genomic Solutions is acknowledged for financial support. Gabriela Ribas and Mario Diniz are acknowledge for kindly provide us with *D. desulfuricans* ATCC27774 and *C. carpio* samples, respectively.

VI.8 References

[1] D. Lopez-Ferrer, B. Canas, J. Vazquez, C. Lodeiro, R. Rial-Otero, I. Moura, J.L. Capelo, Sample treatment for protein identification by mass spectrometry-based techniques. Trac-Trends *Anal. Chem*. 25 (2006) 996-1005.

[2] R.J. Carreira, R. Rial-Otero, D. Lopez-Ferrer, C. Lodeiro, J.L. Capelo, Ultrasonic energy as a new tool for fast isotopic O-18 labeling of proteins for mass spectrometry-based techniques: Preliminary results, Talanta, 76 (2008) 400-406.

[3] D. Lopez-Ferrer, J.L. Capelo, J. Vazquez, Ultra fast trypsin digestion of proteins by high intensity focused ultrasound. J. Proteome Res. 4 (2005) 1569-1574.

[4] H.M. Santos, C. Mota, C. Lodeiro, I. Moura, I. Isaac, J.L. Capelo, An improved clean sonoreactor-based method for protein identification by mass spectrometry-based techniques, Talanta, 77 (2008) 870-875.

[5] H.M. Santos, J.L. Capelo, Trends in ultrasonic-based equipment for analytical sample treatment. Talanta 73 (2007) 795-802.

[6] R.J. Carreira, R. Rial-Otero, D. Lopez-Ferrer, C. Lodeiro, J.L. Capelo, Ultrasonic energy as a new tool for fast isotopic O-18 labeling of proteins for mass spectrometry-based techniques: Preliminary results, Talanta, 76 (2008) 400-406.

[7] Santos, H.M., Glez-Peña, D., Reboiro-Jato, M., Fdez-Riverola, F., Diniz, M.S., Lodeiro, C., Capelo-Martínez. J.L., Novel 18O inverse labeling-based workflow for accurate bottom-up mass spectrometry quantification of proteins separated by gel electrophoresis, Electrophoresis, 31 82010) 3407-3419.

[8] D. Lopez-Ferrer, T.H. Heibeck, K. Petritis, K.K. Hixson, W. Qian, M.E. Monroe, A. Mayampurath, R.J. Moore, M.E. Belov, D.G. Camp II, R.D. Smith, J. Proteome Res. 7 (2008) 3860-3865.

[9] Ultrasonic multiprobe as a new tool to overcome the bottleneck of throughput in workflows for protein identification relaying on ultrasonic energy, Santos, H.M., Carreira, R., Diniz, M.S., Rivas, M.G., Lodeiro, C., Moura, J.J.G., Capelo, J.L., Talanta 81 (2010) 55-62.

[10] Y.K. Wang, Z.X. Ma, D.F. Quinn, W.F. Emil, Inverse O-18 labeling mass spectrometry for the rapid identification of marker/target proteins, Anal. Chem. 73 (2001) 3742-3750.

[11] M. Postema, A. Wamel, C. T. Lancee, N. Jong, Ultrasound-induced encapsulated microbubble phenomena. Ultrasound Med. Biol. 30 (2004) 827-840.

[12] G. Wibetoe, D. T. Takuwa, W. Lund, G. Sawula, Coulter particle analysis used for studying the effect of sample treatment in slurry sampling electrothermal atomic absorption spectrometry. Fresenius J. Anal. Chem. 363 (1999) 46-54.

[13] X. Yao, C. Afonso, C. Fenselau, Dissection of proteolytic O-18 labeling: Endoprotease-catalyzed O-16-to-O-18 exchange of truncated peptide substrates, J. Proteome Res. 2 (2003) 147-152.

Chapter VII

Conclusions and future prospects

VII.1 Conclusions

The work presented in this thesis involves sample preparation adressed for mass spectrometry analysis by MALDI-TOF, to, somehow, contribute for the filing of the existing gap caused by the lack of standard protocols in some application areas of this mass spectrometry in the Laboratory of Analysis of the DQ-FCT-UNL. The results are detailed below.

Ultrasonic energy was used as a tool to improve the protocols for the analysis of polymers by MALDI. Different ultrasonic devices were tested, namely the ultrasonic bath, UB; the sonoreactor and the ultrasonic probe. The device with the best performance was proven to be the ultrasonic bath. With this system it was assayed two different frequencies of sonication, namely 35 kHz and 130 kHz. The homogenization process with the last frequency for the PS 2000 Da in DHB matrix during 120 s, led to low Mw and Mn values, that were found statistically different from the values obtained for the sample homogenization using the standard method of reference (vortex mixing) and from the values giving by the polymer manufacturer. Despite of these results, when the UB at a sonication frequency of 35 kHz was used, the values for Mw and Mn obtained for PS and PEG in dithranol matrix were not statistically different from the ones acquired with vortex mixing or from the values recommended by the manufacturers. As a general role, the sonoreactor and the ultrasonic probe can be also used, but firstly needs to be clearly established by comparison with a standard mixing procedure, such as vortex, that they can be used without troubles in the sample preparation of a given polymer, since in this work the applicability of such devices was shown to be dependent of a series of factors, such as the type of matrix used and the sonication time employed. For PS analysis by MALDI the DHB matrix should not be used. For the analysis of PS 2000 Da, this matrix needs six times more Ag as cationic reagent than dithranol matrix, making necessary to discard the spectrum of the first 50 shots due to the high saline content of the mixture. In addition, it was found a high dependence on the analyte/matrix mixing procedure for DHB matrix. For instance, PS 2000 in DHB cannot be mixed with the ultrasonic bath at 130 kHz with a sonication time of 120 s. Moreover, when the mass of the poly(styrene) was increased from 2000 Da to 10,000 Da, analysis with DHB matrix was not possible for any of the sample mixing procedures studied, even increasing the cationic agent six times more than the amount needed for the analysis of PS 10,000 Da in dithranol. For

PEG analysis in dithranol, significant differences were found for Mn and Mw values, between vortex mixing and the sonoreactor (30 s of sonication time) and the sonication probe (10 s or 30 s of sonication time), the most intense sonication devices. When the matrix for PEG was DHB, Mn and Mw values obtained with vortex mixing were statistically different than those obtained with the sonoreactor (30 s of sonication time). This pioneer work thus suggests that the UB with a sonication frequency of 35 kHz could be used for fast and high throughput sample treatment of polymers for their characterization. Nevertheless, this methodology needs of further confirmation and to be extended to more polymers, and for this reason more works dealing with this subject are anticipated.

A new fluorescence β-naphtol derivative **L**, containing an N2O5 donor set was synthesised in excellent yield by a simple Schiff-base condensation reaction, and its photophysical properties have been evaluated in solution by absorption and fluorescence emission spectroscopy and by MALDI-based mass spectrometry. Its capacity to act as a potential sensor for Cu^{2+}, Zn^{2+}, Cd^{2+} and Hg^{2+}, and the basic anions such as F^-, Cl^-, Br^-, I^- and CN^-, was carried out in DMSO solution. Among the cations and anions studied, the probe has shown a remarkable selectivity for Cu^{2+}, CN^- and F^-. This selectivity means that the new ligand could find an application as the building block to design a more complex chemosensor for these three ions. The interaction of **L** with Cu(II), CN^- and F^- was also studied using MALDI-TOF mass spectrometry (both in positive and negative mode). No peak was observed when the ligand was titrated with fluoride anion in stoichiometry concentrations appearing a peak assigned to $[\mathbf{L}F]^-$ when the concentration of F^- was increased. In the other hand, noteworthy changes in the mass spectrum of the ligand (either in the positive or negative mode) were observed upon titration with Cu^{2+} and CN^-. The results from the MALDI studies suggest that **L** can be used to sense Cu^{2+} in positive mode, and cyanide in negative mode. DFT studies showed that the copper (II) complex is formed by the un-protonated $\mathbf{L}^{2-}$ species as it was predicted experimentally. However, the anionic complexes with fluoride and cyanide take places via supramolecular interactions with the diprotonated **L** form.

Four macrocyclic ligands containing an 8-HQ pendant arm were synthesized and fully characterized. The protonation behaviour and sensing capability of these ligands toward divalent, Cu(II), Zn(II), Cd(II), and trivalent, Al(III) and Cr(III) metal ions have

been studied by UV–vis and fluorescent emission spectroscopy. MALDI was used to characterize titrations of L^2 and L^4 with Zn(II) and Al(III) solutions. In all cases, the formation of the metal complexes was observed by the presence of the expected m/z peaks. These results confirm the formation of the metal complexes also in the gas phase. The results were the same in both cases. Addition of one metal equivalent led to the formation of the mononuclear complex. Addition of increasing amounts of metal ion did not produce any peaks attributable to the formation of dinuclear complexes. The results with Al(III) and Zn(II) confirm both the stoichiometry observed in the synthesized solid metal complexes, and the data obtained in solution by absorption and fluorescence emission spectroscopy. For ligand L^2, in the presence of 1 and 2 equiv of Zn(II), peaks with m/z 619.3 are attributable to the protonated ligand $[L^2H]^+$, and with m/z 462.2 are attributed to the loss of the methyl-8-HQ group. Small peaks at higher mass values are attributable to species with two, three and four pendant arms, and they are indicative of the interaction of the quinoline group with the ligand in the gas phase After addition of the metal salt, the peak corresponding to the protonated ligand disappears, and new peaks at m/z 682.3, 524.2, and 441.2, attributable to the $[L^2Zn–H]^+$, $[L^2Zn–MeQuinoline]^+$, and $[L^2Na\text{-pendant}]^+$ species, respectively, are observed. Overall the results presented above confirms that MALDI can be used to follow titrations of metals and complexes, being an excellent complement to other traditional techniques such as UV–vis and fluorescent emission spectroscopy.

It has been proven that the combination of a 96-well plate and an ultrasonic multi-probe is a powerful tool in sample treatment for proteomics, allowing high sample throughput and a potentially enormous number of different proteomics applications. The huge variety of protocols that can be used with this accomplishment has been demonstrated through different proteomics sample treatments for protein identification and ^{18}O based labelling. Sample preparation steps including distaining, washing, reduction & alkylation, digestion, spotting on MALDI targets or transfer to LC/MS input plates can be combined on a single automated platform making use of ultrasonication. This allows for rapid processing, minimizes the risk of contamination and therefore reduces the chance of application errors and improves the quality of data. The results showed that for protein digestion low or high ultrasonic amplitudes must be avoided when using a 96 well plate and an ultrasonic multiprobe. We have not found differences in performance for protein identification when using ultrasonic amplitudes of 30 (single

probe) or 40 kHz (multiprobe). We have demonstrated that using the direct and reverse ^{18}O labelling the effectiveness of different procedures for in-gel protein digestion can be compared in terms of number and type of peptides produced. In fact our findings showed a similar number of peptides obtained by either the overnight or the ultrasonic method. However, some peptides were preferentially formed for each digestion protocol.

VII.2 Future prospects

The work we have developed along with other ones in the bioscope group related to ultrasonic energy and protein cleavage have received more than 600 references since it was published the first manuscript dealing with this idea in 2005. Currently our work opens the possibility to use the new ultrasonic platforms that allows the treatment of 96 well plates at once. This device is called cup-horn and it entails all the advantages needed for a good work, namely simplicity, reduction of sample handling and time of sample treatment, furthermore, cross contamination is avoided. The most remarkable advantage is the large amount of samples that can be treated at once, namely 96. If this device performs as all the others already tested by our group, sample treatment in proteomics will be no more the bottleneck of proteomics pipelines. It must be stressed out the online applications, another field that has not yet been fully explored, and that it deserves future work.

The promising use of ultrasonic energy as a tool to prepare polymers for their characterization by mass spectrometry is certainly a notable area of progress in science that was open by this research. The work ahead with this application will pass for its large-scale application to a large number of different polymers.

MALDI has also demonstrated to be an excellent technique for characterization of small molecules, and therefore we expect to use it further in our facilities for this purpose. Furthermore, the possibility to use MALDI as a way to follow metals titrations with macrocyclic ligands opens the possibility of using MALDI as a method for the qualitative detection of metals in waters. This is something that is currently on-going in the laboratories of the Bioscope group.